

Dear Editor,
Dr. Kostas Tsigaridis,

Thank you and thank to the staff of ACP for your work. We are glad to notice that all the referees appreciated the experimental effort and the high relevance of the results presented in our paper. Furthermore, all the referees asked for elucidation of a number of technical points. All the raised criticisms and relative answers have been addressed in the revised manuscript. Finally, we added the new figures, required to help the reader understand the vertical behavior of aerosol properties. The whole text was proofread, and edited to improve the language. The manuscript was shortened when possible, as new parts were introduced as required by the referees. We are pleased that this discussion based on the constructive criticisms of the referees has helped us to improve the scientific quality of the work done.

With our best regards,

Yours sincerely,

Dr. Luca Ferrero

Response to Reviewer#1

We thank the reviewer for his or her helpful comments and insight. We respond to the general and to the specific points below. All the comments are addressed in the revised manuscript. As requested, the whole text was proofread and edited, to eliminate the typos and to improve the language.

General Comment 1: This study reports vertical profiles of aerosol number size distribution and black carbon (BC) concentrations from balloon measurements during a field campaign in Ny-Ålesund, Svalbard spring and summer 2011-2012. The authors divide the number size distribution into 3 modes and classify the vertical profiles in four shapes during spring. The authors also discuss secondary aerosol formation and emissions from shipping during summer.

This study is important because 1) the vertical distribution of aerosols affects its radiative forcing and 2) measurements of the vertical distribution of aerosols in the Arctic are particularly sparse. Since such measurements are highly needed and valuable, I think this study is relevant and within the scope of ACP. The Method section is clearly outlined and the different instruments used are sufficiently and well explained. The figures are nice and easy to follow. However, I think the overall presentation of the results should be improved before it can be published. The manuscript needs more work in terms of language and structure. If this can be achieved, I recommend the manuscript for publication.

Answer to the General Comment 1 (AGC)1: Thank you very much for your comment which underline the experimental efforts and the high relevance of the results presented in our paper. We agree with you that an improved organization of the manuscript and a better presentation of the results is necessary. For this reason, we managed the paper accordingly to your suggestions (here below answered). The whole text was also proofread and edited, to eliminate the typos and to improve the language.

General comment 2. The quality of the English language in this manuscript is variable (some parts are good, but others less good), and I think it would benefit by a thoroughly review of the language (and a spell check!). I have added a few examples under minor comments.

AGC2: The manuscript was proofread and edited, to eliminate the typos and to improve the language as required. A particular attention was given to shorten the several long sentences present in the paper, as also required in your minor comment 4. Thank you for the suggestion.

General comment 3. The Results section would be easier to read if it was shortened a bit. Description of the methodology should always be under Methods, not Results. I have a few specific suggestions below.

AGC3: Thank you for this comment. We agree with you. The description of the methodology was moved to the method section (section 2.2.1, page 9, lines 17-36; section 2.2.3, page 13, lines 1-13). Moreover, sections 3.1 and 3.2 were shortened and merged together in the revised version of the paper (new section 3.1, pages 13-15).

General comment 4. I miss a broader implication of this study. Why did you separate the profiles into the four shapes? Comprehensive measurement studies like this can provide physical understanding for evaluation/improvement of the modeling of aerosol processes. Do you have any suggestions? I understand that you cannot add any modeling, but I would like to know more what we can learn from this study.

AGC4: Thank you for this question. Our answer is also related to that reported below for your specific comment SC22 (see our answer ASC22).

We separated the profiles in the four shapes because each shape is the result of an interplay of several processes: 1) transport events, 2) the planetary boundary layer dynamics and 3) the local formation of aerosol. The different combinations of these factors result in a specific profile class.

Figure 7 represents a good example in which the transport of polluted air masses from mid-latitudes generated initially PG profiles that naturally evolved (due to the entrance into the PBL) into a NG profile.

Even though a modelling simulation is beyond the scope of the present paper, some indication can be obtained. One of this is related to your question about the validity of ground-based measurements with respect to the vertical aerosol distribution in modelling comparison (SC21). HO profile showed that ground measurements are fully representative of the vertical column (up until ~1 km, our vertical limit) while during NG and PG profiles the ground based measurements are representative for the column up to the PBL. DNG profiles show that ground-based measurements differ from the measurements performed within the column. However, the last case is influenced by secondary aerosol formation that can be easily detected by an SMPS.

Thus ground-based measurements (coupled with a proper PBL determination) are fundamental for model validation. Due to your question we added the aforementioned consideration in the conclusions (section 4, pages 23-24, lines 36-40 and lines 1-4).

General comment 5. Measurements of vertical profiles in the Arctic are sparse, but there are a few, e.g.:

- two ARCTAS campaigns in the North American Arctic (Jacob et al. 2010) in April and June/July 2008
- the ARCPAC campaign conducted together with ARCTAS in spring 2008 (Brock et al. 2011)
- the PAMARCMIP campaign in April 2009 (Stone et al. 2010) - the HIPPO campaign (Schwarz et al. 2010, 2013; Wofsy 2011) January and October 2009 + winter and autumn 2009
- the ARCTAS/ARCPAC campaign in spring 2008,
- the ARCTAS campaign in summer 2008
- the PAMARCMIP campaign in spring 2009.

On a general basis; How are those compared to your study? I suggest you also include more of these studies in the introduction.

Jacob, D.J., J.H. Crawford, H. Maring, A.D. Clarke, J.E. Dibb, L.K. Emmons, R.A. Ferrare, C.A. Hostetler, P.B. Russell, H.B. Singh, A.M. Thompson, G.E. Shaw, E. McCauley, J.R. Pederson and J.A. Fisher, 2010. The Arctic Research of the Composition of the Troposphere from Aircraft and Satellites (ARCTAS) mission: design, execution, and first results. *Atmospheric Chemistry and Physics*, 10:5191-5212.

Brock, C.A., J. Cozic, R. Bahreini, K.D. Froyd, A.M. Middlebrook, A. McComiskey, J. Brioude, O.R. Cooper, A. Stohl, K.C. Aikin, J.A. De Gouw, D.W. Fahey, R.A. Ferrare, R.-S. Gao, W. Gore, J. Holloway, G. Hubler, A. Jefferson, D.A. Lack, S. Lance, R.H. Moore, D.M. Murphy, A. Nenes, P.C. Novelli, J.B. Nowak, J.A. Ogren, J. Peischl, R.B. Pierce, P. Pilewskie, P.K. Quinn, T.B. Ryerson, K.S. Schmidt, J.P. Schwarz, H. Sodemann, J.R. Spackman, H. Stark, D.S. Thomson, T. Thornberry, P. Veres, L.A. Watts, C. Warneke and A.G. Wollny, 2011. Characteristics, sources, and transport of aerosols measured in spring 2008 during the aerosol, radiation, and cloud processes affecting Arctic climate (ARCPAC) project. *Atmospheric Chemistry and Physics*, 11:2423-2453.

Wofsy, S.C., 2011. HIAPER Pole-to-Pole Observations (HIPPO): finegrained, global-scale measurements of climatically important atmospheric gases and aerosols. *Philosophical Transactions of the Royal Society*, 369:2073-2086.

Stone, R.S., A. Herber, V. Vitale, M. Mazzola, A. Lupi, R.C. Schnell, E.G. Dutton, P.S.K. Liu, S.M. Li, K. Dethloff, A. Lampert, C. Ritter, M. Stock, R. Neuber and M. Maturilli, 2010. A three-dimensional characterization of Arctic aerosols from airborne Sun photometer observations:

PAMARCMIP, April 2009. Journal of Geophysical Research: Atmospheres, 115:doi 10.1029/2009jd013605.

Schwarz, J.P., J.R. Spackman, R.S. Gao, L. Watts, P. Stier, M. Schulz, S.M. Davis, S.C. Wofsy and D.W. Fahey, 2010. Global-scale black carbon profiles observed in the remote atmosphere and compared to model. Geophysical Research Letters, 37:L18812, doi:10.1029/2010gl044372.

Schwarz, J.P., B.H. Samset, A.E. Perring, J.R. Spackman, R.S. Gao, P. Stier, M.G. Schultz, F.L. Moore, E.A. Ray and D.W. Fahey, 2013b. Global-scale seasonally resolved black carbon vertical profiles over the Pacific. Geophysical Research Letters, 40:5542-5547.

AGC5: Thanks for this comment.

An important comparison was reported in the manuscript (section 3.2, page 16, lines 21-25), where “the columnar averages of both total aerosol number and eBC concentrations [$236.1 \pm 23.9 \text{ cm}^{-3}$ (N_{14-260}), $21.1 \pm 1.3 \text{ cm}^{-3}$ ($N_{260-1200}$), $0.2 \pm 4 \cdot 10^{-2} \text{ cm}^{-3}$ ($N_{>1200}$) and $52 \pm 8 \text{ ng m}^{-3}$ (eBC)]” were successfully compared with long-term data series collected over Ny-Ålesund at the Zeppelin observatory (Eleftheriadis et al., 2009; Tunved et al., 2013) during Spring.

This comparison underlined the accuracy of the collected data and, most importantly, suggested that all the investigated vertical profile classes may influence the background Arctic aerosol measured by Arctic observatories within GAW and EMEP observation programs.

Moreover, at page 3 lines 23-25 (original version of the manuscript) we cited some of the Arctic campaigns (i.e. Kupiszewski et al., 2013; Schwarz et al., 2010).

However, we fully agree with you that a better contextualization of the measuring campaign is required.

Thus, we modified the introduction section, adding and discussing the suggested campaigns (and related references). Moreover, we discussed the obtained results with respect to the same references.

Particularly we modified the introduction section at page 3, lines 26-40 and at page 4, lines 1-10. The result section was modified at the following points: section 3.2 (page 16, lines 24-29), section 3.2.1 (page 17, lines 1-2 and lines 17-24), section 3.2.2 (page 18, lines 4-6 and lines 12-17), section 3.2.3 (page 19, lines 4-10), section 3.2.4 (page 20, lines 12-14, page 21, lines 13-25).

Specific Comment 1 (SC1): Abstract: You should mention in the abstract that these were balloon measurements up to 1200 meters height.

Answer to the Specific Comment 1 (ASC)1: *Thank you very much, we modified the abstract accordingly to your suggestion at page 1, lines 26-27.*

SC2: Page 2, L 17: ‘to influence with semi-direct effects the atmospheric properties’. Could this be rewritten and explained further, maybe by 1 or 2 examples?

ASC2: *The sentence was rewritten at page 2, lines 15-20, as follows: “Many of these processes depend on aerosol absorption and scattering of the solar radiation (direct effect). Additionally, indirect effects play an important role as the aerosols seed and modify the cloud properties. Lastly, light absorption by BC can alter the atmospheric thermal structure within, below, or above clouds consequently affecting cloud distributions (IPCC, 2013; Bond et al., 2013; Ramanathan and Feng, 2009; Koren et al. 2008; Koren et al., 2004; Kaufman et al., 2002)”.*

SC3: Page 2, L 34: You mention Arctic Haze here without explaining it. Since this is an important part of your study, I think you should briefly explain the phenomena with a few references (e.g. Stohl 2006). Stohl, A. (2006), Characteristics of atmospheric transport into the Arctic troposphere, J. Geophys. Res., 111, D11306, doi:10.1029/2005JD006888.

ASC3: Thanks for raising this point, we agree with you that a better description of the Arctic Haze could help the reader. For this reason, we added to the introduction section (pages 2-3, lines 34-39 and line 1) the following description: “During the Arctic Haze, an inflow of pollution (aerosol and gases) from northern mid-latitudes (during winter-spring) results in a reduction in visibility (Jacob et al., 2010; Stohl et al., 2006; Radke et al., 1984; Barrie and Hoff, 1985; Brock et al., 1989; Shaw, 1995). The Arctic Haze occurs under meteorological conditions with stable stratifications and the frequent and persistent occurrences of surface-based inversions. According to Stohl et al. (2006), within these conditions, the air pollution can be transported into the Arctic at low-level (followed by ascent in the Arctic or low-level alone) or with an uplift outside the Arctic, followed by descent in the Arctic itself”.

SC4: Page 3, L 25: ‘These reports may well highlight opposing forms of behavior ‘. I am not quite sure what this means?

ASC4: The intention was to underline the differences in the vertical aerosol behavior found during the reported field campaigns. However, to avoid any confusion, we deleted this sentence.

SC5: Page 3, L 25: One reason for this difference between the observations could be the strong influence of biomass burning during spring 2008 (Warneke et al. 2010).

Warneke, C., K.D. Froyd, J. Brioude, R. Bahreini, C.A. Brock, J. Cozic, J.A.de Gouw, D.W. Fahey, R. Ferrare, J.S. Holloway, A.M. Middlebrook, L. Miller, S. Montzka, J.P. Schwarz, H. Sodemann, J.R. Spackman and A. Stohl, 2010. An important contribution to springtime Arctic aerosol from biomass burning in Russia. *Geophysical Research Letters*, 37:L01801, doi:10.1029/2009GL041816.

ASC5: Thank you very much for the suggestion, we added the reference to the introduction section (page 3, line 33).

SC6: Page 3, L 30: Drop ‘should’, as this is written it seems like you tell the emissions to do so? In bracelets: we do not know for sure if these emissions will warm the surface and be deposited, but as you write above; studies show that there are higher probability for this to happen when the concentrations are located close to the surface.

ASC6: Thank you. We modified the sentence.

SC7: Page 4, L 23: Could you add just one sentence summarizing this table? E.g. 25 measurement days, balloons measured 2-14 profiles each day, altitude range?

ASC7: Thank you for the suggestion. The new sentence (page 5, lines 11-13) is as follows: “Table 1 lists the dates of the campaign (25 measurement days), the number of flights (197 measured profiles), the maximum altitudes (~700-1300 m) and the cloud base height (clouds present for 48% of the campaign).”

SC8: Page 5, L 5: Is there a reference for this instrument and the calculated uncertainty in mass concentrations?

ASC8: As stated at page 5, line 32, we used the 5-digit Sartorius ME235P microbalance. In this respect, 5% is the uncertainty related to the weighing procedure experimentally evaluated. The text is changed as follows (page 5, lines 32-33): “The reproducibility error for filter weighing was lower than 5% (experimentally evaluated)”.

SC9: Page 6; L 18: Could you briefly here explain what you mean when the atmosphere is ‘stable’ and does not encourage vertical mixing? (in terms of potential temperature)

ASC9: *We modified the sentence as follows (page 7, lines 1-6): “The term stability refers to the propensity of air masses to move vertically: stable air resists any vertical motion, while unstable air masses are prone to vertical movements. A parcel of air results to be stable/unstable if the temperature lapse rate is lower/higher than the adiabatic one, i.e. if the potential temperature is increasing/decreasing with height, respectively. In stable stratification, turbulence and vertical mixing is suppressed, leading to trapping of pollutants near ground level”.*

SC10: Page 8, L 28: In this paragraph you define the 3 modes of particles, ‘Aitken’, ‘Accumulation’ and ‘coarse’ and say that you will also use these names for the rest of the discussion, but most of the time you use N_{14-260} , $N_{260-1200}$, and $N_{>1200}$ anyway. I suggest you use the names Aitken etc. throughout the text once you have defined them, as this is easier to read.

ASC10: *Thank you for addressing it. With these sentences we wanted to explain the meaning of each investigated broadsize range. We carefully considered your comment. However, “ N_{14-260} includes a small fraction of the Nucleation mode (from 14 to 20 nm), the totality of the Aitken mode (20-100 nm) and a fraction of the Accumulation mode (from 100 to 260 nm)” (page 9, lines 4-5); in addition, “the mode $N_{260-1200}$ includes most of the Accumulation mode particles” (page 9, lines 5-6). Thus, as both N_{14-260} and $N_{260-1200}$ are not “pure/whole” Aitken and Accumulation modes we decided to maintain the manuscript in the present form. A similar approach was also used in Kupiszewski et al. (2013).*

SC11: Page 8, L 36: Since there are many figures in this paper; I suggest removing fig 2 (or move to the supplementary).

ASC11: *Figure 2 was moved to the supplemental material (now Figure S1).*

SC12: Page 9: There are various methods to measure BC concentrations, and they can disagree by a factor of seven or more (Petzold et al 2013). Since the (common) filter-based method like you have used is not a direct measurement of BC, it is recommended to report the resulting BC concentration (eBC) together with the assumed MAC value. Maybe you should change ‘BC’ to ‘eBC’ to make sure that we know that this is equivalent BC? I also think you should add a brief discussion on how your measurements depend on the assumed MAC number (you use 12.5 m²/g?) (or at least make a note about this).

Petzold, A., J.A. Ogren, M. Fiebig, P. Laj, S.M. Li, U. Baltensperger, T. Holzer-Popp, S. Kinne, G. Pappalardo, N. Sugimoto, C. Wehrli, A. Wiedensohler and X.Y. Zhang, 2013. Recommendations for reporting “black carbon” measurements. *Atmospheric Chemistry and Physics*, 13:8365-8379.

ASC12: *Petzold et al. (2013), Andreae and Gelencser (2006) and other authors (Gilardoni et al., 2010; Sthol et al., 2013; Eckhardt et al., 2013) suggest reporting BC concentrations with the term equivalent Black Carbon (eBC), arising from the need to report the method to determine BC and the parameters used in the method. We specified it in section 2.2.2 (page 9, line 40 and page 10, lines 1-4). Moreover, we used the term eBC throughout the whole paper.*

When optical methods are used to measure light transmission through the filter loaded with BC, the mass equivalent concentration is determined using the mass attenuation cross-section (σ_{ATN}). For the case of our measurements, we report the σ_{ATN} value 12.5 m² g⁻¹. We note this value (Ferrero et al., 2011) in the method section, as the one used in the micro-Aethalometer AE51 (page 10, line 20). This approach was also used by Eleftheriadis et al. (2009) when reported ten years of BC measurements in Ny-Ålesund.

Moreover, the σ_{ATN} value ($12.5 \text{ m}^2 \text{ g}^{-1}$) “was obtained by comparing the BC values measured with the microAeth® Model AE51, with an AE31 Aethalometer (880 nm wavelength) operating in a test chamber with different BC concentrations at low attenuation values. The comparison was then repeated using ambient air” (as reported in Ferrero et al., 2011).

This value is not far from the σ_{ATN} values of $15.2 \text{ m}^2 \text{ g}^{-1}$ and $15.9 \text{ m}^2 \text{ g}^{-1}$ reported in Eleftheriadis et al. (2009) and applied to the attenuation coefficient measured at the Zeppelin station (Ny-Ålesund) with the Aethalometers AE9 and AE31, respectively. The difference between these values results from the use of different filter materials to collect the sample in the different Aethalometers, which was quantified in Ferrero et al. (2011) and Drinovec et al. (2015).

Due to your question we added the aforementioned specifications to section 2.2.2 (page 10, lines 21-28).

We compare our results with those previously measured at Ny Ålesund in the manuscript (page 16, lines 21-24), where we state: “the columnar average of BC concentrations obtained by averaging the profile classes was $52 \pm 8 \text{ ng m}^{-3}$ (eBC)”. This value “perfectly agrees with long-term data series collected over Ny-Ålesund at the Zeppelin observatory (Eleftheriadis et al., 2009) during Spring.”

Finally, considering the relationship between the attenuation and absorption coefficients (page 11, equation 11), the apparent mass attenuation cross-section of $12.5 \text{ m}^2 \text{ g}^{-1}$ corresponds to the mass absorption cross-section (MAC) of $6.1 \text{ m}^2 \text{ g}^{-1}$ (using $C=2.05 \pm 0.03$). As suggested by Petzold et al. (2013), we report the wavelengths, the mass attenuation cross-section and the mass absorption cross-section used in the determination of the absorption coefficients, using the methodology reported in Weingartner et al. (2003). The MAC of $6.1 \text{ m}^2 \text{ g}^{-1}$ is in agreement with the previously published range of values (see for example Petzold et al. (2013) and references therein).

SC13: Page 9: Filter-based methods are sensitive to absorbing and non-absorbing non-BC particles. Could you please add a few sentences about the uncertainties in your method as well?

ASC13: Considering the absorbing non-BC particles, different types of aerosol may in principle contribute to the signal in Aethalometers (i.e. Brown Carbon, dust). However, Brown Carbon (BrC) is characterized by negligible absorption in the infrared (Andreae and Gelencsér, 2006), the wavelength range of the eBC measurements (micro-Aeth AE51 uses 880 nm). In this respect, Massabò et al. (2013) show the potential contribution of BrC to the determination of eBC to be below 10%.

To estimate the possible influence of BrC on eBC measurements carried out during the spring 2011 campaign, the few data collected with the micro-Aeth prototype at 370 and 880 nm were considered. Particularly, the Aethalometer model (Sandradewi et al., 2008) was applied to the apportionment of absorption due to both BC and BrC as reported in Massabò et al (2013) and in Shamjad et al. (2015) as follows:

$$\frac{b_{abs}(370 \text{ nm})_{BC}}{b_{abs}(880 \text{ nm})_{BC}} = \left(\frac{370}{880}\right)^{-\alpha_{BC}} \quad (1)$$

$$\frac{b_{abs}(370 \text{ nm})_{BrC}}{b_{abs}(880 \text{ nm})_{BrC}} = \left(\frac{370}{880}\right)^{-\alpha_{BrC}} \quad (2)$$

$$b_{abs}(\lambda) = b_{abs}(\lambda)_{BC} + b_{abs}(\lambda)_{BrC} \quad (3)$$

where α_{BC} and α_{BrC} represent the Absorption Angstrom Exponents of BC and BrC, respectively. The value for α_{BC} was taken to be 1 as suggested by Massabò et al (2013) and Sandradewi et al. (2008), while α_{BrC} was set at 3.5 (Yang et al., 2009), 3.95 (Massabò et al., 2013), 6.6 (Shamjad et al., 2015) and 9.0 (Bikkina and Sarin, 2013), respectively. With this inputs, the percentage of absorption at 880 nm due to BrC instead that BC was 8.5%, 5.8%, 0.5% and 0.1%, respectively. Thus, it is

possible to estimate that the BrC positive artifact on eBC measurements was less than 10% during the campaign.

The effect of non-absorbing particles on the filter photometer measurements was also quantified for the Aethalometer AE33. Drinovec et al. (2015), which uses the same filter material as the AE51, and was shown to be below 2.5%. To reduce the effect of the non-absorbing particles sampled onto the filter, the experimental protocol during the campaign followed that reported in Ferrero et al. (2011): all vertical BC profiles were conducted by changing the filter ticket regularly. As a result, ATN never achieved values higher than 20 during all profiles. This means that the total amount of aerosol collected on each filter during the vertical profile was very low resulting in a negligible effect of non-absorbing particles.

We added the aforementioned considerations to the supplemental material and referenced them in section 2.2.2 (page 12, lines 3-9).

SC14: Page 11, L 15: ‘Figure S1a shows a larger interannual springtime variability.’ Of what?

ASC14: Thanks for addressing this point, with this sentence we meant that Figure S1a (now Figure S3a) shows a larger interannual springtime variability of temperature measured close to the ground. Due also to your question here below (SC15) we rewrite the manuscript text (page 13, lines 27-33) with the following sentence: “First of all, the observational periods (spring 2011, summer 2011 and summer 2012) were addressed in a climatological context. In this respect, the temperature measured in spring 2011 was within the standard deviation range of the long-term observations, while a 10-day period at the end of April 2011 was slightly warmer than the climatological mean (Figure S3a). The temperatures during the summer seasons 2011 and 2012 were mostly within the range of the long-term observations (Figure S3b). Neither of the campaign periods was conducted under exceptional meteorological conditions, so the vertical profile measurements can be considered to have been obtained under typical meteorological conditions representative for the Ny-Ålesund environment.”

SC15: Page 11, L 13 - 20: Since you are referring to figures in the supplement, maybe you could rewrite this paragraph so this is easier to follow without the figures? Not ‘Fig Sxx shows ..’ but instead just briefly state that the spring season had surface temperatures close to the climatology, summer season had .. etc. and then mention that figures are in Supplementary (–OR– move the sup. figures to the paper, but then you already have many figures there).

ASC15: We modified the paper accordingly to your observation (see ASC14 and pages 13, lines 27-33).

SC16: P11: ‘Particularly, the maximum wind speeds registered at ground during balloon flights in spring 2011 and in summer 2011 2012 were 4.9 m s and 10.7 m s lower than the absolute wind speeds registered during the same periods: 27.9 m s and 16.3 m s.’ I’m not sure if I understood this. The absolute winds measured by ..? With movement? How do you conclude that the measurement periods are representative for days with low winds?

ASC16: The wind speed was measured at the Amundsen-Nobile Climate Change Tower as described in section 2.1.2 (page 6, lines 36-38). The wind speed (average, max value) measured during balloon flights was lower than that during the whole period (April 2011, June and July 2011-2012) of the campaign. Thus, we reported that balloon flights have limitations with respect to its launch conditions, in particular they favor low wind conditions as it is very difficult to launch the balloons during high winds. We understand from your question that the sentence was not clear. Thus, we rephrased it as follows (pages 13-14, lines 34-40 and lines 1-2): “We note, however, that the tethered balloon measurements have limitations with respect to its launch conditions (section

2.2). Particularly, balloon profiles were measured in low wind conditions, as it is very difficult to launch the balloons during high winds. This introduces a bias in respect to average meteorological conditions above the launch site. The maximum wind speed measured at the Amundsen-Nobile Climate Change Tower (section 2.1.2) during balloon flights was lower than that during the whole period of the campaign (April 2011, June and July 2011-2012): 4.9 m s^{-1} and 10.7 m s^{-1} (springtime and summertime balloon profiles) compared to 27.9 m s^{-1} and 16.3 m s^{-1} (full spring 2011 and summer 2011-2012). Table 1 resumes the conditions for all the measured profiles. The majority of vertical profile measurements was conducted under clear sky conditions (no clouds) or with clouds with base height above the balloon payload.”

SC17: Page 11, line 32 - page 13, line 14: I think you spend too much time explaining figure 3. Parts of this can be moved to Methods, e.g. what type of information you can retrieve from the measurements. You can also move parts to Introduction as a way of motivating the study. When I read the ‘Results’-chapter I want to read about the results right away. Could you also try to merge some of this information when you present the other results? I would skip everything between L31, p11 to L21,p12 and start on ‘An example ..’. Is fig 3 needed at all? Why cannot the measured potential temperature and the RH for each group be plotted in fig 5 instead? On the other hand, figure 7 is hardly mentioned. Can the wind roses be put in better context with the profiles described in 3.3.1-3.3.4? Also, this text is a bit hard to read, because of all the numbers listed. Do you need to list them all? Maybe put them in a table?

ASC17: *We agree with your observations. Particularly, as we reply in AGC3 to your general comment, all the description of the methodology presently in the result section was moved under the method section. Sections 3.1 and 3.2 were shortened and merged together in the revised version of the paper. Figure 3 (now Figure 2) was maintained in the revised version to introduce the set of vertical profile measurements. We added averaged meteorological parameters to figure 5 (now Figure 4 in the revised version of the manuscript).*

Figure 7 (now Figure 5) was put in evidence in the revised version of the paper when discussing each profile class (section 3.2.1, page 17, lines 2-5; section 3.2.2, page 17, lines 29-32; section 3.2.3, page 18, lines 21-22; section 3.2.4, page 19, lines 15-17; section 3.3.1, page 22, lines 5-8; section 3.3.2, page 22, lines 31-32. Finally, a table (Table 3) resuming data of the campaign was added to the revised version of the manuscript.

SC18: Page 17, L3: does this text and forward belong to 3.3.4 or should it have a separate heading?

ASC18: *Page 17, line 3 and the following lines (original version) belong to section 3.3.4 (now section 3.2.4). Section 3.2.4 was quite long, but we shortened it following your suggestion (see AGC3) moving the methodology present here in the method section.*

SC19: Page 18: anything that has to do with methodology should be under Methods, not Results.

ASC19: *We agree with you and we modified the paper accordingly (see AGC3).*

SC20: Page 19, L16: what is meant by a ‘meaningful’ impact of ship emissions?

ASC20: *The intention was to point out that profiles were affected by a local, high, plume emitted from the ships. We agree that the sentence, as stated, was not clear and thus we rephrased it as follows (page 21, lines 34-35): “Type 2, profiles characterized by the presence of shipping emissions (hereinafter addressed as SP), Figure 11d-f.”*

SC21: Page 20: It is interesting to see the impact of ship emissions. Could you remind us here how far the measurements were from the ships? This also relates to your final conclusion on page 21 (where you suggest that increased shipping could significantly increase BC concentrations during summer and enhance climate change in the Arctic). Currently, BC emissions from shipping in the Arctic comprise a small fraction of within- Arctic BC. Browse et al. 2012 found that even under a high-projection of shipping, by 2050 BC emissions from shipping would still contribute less than 1 % of total Arctic deposition. Do you suggest that current emission inventories are too low and that future emission projections should also be higher?

Browse, J., K.S. Carslaw, S. Arnold, K.J. Pringle and O. Boucher, 2012. The scavenging processes controlling the seasonal cycle in Arctic sulphate and black carbon aerosol. *Atmospheric Chemistry and Physics*, 12:6775-6798.

ASC21: *Vertical profile measurements in summer were carried out from the German-French AWIPEV research base (78°55'24" N 11°55'15"E), 600 m far from the harbor (we added this information to section 2, page 5, line 10). Thus, the reported results (section 3.3.2, Figure 11d-f and Figure 12) refer to the local impact of ships.*

The obtained results are in agreement with those reported in Eckhardt et al. (2013), who showed an enhancement of 72 and 45 % (up to 81 and 72 % in stagnant conditions) of eBC, when ships cruised in the Kongsfjord, compared to values when ships were not present.

From these results, yet Eckhardt et al. (2013) concluded that the eBC increase due to shipping emission can "be taken as a warning signal of future pan-Arctic conditions if Arctic shipping becomes more frequent and emission regulations are not strict enough".

On the other hand, as you addressed, shipping contribution was less than 1% of BC emissions in the Arctic as reported in the study of Stohl et al. (2013) where, conversely, gas flaring was estimated to contribute 42% to the annual mean BC surface concentrations in the Arctic dominating the estimated BC emissions north of 66° N.

However, even also Corbett et al. (2010) reported that "the magnitude of emissions from shipping on a mass basis may be modest compared to other anthropogenic sources, the proximity of activity to the Arctic may help explain regional effects important for global and regional climate change". The possible implications of shipping emissions were also addressed in the work of Sand et al. (2013), who underlined that the BC aerosols would be emitted by ships directly into the Arctic planetary boundary layer with a stronger interaction with the surface (both by deposition of BC on snow and ice and by radiative and sensible heat fluxes down to the surface).

Given the aforementioned considerations and the experimental conditions of vertical profile measurements, we rephrased the conclusion referring to the impact of shipping emission at a local scale (page 23, line 10).

The emission inventories are beyond the scope of the present work. We report the increased number of ships (page 22, lines 19-23) and passengers (a proxy of ship dimensions) in summer 2012 (78 days with 138 ships) relative to summer 2011 (57 days with a total of 103 ships). The obtained results can be thus considered an important phenomenon which should remain under observation in the future due to the sensitivity of the Arctic environment.

SC22: Page 20, L22: 'forbidden' – by who/what? What is meant by: ' . And the locally formed aerosol becomes in summer' ?

Do you find any (systematic) correlation between the different vertical profiles and the measurements at the ground? E.g. for special ground conditions, one can assume (with some certainty) a particular profile? Or that when using ground measurements (which are more abundant) when comparing to models, it is not such a bad assumption?

ASC22: *Thank for addressing this point, the sentence was incomplete due to an erroneous application of tracking changes in the word processor. We rewrote the sentence as follows (page*

23, lines 5-8): “It is important to note that SP profiles were observed in summer. In summer the long-range transport of aerosol from mid-latitudes is minor (Browse et al., 2012; Quinn et al., 2008; Stohl et al., 2006) and the locally formed aerosol becomes dominant (Giardi et al., 2015; Tunved et al., 2013; Ström et al., 2009 and 2003)”.

Figure 4 clearly shows that for HO profiles ground measurements are fully representative of the vertical column (up until ~1 km, our vertical limit); during NG and PG profiles the ground based measurements are representative for the column up to the planetary boundary layer. DNG profiles show that ground-based measurements differ from the measurements aloft. However, the last case is influenced by secondary aerosol formation that can be easily detected by an SMPS (or similar experimental devices).

Given the above considerations, in our opinion, ground-based measurements (coupled with a proper PBL determination) are fundamental and very useful for model validation. We added these considerations in the conclusion section (pages 23-24, lines 36-40 and lines 1-4).

Minor Comment 1 (MC1): Line 28 page 2: write the Q as a full sentence, e.g. How does the aerosol (. . .) vary by season?

Answer to the Minor Comment 1 (AMC)1: The sentence was changed into: “To adopt the right mitigation strategies, key scientific issues in the study of Arctic aerosols has to be solved. They include the identification of the relative importance of long-range advection with respect to local emissions (Flanner, 2013; Sand et al., 2013; Shindell and Faluvegi, 2009).

Most important, the seasonal characterization of the aerosol vertical structure, a very poorly determined piece of information, is required” (page 2, lines 25-29).

MC2: Page 2, line 31: ‘Very pronounced’ → drop ‘very’

AMC2: Done

MC3: Page 3, line 1: know → known

AMC3: Thanks, corrected.

MC4: There are several long sentences in this paper, which makes it a bit hard to read. E.g. Page 3. Line 2-7 is one sentence over 6 lines. Could this be split in 2? Also in this sentence: ‘leads’ → ‘could lead’.

AMC4: We agree with you. We modified the sentence at page 3 and we shortened the long sentences present in the paper. Thanks for the suggestion.

MC5: Page 4, line 28: form → from

AMC5: Thanks, corrected.

MC6: Page 6, line 5 double ..

AMC6: Thanks, corrected.

MC7: Page 6, line 13: operates since 2009 → ‘have operated’

AMC7: Thanks, corrected.

MC8: Page 6, line 21: ‘during snow covered or not periods’ Please rewrite.

AMC8: *We rephrased and move the sentence at page 14, lines 11-16 (section 3.1).*

MC9: Page 8, line: closets → closest

AMC9: *Thanks, corrected.*

MC10: Page 11, line 2: ‘Aerosol and BC and vertical profile (. . .)’ Please rewrite. By vertical profile do you mean the meteorological fields? And aerosol are the size distributions?

AMC10: *We rephrased the sentence as: “Vertical profiles of aerosol number size distribution and eBC concentrations were measured to assess changes in aerosol properties within the vertical column in the Arctic region” (page 13, lines 16-17). Here the intention was to draw the reader’s attention towards the topic of this paper: the determination of the vertical behavior of the aerosol properties (number size distribution and eBC concentration) in the Arctic.*

MC11: Page 11, Line 10: ‘Before to introduce’ .. please change

AMC11: *We rephrased the sentence as: “Here below, the ambient conditions under which the vertical profiles were measured are briefly described” (page 13, lines 25-26).*

MC12: P 11, L 24: ‘Moreover, quite all measurements were conducted’ quite all? You mean ‘all’?

AMC12: *Table 1 summarizes the conditions during the measuring campaign. It can be observed that, during the majority of vertical profile measurements, clear sky conditions were present. Due to your question we rephrased the sentence to clarify this point (page 14, lines 1-2).*

MC13: P11, L31: drop ‘now’

AMC13: *Done*

MC14: P11, L34: ‘Several information can be derived’ please rewrite

AMC14: *We rephrased the sentence as (page 13, lines 1-3): “Examples of AS_h , accompanied with the corresponding potential temperature (θ) and RH profiles, are presented in Figure 2a-d. The presented data, accurately describe the vertical distribution of the aerosol and its properties in the first kilometer above Ny-Ålesund”.*

MC15: P11, L34: P20, L24: reasing → rising?

AMC15: *Yes, rising. Thanks, corrected.*

Response to Reviewer#2

We thank the reviewer for his or her helpful comments and insight. We respond to the general and specific points below. All the comments are addressed in the revised manuscript. As requested, the whole text was proofread and edited, eliminate the typos and to improve the language.

General Comment 1: This manuscript describes vertical profiles of aerosol number density over Arctic during spring and summer and presents authentic and original scientific material that has relevant implications for atmospheric science (aerosol, clouds, CCN, and others). This study is based on very important aerosol data over Ny-Ålesund, Svalbard, although the tethered-balloon-borne aerosol measurements are restricted to the good weather (i.e., clear sky, calm winds etc.). On the whole, the topic of the manuscript is relevant and suitable for the scope of the “ACP”. However, there are several points which require some careful revision and corrections before publication.

Answer to the General Comment 1 (AGC)1: *Thank you very much for your comment which underline the originality and the high relevance of the results presented in our paper. Concerning your request of revision and correction we managed the paper accordingly to your suggestions (here below answered). The whole text was also proofread and edited, to eliminate the typos and to improve the language.*

General comment 2. Quality of English I found many typo, miss-spell, and grammatical errors (e.g., location of “,”).

AGC2: *The manuscript was proofread and edited, to eliminate the typos and to improve the language as required.*

General comment 3. Comparison with previous airborne aerosol measurements Several airborne aerosol measurements have carried out in Arctic area since 2000, for instances, ASTAR (2000, 2004, and 2007), ARCTAS (2008), ARCPAC (2008), and PAMARCMiP (2009 and 2011). Particularly, ASTAR campaigns were made around Svalbard. I suggest strongly that your data are compared to these previous results, and that these campaigns should be added into description of introduction.

AGC3: *Thank you for this comment. An important comparison was reported in the manuscript (section 3.2, page 16, lines 21-25), where “the columnar averages of both total aerosol number and BC concentrations [$236.1 \pm 23.9 \text{ cm}^{-3}$ (N_{14-260}), $21.1 \pm 1.3 \text{ cm}^{-3}$ ($N_{260-1200}$), $0.2 \pm 4 \cdot 10^{-2} \text{ cm}^{-3}$ ($N_{>1200}$) and $52 \pm 8 \text{ ng m}^{-3}$ (BC)]” were successfully compared with long-term data series collected over Ny-Ålesund at the Zeppelin observatory (Eleftheriadis et al., 2009; Tunved et al., 2013) during Spring. Moreover, at page 3 (lines 23-25, original version of the manuscript) we cited some of the Arctic campaigns (i.e. Kupiszewski et al., 2013; Schwarz et al., 2010).*

However, we fully agree with you that a better contextualization of the measuring campaign with respect to the international is required. Thus, as also required by reviewer#1, we modified the introduction section adding and discussing the suggested campaigns. Moreover, as you suggested, we discussed the obtained results with respect to the same references.

Particularly we modified the introduction section at page 3, lines 26-40 and at page 4, lines 1-10. The result section was modified at the following points: section 3.2 (page 16, lines 24-29), section 3.2.1 (page 17, lines 1-2 and lines 17-24), section 3.2.2 (page 18, lines 4-6 and lines 12-17), section 3.2.3 (page 19, lines 4-10), section 3.2.4 (page 20, lines 12-14, page 21, lines 13-25).

General comment 4. Classification of aerosol type In this study, authors classified aerosol profiles into four groups. I agree with the classification of aerosol profiles. Unfortunately, typical weather/meteorological conditions and air mass origins in each type were not mentioned in the text. These information is very important to characterize vertical features of aerosols in Arctic region, and to be compared to aerosol data taken in the other project.

AGC4: Thank you for your comment, which supports the classification of aerosol profiles.

The weather and meteorological conditions for each profile class were addressed in Table 2, Figure 7 (now Figure 5) and discussed along section 3.2 and 3.3. However, they were mainly addressed to illustrate the differences between DNG profiles and the other profile classes. We modified the paper introducing the meteorological context for each profiles class.

In this respect, we modified the result section at the following points: section 3.2 (page 16, lines 30-33), section 3.2.1 (page 17, lines 3-11), section 3.2.2 (page 17, lines 29-34), section 3.2.3 (page 18, lines 21-25), section 3.2.4 (page 19, lines 15-19) section 3.3.1 (page 22, lines 5-9), section 3.3.2 (page 22, lines 31-35).

The air mass origins are addressed below and we refer to the following explanation also for the answer to your specific comment 9.

We agree with you that air mass origin was shown and explained (in the original version of the manuscript) only for the case study reported in figure 6 (now Figure 7) and discussed in sections 3.2.2 and 3.2.3 for both PG and NG profiles.

However, before trying to find a relationship between the type of the vertical profile and air mass origin, it is necessary to consider that each profile shape is the result of an interplay among several processes: 1) transport events, 2) the planetary boundary layer dynamic and 3) the local formation of aerosol. Among this, only the transport event process is strongly related to the air mass origin (some precursors transported may also affect secondary aerosol formation), while the final profile shape is the result of the specific combination of the aforementioned processes.

Figure 7 represents a good example in which the same air mass origin that transported polluted air masses from mid-latitudes generated initially PG profiles that naturally evolved (due to the entrance into the PBL) into NG profiles.

Thus, the same air mass origin could be related to different profile classes.

Due to your question, even with the aforementioned limitations, we performed a cluster analysis of back-trajectories corresponding to each profile class obtained at using the Hysplit 4 (rev. 513). The result is attached here below (Figure AGC4.1).

From Figure AGC4.1 it is possible to observe first that back-trajectories were close in the Arctic area during HO profiles. HO profiles were then representative for background conditions in the Arctic. Both PG and NG can be affected by transport from mid-latitudes. The same happened for DNG profiles, which are a special type of NG profiles.

We added this figure and the aforementioned discussion to the supplemental material (Figure S6) and we address them in the revised version of the manuscript (page 16, lines 35-36).

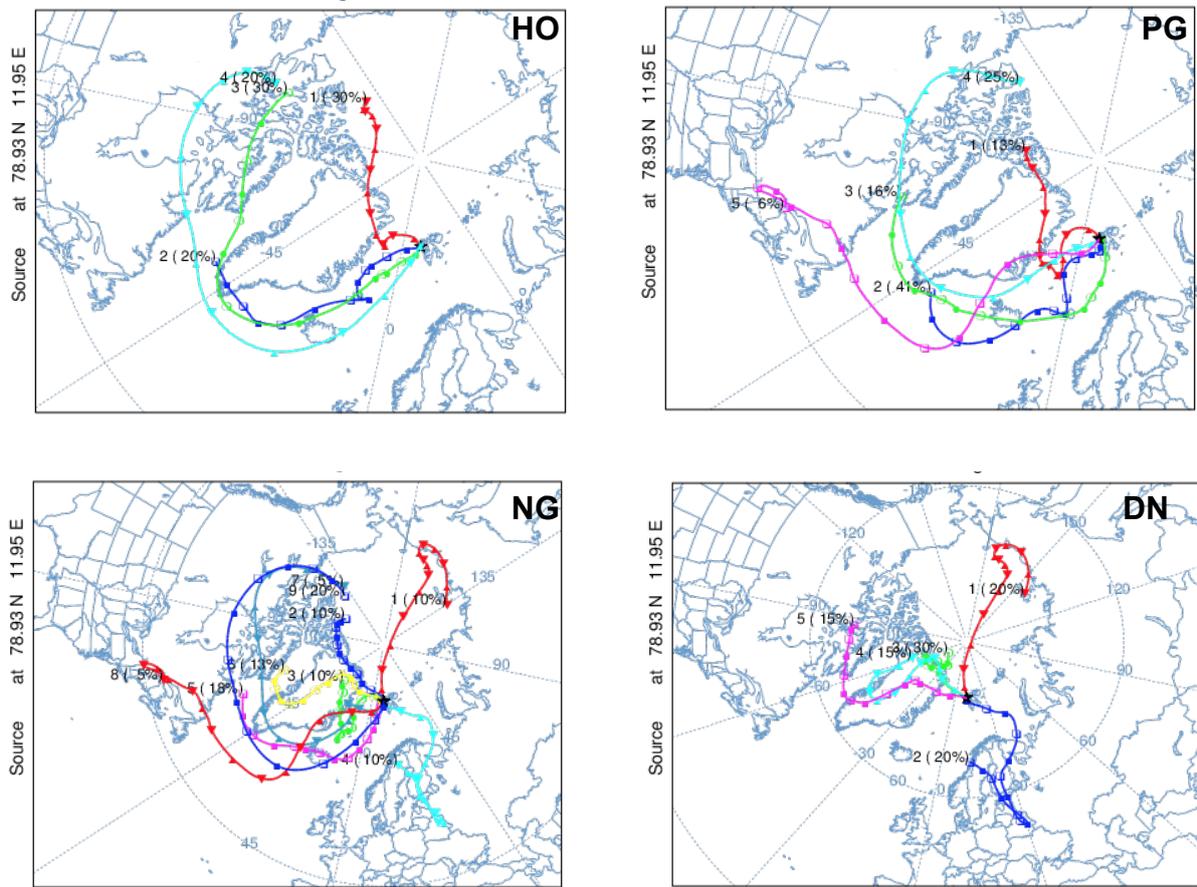


Figure AGC4.1. Cluster analysis of springtime back-trajectories for each profile class (Figure S6 in supplemental material).

General comment 5. Relation between aerosol vertical profiles and structure of boundary layer
Vertical features of aerosols in the lower troposphere are associated with the structure of boundary layer (i.e., surface inversion and height of boundary layer). What is typical height of top of boundary layer in each type? Aerosol data should be compared to vertical structure of boundary layer (surface inversion and top of the layer).

AGC5: We fully agree with you that the relationship between the aerosol vertical profiles and structure of boundary layer is very important. In fact, section 3.1 and figures 2-3 address this topic. Figure 2 illustrates the discussion of the case studies chosen as representative for each profile class. The relationship between θ inversions and AS_h was well documented in section 3.1. Figure 3 reports the frequency distribution with altitude of both AS_h and θ and RH gradient and section 3.1 is essentially dedicated to the discussion of figure 3.

What is missing, and we agree with on this point, is the average values of AS_h corresponding to $H_s=0$ for the profile classes reported in figures 4 and 11; they are: 417 ± 266 m (PG), 506 ± 212 m (NG), 585 ± 90 m (DNG), 474 ± 204 m (SP). We added these values to the sections in which each profile class was discussed.

Finally, as you also requested in your specific comment 6 (see ASC6), we added averaged profiles of normalized θ and RH to Figure 4 in order to relate the mean vertical behavior of aerosol to that of meteorological parameters.

Specific Comment 1 (SC1): Abstract: Height range of aerosol measurements are added in the text of abstract.

Answer to the Specific Comment 1 (ASC1): Thank you very much, we modified the abstract accordingly to your suggestion at page 1, lines 26-27.

SC2: Page 5 Line 11, Unit of conductivity: $M \Omega \text{ cm}^{-1}$ (not $M \Omega \text{ cm}$)

ASC2: The measuring unit is right ($M\Omega \text{ cm}$) as it is the resistivity of the ultrapure (Milli-Q) water. We added to the text the specification: "resistivity" (page 5, line 38).

SC3: Page 9 – 10, Sensitivity (detection limit) of BC measurement. In general, high flow rate is required for BC measurements in regions with lower BC concentration. Flow rate for BC measurement was $2.5 \times 10^{-6} \text{ m}^3 \text{ s}^{-1}$ (0.15 L min^{-1}) in this study. I understand that authors chose the largest flow rate of the micro-aethalometer. However, this flow rate might be not enough in lower BC concentrations. Although BC concentration increases during winter –spring in the Arctic regions, the BC level is lower than that in the mid-latitudes. What is the sensitivity (detection limit) of BC measurement in your measurement setting and analytical procedures?

ASC3: At page 10, lines 31-32, a first determination of the accuracy of equivalent BC (eBC) determination was reported by comparing the AE51 and the prototype measurements carried out simultaneously during spring 2011. The result of this intercomparison was reported in Figure 2c (now Figure S1c, supplemental material). As shown, eBC measurements obtained by the two micro-Aethalometers agreed very well ($R^2=0.852$; slope=0.976) with a RMSE of 2 ng m^{-3} (considering the average of the two measurements as the target value).

This result is important because the prototype operated at 265 ml/min ($4.42 \times 10^{-6} \text{ m}^3 \text{ sec}^{-1}$) and the AE51 at 150 ml/min (AE51 commercial version). We added a sentence which describes the two flowrates in the revised version of the manuscript at page 10, lines 32-34 (section 2.2.2).

We present below the analysis calculating the error (in percentage) of each eBC data considering the average of the two eBC measurements (AE51 and the prototype) as the target value. The result is reported in Figure S2a (supplemental material; attached also here below as Figure ASC3.1). Figure ASC3.1 reports the mean (\pm standard deviation) and the 90th percentile of the absolute value of the error in percentage of the measured eBC as the function of eBC concentration using intervals of 5 ng m^{-3} . As it possible to observe at low concentration the error can exceptionally reach values of 90%. The error decreases with increasing eBC concentration, dropping below 20% for concentrations above 20 ng m^{-3} . Thus, it is possible to consider this value as the limit above which a single BC measurement point is not affected by instrumental noise.

Even though this limit for a single eBC measurement is close to the BC concentrations that have been previously measured in the Arctic (Eleftheriadis et al., 2009), the eBC profiles presented in the manuscript are an average of many measurements, hence the effect of the noise on the reported eBC concentrations is further reduced. The aim of this paper is to determine the seasonal phenomenology of the aerosol behavior along vertical profiles classifying the collected experimental data, according to their shape and averaging them for each season. This is very important as, even the error in percentage of each data point can reach high values (especially at low concentrations), the average of the data stabilizes the instrumental fluctuations. This effect is demonstrated by Figure ASC3.2 (Figure S2b in supplemental material) which reports the correlation between the eBC concentrations (AE51 and the prototype) averaged on the same intervals of 5 ng m^{-3} used in Figure ASC3.1 ($R^2=0.986$; slope=1.017).

The aforementioned results demonstrate the reliability of the seasonal phenomenology of the aerosol vertical profiles reported in Figure 4 and 11 and sections 3.2 and 3.3 along the manuscript for what concern BC concentrations.

Due to your question we added the aforementioned analysis to the revised version of the manuscript in section 2.2.2 (pages 10-11, lines 35-39 and lines 1-11).

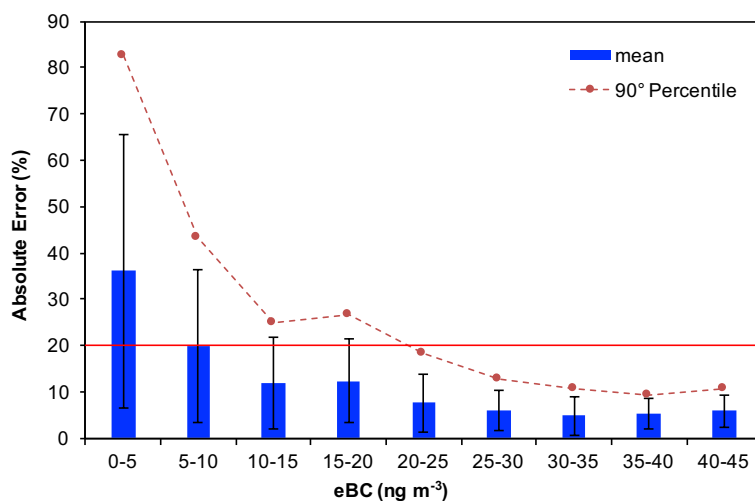


Figure ASC3.1. Absolute value of the error in percentage of the measured eBC in function of its concentration.

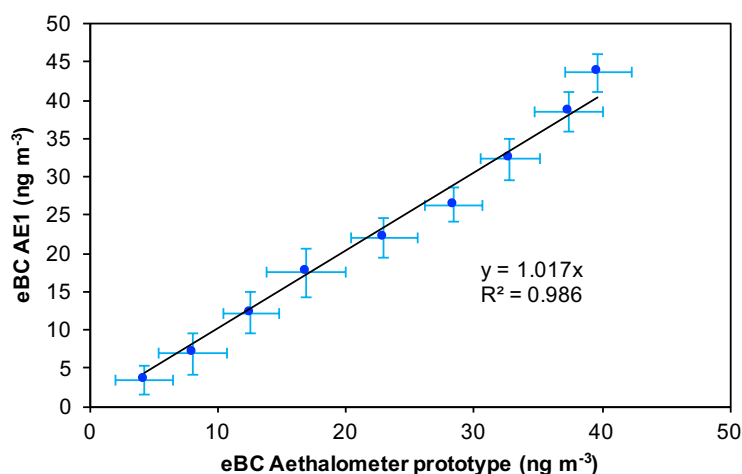


Figure ASC3.2. Absolute value of the error in percentage of the measured eBC in function of its concentration.

SC4: Page 10, Aerosol stratification height (ASh) Procedure for ASh estimation should be mentioned in the text.

ASC4: The procedure to estimate the AS_h was described in the manuscript at page 10 (lines 21-38) and page 11 (lines 1-2) (original version of the manuscript). It is based on the gradient method, which considers the minimum of the vertical derivative of the aerosol concentration as the AS_h . It is reported in the review of Seibert et al. (2000) and its application to vertical profile data has been widely described in previous works (Ferrero et al., 2012, 2011a, 2011b and 2007; Sangiorgi et al., 2011; Di Liberto et al., 2012). For this reason, we refer to the aforementioned publications in the manuscript.

However, due to your question, we briefly explained the gradient method in section 2.2.3 in more detail (page 12, lines 17-23; revised version of the manuscript).

SC5: Sections 3.1 - 3.2 In the sections of 3.1 – 3.2, typical examples of vertical profiles of aerosols and meteorological parameters were mentioned. The description is slightly redundant. Some sentences can be simplified. In addition, general vertical structure of the boundary layer over Ny-Ålesund (i.e., thickness of surface inversion layer, and height of top of boundary layer) should be mentioned to understand characteristics of the vertical profiles. The vertical structure is associated closely with vertical features of aerosols.

ASC5: Thank you for this comment. We agree with you that description of the results in section 3.1 and 3.2 was slightly redundant. Thus, sections 3.1 and 3.2 were shortened and merged together in the revised version of the paper.

A comprehensive description of the general vertical structure of the boundary layer over Ny-Ålesund, is beyond the scope of the paper as the campaign was limited just to three months (April 2011, July 2011 and June-July 2012). We focus on the vertical structure of the boundary layer for the relevant periods.

With respect to the field campaign, θ and RH vertical behavior was described in sections 3.1-3.2 (now section 3.1) and figures 2-3. Figure 2 aims to the discussion of the case studies chosen as representative for each profile class and Figure 3 reports the frequency distribution with altitude of both AS_h and θ and RH gradient.

With respect to the general behaviour of the PBL over Ny-Ålesund, we refer to the comprehensive work of Vihma et al. (2011) that describes the characteristics of temperature and humidity inversions and low-level jets over Svalbard fjords in spring.

Moreover, the long-term upper-air observations by daily radiosondes provide an overview of the atmospheric vertical structure above Ny-Alesund, including the PBL altitude range (Maturilli and Kayser, 2016). In this climatological approach, Maturilli and Kayser (2016) identify the frequent occurrence of a temperature inversion layer in the shear zone above the mountain ridges that is typically present throughout the year, leading to a decoupling of the lowermost kilometer of the atmosphere from the free troposphere above. In between the mountains, the atmosphere is characterized by wind channeling along the fjord axis, disturbed by e.g. glacier outflow or land-sea breeze. Stable atmospheric conditions with suppressed vertical exchange occur frequently during polar night conditions, when a radiative surface-based inversion develops. Once the snow-melt leads to considerable sensible and latent heat fluxes at the surface, atmospheric stratification gets neutral or unstable, allowing convection and vertical mixing.

We added these references to the introduction section (page 4, lines 22-32) and we discussed the results reported in section 3.1 (page 15, lines 1-5) with respect to these references.

SC6: Figure 5 In addition to four groups, general vertical profiles (all data) should be shown in the Figure. The general profiles can be useful, when authors want to know general (average) vertical profiles. Because the vertical profiles of aerosols related to profiles of meteorological parameter (potential temperature and relative humidity), mean profiles of meteorological parameter (or normalized meteorological parameter) should be shown together with those of aerosols.

ASC6: *Thanks for the suggestion. We prepared the figure with all data for the revised version of the paper and we added this figure to the supplemental material (Figure S5 for spring and Figure S8 for summer, here below attached as Figure ASC6.1 and ASC6.2). We also added the mean profile of normalized meteorological parameters (and related all data) to both Figures 4 and 11 and Figure S5 and S8. For normalized meteorological parameters we report absolute differences (Δ) of θ and RH along H_s with respect to the value assumed at $H_s=0$.*

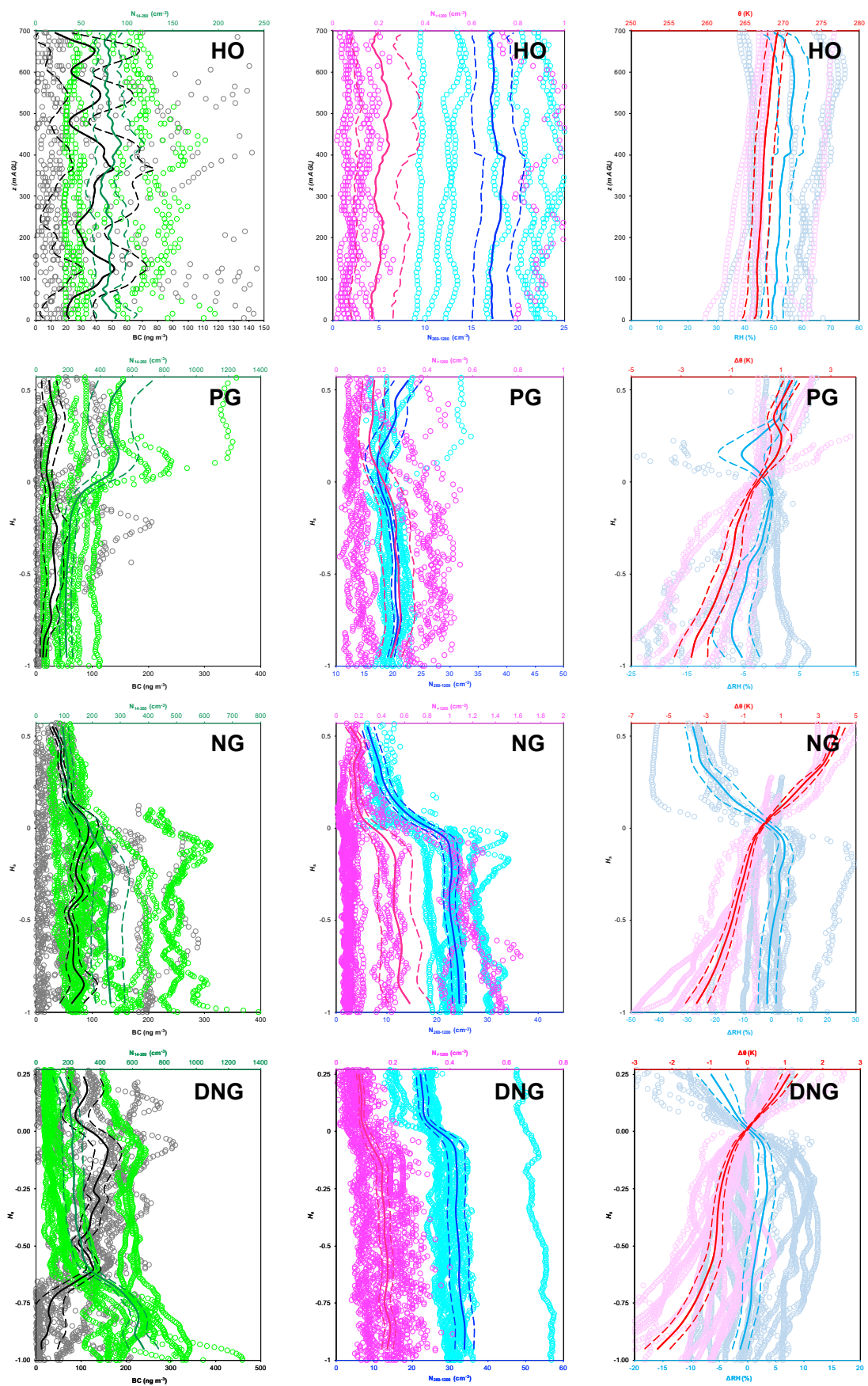


Figure ASC6.1. All data point of the collected vertical profiles during spring for each profile class. The average (solid line) and the mean standard deviation (dashed lines) are also reported (Figure S5 in supplemental material).

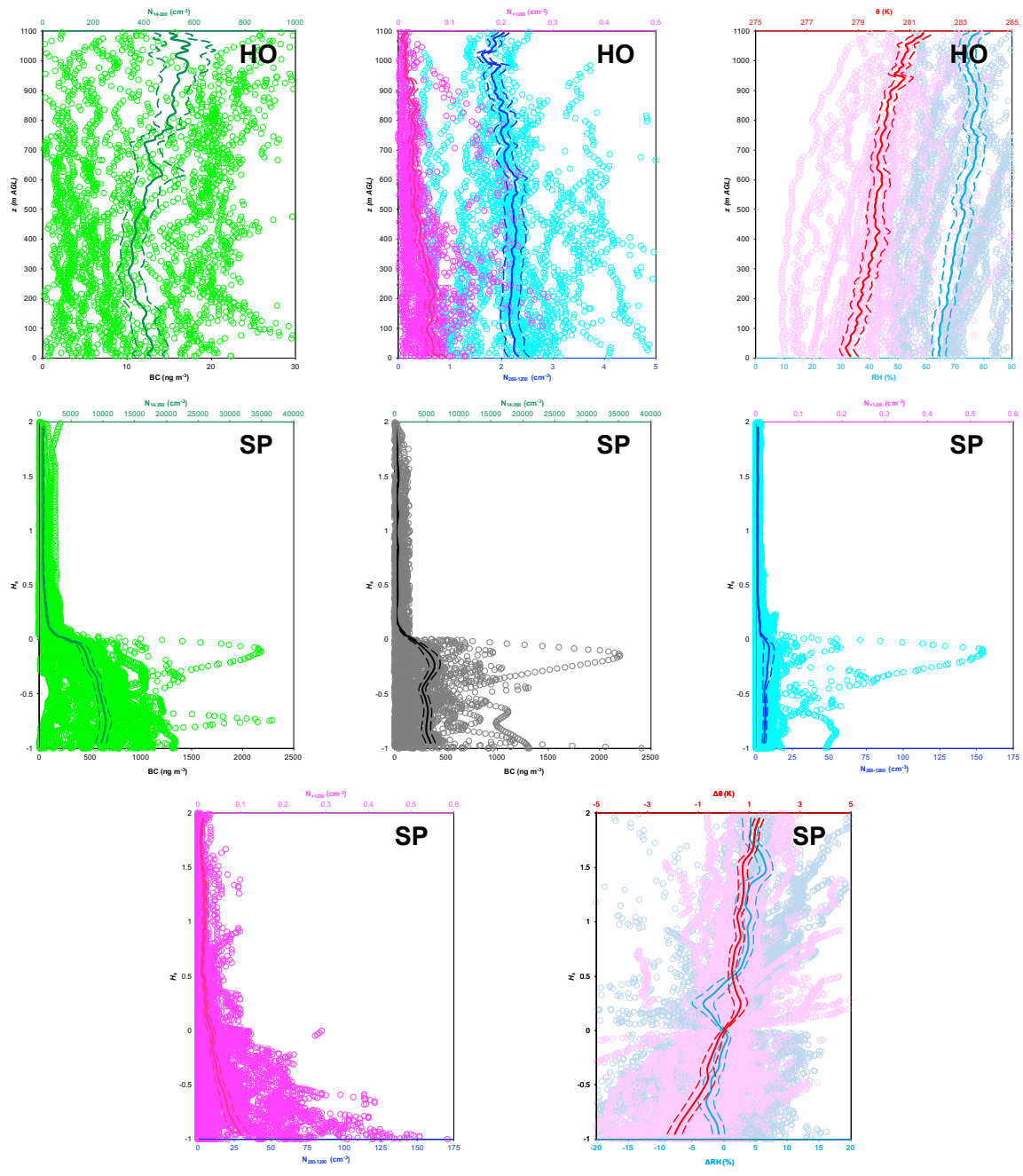


Figure ASC6.2. All data point of the collected vertical profiles during summer for each profile class. The average (solid line) and the mean standard deviation (dashed lines) are also reported (Figure S8 in supplemental material).

SC7: Page 15 Line 8 Before statement about Figure 6, Figure 7 and explanation appeared here. Check or arrange figure number or description in the text.

ASC7: We arranged the figure number in the revised version of the manuscript accordingly to your observation. Thanks.

SC8: Page 15 Line 30 – 34 It is true that wet removal processes have an impact on aerosol number density, but dry deposition make an important contribution to the aerosol number density, especially in coarse particles.

ASC8: Thank you for this comment. We agree with you and we modified the sentence accordingly (page 18, line 1).

SC9: Page 15 Line 35-39 Air mass origins was shown and explained in only in “positive gradient profiles”. However, transport pathway should be discussed together with aerosol source areas to show “plume” transport. In addition, general pattern and characteristics of transport processes in each type should be shown and discussed to understand relation between vertical profiles of aerosols and air mass origins.

ASC9: Please see our answer AGC4 to your general comment 4.

SC10: Page 15 Line 38- Some of particulate organics can be derived from secondary formation. However, there are matters to be discussed whether organics can play an important role in “new particle formation” or not. Actually, organics are condensable vapors to grow aerosol particles in ultrafine mode. So, authors should distinguish between new particle formation and secondary formation and mention them in the text.

ASC10: In section 3.2.4, during the discussion of DNG profiles, we summarized that the experimental results show high acidic sulfate fraction, low BC fraction, low temperature, high relative humidity, low wind speed during (page 20, lines 21-23) at the same time of the presence of a huge Aitken mode (page 20, lines 31-32). All of the aforementioned results pointed towards the presence of a ground-based plume of locally formed secondary aerosol (page 20, lines 35-36). With the last sentence, we meant newly formed particle. Thus, to clarify the sentence we modified the paper accordingly to your suggestion.

For what concern the organics, at page 20, lines 24-30 we reminded that non only binary H_2SO_4 – H_2O system is important for new particle formation but also the presence of organics, as well demonstrated in the work of Riccobono et al. (2014; cited in the paper). This was done to complete the discussion as several organics that can participate to this process were measured in spring at the Gruebadet site (the site of the vertical profile campaign) in spring as reported in Zangrando et al. (2013).

Thus, for this reason we modified section 3.2.4 in the revised version of the paper accordingly to your observation (page 20, line 36).

SC11: Section 3.4 Different condition of solar radiation between spring and summer can engender change of height of top of the boundary layer. This change is very important to vertical profiles of aerosols and meteorological parameters. Other comments about section 3.4 is similar to previous comments about section 3.3.

ASC11: Thank you very much for this comment. We added the radiation data in section 3.1 of the revised version of the paper. The new sentence (page 14, lines 11-16) is as follows: “Convective conditions generally are observed more frequent during summer in Ny-Ålesund related to the

different level of radiation energy at disposal and surface properties. In summer homogenous profiles were observed often (37%) than in spring (15%), due to a synergy of the higher solar power density at disposal ($186.4 \pm 71.2 \text{ W m}^{-2}$ in summer and $109.2 \pm 35.9 \text{ W m}^{-2}$ in spring) together with a lower albedo (0.15 ± 0.01 in summer and 0.87 ± 0.04 in spring) induced by the summer snowmelt in Svalbard”.

Response to Reviewer#3

We thank the reviewer for his or her helpful comments and insight. We respond to the general and specific points below. All the comments are addressed in the revised manuscript. As requested, the whole text was proofread and edited, to eliminate the typos and to improve the language.

General Comment 1: This manuscript is based on vertical profiles of aerosol number density, eBC and ground measurements of the above at the Ny Alesund Arctic research station. This study is providing very useful data for the vertical structure of the aerosol column at a well studied area, where this type of data are still missing.

As a general outcome, the topic of the manuscript is relevant and suitable for the scope of “ACP”. However, there are several points where the manuscript is failing to follow and deliver the methods and data quality needed for this study.

The description of the vertical structure of the atmosphere is well documented and useful and the classification of the different structures useful to relate to known aerosol properties based on the aerosol number size distributions from OPCs. There is also a good documentation of aerosol contamination events from harbor traffic of large boats.

Answer to the General Comment 1 (AGC)1: Thank you very much for your comment which underline the importance of the collected experimental data as well as the high relevance of the results presented in our paper. Here below we answer to the raised points.

General comment 2. The classification and discussion of results is not based on the understanding we can derive for the aerosol microphysics based the origin of aerosol during the study.

AGC2: The aim of the paper is to determine the seasonal phenomenology of the aerosol behavior along vertical profiles; this goal was achieved classifying the collected experimental data, according to their shape, both during spring and summer. Thus, attention was paid to the description of the vertical structure of the atmosphere and its relationship to the aerosol number size distribution.

We underline that, within the context of vertical profile classification, the aerosol microphysics and aerosol/air mass origin were investigated, when necessary, with the aim to deepen the understanding on aerosol vertical behavior for a specific vertical profile class.

In this respect, Figure 7 and related results reported in section 3.2.2 describe the influence of transport from mid-latitudes and the formation of PG profiles. Another example is related to the DNG profiles, which are related to the secondary aerosol formed close to the ground (section 3.2.4 and Figures 6, 9, 10).

General comment 3. There is no attempt to compare with data obtained by numerous studies in the area using aircraft or lidar techniques. Although several studies are mentioned no quantitative comparison is given at least for the ground measurements or data published.

AGC3: Thank you for this comment as a comparison with previous studies is very important.

An important comparison is reported in the manuscript at page 16 (lines 21-24), where “the columnar averages of both total aerosol number and BC concentrations [$236.1 \pm 23.9 \text{ cm}^{-3}$ (N_{14-260}), $21.1 \pm 1.3 \text{ cm}^{-3}$ ($N_{260-1200}$), $0.2 \pm 4 \cdot 10^{-2} \text{ cm}^{-3}$ ($N_{>1200}$) and $52 \pm 8 \text{ ng m}^{-3}$ (eBC)]” were successfully compared with long-term data series collected over Ny-Ålesund at the Zeppelin observatory (Eleftheriadis et al., 2009; Tunved et al., 2013) during Spring.

This comparison underlined the accuracy of the collected data and, most importantly, suggested that all the investigated vertical profile classes may influence the background Arctic aerosol measured by Arctic observatories within GAW and EMEP observation programs.

However, we fully agree with you that a better contextualization of the measuring campaign is required. Thus, we modified the introduction section referencing to previous airborne aerosol measurements carried out in Arctic area. Here below a brief resume.

Particularly we modified the introduction section at page 3, lines 26-40 and at page 4, lines 1-10 as follows: “At this purpose, several field campaigns have been performed in the Arctic in recent years with the aim to characterize aerosol properties along the vertical direction.

The ARCTAS mission (Jacob et al., 2010 and reference therein) showed highly-layered air pollution transport from North America and East Asia in spring, characterized by anthropogenic aerosol below 2 km and by biomass burning in the 2–4 km layer. The ARCPAC campaign (Brock et al. 2011) grouped the aerosol affecting the Arctic in spring in four categories: background troposphere (relatively diffuse, sulfate-rich aerosol); depleted aerosol within the surface inversion layer over sea-ice; layers of organic-rich biomass burning aerosol (above the top of the inversion layer) (see also Warneke et al., 2010) and layers dominated by fossil fuel combustion. The ASTAR campaign (Engvall et al., 2008), focussed on the spring to summer transition period in Svalbard, found Aitken and accumulation mode particles more concentrated in the free troposphere compared to the boundary layer. Kupiszewski et al. (2013), reported new particle formation events in the near-surface layer (possibly related to biological processes) during the summer ASCOS campaign.

Considering the BC, the springtime, PAM-ARCMIP (Stone et al., 2010) and HIPPO (Schwarz et al., 2010) campaigns showed high BC concentrations close to the ground, below the thermal inversion, but also dense pollution and BC at high altitudes over the Arctic (Wofsy et al., 2011). Interestingly, the PAM-ARCMIP results show a decrease of BC compared to past measurements (i.e. AGASP, Hansen and Novakov, 1989). In addition, the HIPPO campaign revealed that in the lower troposphere the BC vertical gradient can change seasonally from positive to negative (Schwarz et al., 2013). In this respect, Spackman et al. (2010) and Koch et al. (2009) reported BC located mainly in the Arctic free troposphere with a positive gradient in the lower troposphere.

The aforementioned campaigns were conducted mainly using aircraft (or helicopters) that for their inner nature are limited to intensive observational periods (Kupiszewski et al., 2013; Bates et al., 2013; Spackman et al., 2010; Schwarz et al., 2010; Koch et al., 2009). Thus, aerosol vertical profiles in the Arctic appear scarce if compared with the number of available data collected at ground level (Samset et al., 2013; Koch et al., 2009). There is the need for regular vertical aerosol profiling campaigns to improve the description of a seasonally resolved aerosol and BC vertical behavior”.

In order to also discuss the results in the context of the aforementioned campaigns, we modified the result sections including them.

The result section was modified at the following points: section 3.2 (page 16, lines 24-29), section 3.2.1 (page 17, lines 1-2 and lines 17-24), section 3.2.2 (page 18, lines 4-6 and lines 12-17), section 3.2.3 (page 19, lines 4-10), section 3.2.4 (page 20, lines 12-14, page 21, lines 13-25).

General comment 4. The use of micro aethalometers in this area can be only used for obtaining EBC concentrations at minimum concentrations, which the authors have yet to derive. They show in figure 2c) a good correlation between the two micro-aethalometers used. This also shows an uncertainty at a 100% level for concentrations below 30 ug/m³. The other serious flaw in the processing of these data is the calculation of the absorption coefficient using a well established methodology and an unrealistic “C” factor. They quote a study in Milan where the “C” factor was derived for urban concentration levels and mixture of urban aerosol species. The authors must remove all absorption coefficients calculated in this manner and reported in this manuscript.

AGC4: Your comment is divided in three parts. Here below we answer to each one:

1. Terminology for BC: we agree with you with the need to report the BC concentrations with the term eBC as suggested by Petzold et al. (2013) and by Andreae and Gelencser (2006) and as widely reported in literature (Gilardoni et al., 2010; Sthol et al., 2013; Eckhardt et al., 2013). We specified it in the method section (pages 9-10, lines 40 and lines 1-4).

2. *Figure 2c (now Figure S1c, supplemental material): data reported in Figure S1c showed a good correlation. This result is first important because the prototype operated at 265 ml/min ($4.42 \cdot 10^{-6} \text{ m}^3 \text{ sec}^{-1}$) and the AE51 at 150 ml/min (AE51 commercial version). However, we agree with you that a single point can be affected by a high level of uncertainty and that a deeper analysis of this comparison is required. Moreover, your question allows us to better explain our approach. In this respect, considering the average of the two eBC measurements (AE51 and the prototype) as the target value (as reported at Page 10, line 36) the absolute error (in percentage) of each eBC data was calculated. Figure AGC4.1 (Figure S2a) reports the average (\pm standard deviation) and the 90° percentile of the Absolute value of the error in percentage of the measured eBC in function of eBC concentration using intervals of 5 ng m^{-3} each. As it possible to observe at low concentration the error can reach values of 90% and more. This error decrease with increasing eBC concentration and reach a reasonable value (less than 20% for both the average and the 90° Percentile) above 20 ng m^{-3} . We have to remind that the aim of this paper is to determine the seasonal phenomenology of the aerosol behavior along vertical profiles classifying the collected experimental data, according to their shape, and averaging them for each season. This is very important as, even the error in percentage of each data point can reach high values (especially at low concentrations), the average of the data stabilize the instrumental fluctuations. This effect is demonstrated by Figure AGC4.2 (Figure S2b) which reports the correlation between the eBC concentrations (AE51 and the prototype) averaged on the same intervals of 5 ng m^{-3} used in Figure AGC4.1 ($R^2=0.986$; slope=1.017). The results demonstrate the reliability of the seasonal phenomenology of the aerosol vertical profiles reported in Figure 4 and 11 and sections 3.2 and 3.3 along the manuscript for what concern eBC concentrations. We added the aforementioned analysis to the revised version of the manuscript in section 2.2.2 (pages 10-11, lines 31-39 and lines 1-11).*
3. *“C” factor: the reviewer’s statement does not consider the experimental conditions of the C determination reported in Ferrero et al. (2011). Ferrero et al. (2011) (page 2832) state that: “The experimental design of vertical profiles does not require any estimation of the aerosol loading factor $R(ATN)$: all vertical BC profiles were conducted by changing the filter ticket after each profile. Every Aethalometer measurement cycle (ascent and descent of the balloon) took less than 40–50 min. As a result, ATN never achieved values higher than 20 during all profiles, meaning that the b_{ATN} measurements were not affected by the “shadowing” effect due to filter loading. The average ATN measured along vertical profiles was 5 ± 1 ”. The experimental conditions for the study in Milano (Ferrero et al., 2011) were intentionally selected not to be influenced by the accumulation of the sample on the filter. This means that the total amount of aerosol collected on each filter during the determination of the parameter C was negligible, making the determined C values a function of the “filter material and the instrument specification” as again stated at page 2832. It is also possible to estimate the total amount of aerosol collected on each filter (ascent and descent of the balloon) during the C determination using the data reported in the paper. Considering the average BC concentrations below and above the mixing layer; the AE51 flowrate, the sampling time and the percentage of BC in PM (both below and above the mixing layer), it is possible to determine that on each filter (changed for each balloon launch) the total PM collected was less than 400 ng. The influence of the type of PM on the C values is therefore negligible, and the C reflects the instrumental properties, which are dominated by the highly scattering filter material. Finally, it is also necessary to observe that the C value was determined using data collected not only below the mixing layer but also above it, in a cleaner atmosphere, along the vertical profiles. The reliability of the obtained C (2.05 ± 0.03) was also demonstrated further in Ferrero et al. (2014), both below the mixing layer and in the free troposphere. For the all the aforementioned reasons, considering that also the detailed explanation of the measurement protocol using the Aethalometer AE51 on page 11*

(lines 27-28) of the manuscript, which ends with: “all eBC vertical profiles were conducted in the clean Arctic environment and the filter tickets were changed regularly to always keep ATN lower than 20 as recommended by Weingartner et al. (2003)”, we maintain the estimation of the absorption coefficient. However, as the value of the absorption coefficient is very important in the Arctic, due to your question we decided to add the reference of Ran et al. (2016, ACPD) to the paper. In fact, until now, the C (2.05 ± 0.03) reported in Ferrero et al. (2011 and 2014) was the only one for the AE51. Recently, on ACPD Ran et al. (2016) proposed 2.52 as C determined at ground-level in China. This value of the parameter C was determined in a completely different environment and, unfortunately the authors have not (yet) reported its uncertainty. Due to your question we added the aforementioned considerations in the revised version of the manuscript (section 2.2.2, pages 11-12, lines 28-38 and lines 1-2).

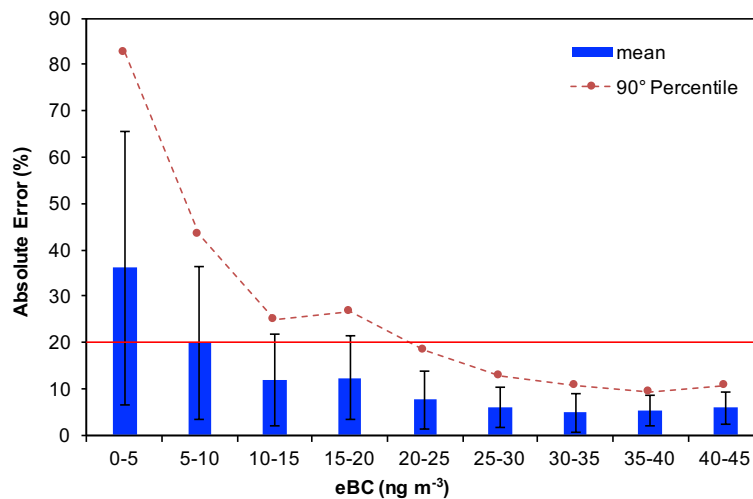


Figure AGC4.1. Absolute value of the error in percentage of the measured eBC in function of its concentration.

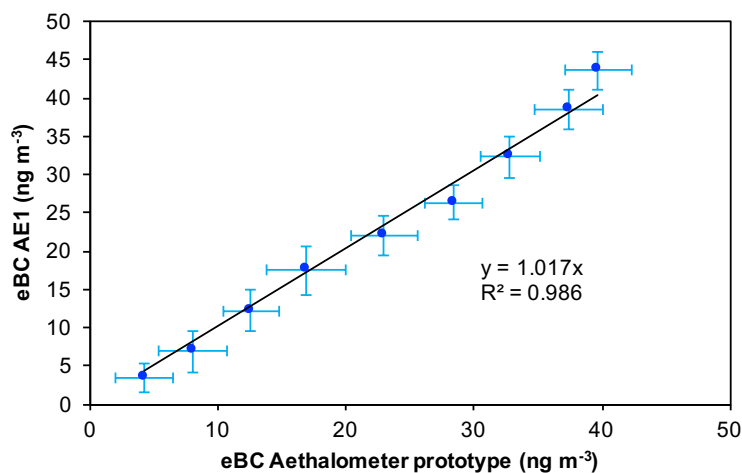


Figure AGC4.2. Absolute value of the error in percentage of the measured eBC in function of its concentration.

General comment 5. The chemical composition reported in figure 8 is given only in % of the total mass. How is the total mass derived and what are the actual mass concentrations of the different species reported in otherwise incredible detail where the non sea salt and non crustal fractions are calculated? These data do not appear realistic. For example in most cases the EC is found to 0.1 % of the aerosol mass. If one assumes that in the worst case eBC and EC mass concentrations can differ by a factor of 2 (+/- 100%) in the HO case where the eBC is found on average at 25 ng/m³ the aerosol mass concentration levels would range between 1 to 50 ug/m³. This upper limit is totally unrealistic and even the 25 ug/m³ is extremely high. The other cases would produce even more grossly biased results.

This comparison puts in doubt the whole dataset of eBC and chemical data leaving the OPC and ground SMPS measurements as the only dataset worth considering for this manuscript.

AGC5: Thank you for this question which allowed us both to deepen the chemical characterization of the aerosol and to better describe the approach reported in the manuscript. Here below we answer to your questions following their order.

1- *The chemical composition reported in Figure 8 was given in percentage. This choice was done to put in evidence (section 3.3.4, page 16, lines 21-29, original version of the manuscript) that “the total sulphate fraction in DNG profiles was double than that observed in the other profile classes ... while both the ss-SO₄²⁻ and the cr-SO₄²⁻ fractions remained quite constant”. These observations, coupled with the lowering of eBC fraction in proximity of the ground (Figure 4l) and the SMPS data reported in Figure 6 show that the ground-based N₁₄₋₂₆₀ concentration peak was due to secondary origin. Thus, the percentage of aerosol chemical composition was used in support of the other datasets to describe the origin of the aerosol found at ground in DNG profiles (see also AGC2)*

However, do to your question we changed figure 8 to report the absolute concentration values (ng m⁻³) of each aerosol chemical component. We moved the previous figure 8, reporting relative contributions, to the supplemental material (Figure S7).

2- *The total mass was measured by weighing the filters before and after the sampling, using a 5-digit microbalance (Sartorius ME235P) after they were conditioned for 48 hours (25°C and 50% relative humidity). The reproducibility error on filter weighing was lower than 5% (experimentally evaluated) as described in section 2.1 (page 5, lines 32-33).*

The absolute concentration values (ng m⁻³) of each aerosol chemical component were added in the new figure 8. Moreover, the same concentration values (ng m⁻³), together with the corresponding detection limit (ng m⁻³) of each aerosol chemical component were reported in a new Table in the supplemental material (Table S1). This table is attached here below as Table AGC5.1. The detection limits refer to the sampling conditions and the analytical procedures. Particularly, as reported in section 2.1.1, for the ion chromatography, only half filter was used (extraction in 12 ml of ultrapure water), 55 m³ of air were filtered for each sample (24 h sampling). For the EC/OC analysis, a 1.5 cm² punch was used and the volume of air filtered for each sample (96 h sampling) was 220 m³.

Table AGC5.1 shows that all the analyzed chemical components were characterized by ambient concentrations largely above the detection limit.

The non-sea salt and crustal fractions of sodium, calcium and sulphate were determined as well documented in section 2.1.1 (equations 1-4). This approach produce reliable results as documented in previous works (Udisti et al., 2016; Giardi et al., 2016; Becagli et al., 2012; Udisti et al., 2012) already referenced in the paper text (page 6, line 13).

When comparing the eBC and EC several points has to be considered. First of all, they are not the same quantity and, as reported by Petzold et al. (2013), they can differ by a factor of 7 and depend on the assumed MAC (for optical measurements) and the thermal protocol for EC/OC analysis. As EC is the only component which is at the limit of detection, we decided

to not report this component in the new figure 8 (EC is also not important in the discussion reported in section 3.2.4 in relation to DNG profiles).

Most important, it has to be considered that vertical profile data are “quasi instantaneous” while the reported chemical composition was determined with the time resolution of 24 h for ionic species and 96 h for EC/OC. In this respect, the chemical speciation and in particular the sulfate content was only used along the paper to support the secondary origin of the ground-based concentration peak of N_{14-260} in DNG profiles. For this purpose, the chemical composition was coupled with information coming from the vertical profiles, the SMPS data and the meteorological parameters.

All the aforementioned observations underline the reliability of the whole dataset used in the paper, and therefore we absolutely reject the statement that these data appear non-realistic.

Conc (ng m ⁻³)	HO		PG		NG		DNG		Detection Limit
	mean	σ_m	mean	σ_m	mean	σ_m	mean	σ_m	
Na⁺	410.85	252.44	655.24	293.67	590.94	192.18	325.71	84.23	0.04
NH₄⁺	66.33	13.85	74.61	12.22	85.04	15.89	128.31	29.21	0.4
K⁺	21.73	8.43	28.81	9.50	27.34	5.98	23.94	2.40	0.04
Mg²⁺	54.21	27.28	79.34	31.70	73.35	20.50	51.21	13.16	0.04
Ca²⁺	39.45	7.67	43.28	7.07	38.88	4.71	33.45	3.17	0.04
Cl⁻	495.82	332.03	871.20	392.54	745.67	267.28	357.20	173.05	0.04
NO₂⁻	22.51	10.00	36.00	15.66	31.43	11.98	20.06	2.33	0.04
NO₃⁻	59.92	12.96	68.66	12.22	51.64	9.59	49.37	15.90	0.04
SO₄²⁻	504.71	93.15	584.69	72.69	779.09	204.18	1441.91	354.09	0.04
Oxalates	4.79	0.98	5.46	0.54	4.99	0.50	6.97	1.12	0.4
F⁻	0.18	0.08	0.21	0.13	0.07	0.09	<DL	<DL	0.004
Glycolate	1.16	0.16	1.29	0.29	1.05	0.14	1.27	0.19	0.4
Formate	2.15	0.70	2.92	0.68	2.99	0.47	2.78	0.38	0.4
MSA	2.28	0.58	4.47	1.07	3.57	0.81	1.84	0.36	0.04
EC	<DL	<DL	<DL	<DL	<DL	<DL	31.85	0.20	11
OC	534.36	39.52	522.87	52.69	517.13	43.96	689.94	19.59	120

Table AGC5.1. Ambient concentrations (ng m⁻³) of the aerosol chemical components (mean±mean standard deviation) and their analytical detection limits (DL).

References:

1. Andreae, M.O and Gelencsér A.: *Black carbon or brown carbon? The nature of light-absorbing carbonaceous aerosols*, *Atmos. Chem. Phys.*, 6, 3131–3148, 2006.
2. Barrie, L. A., and Hoff, R. M.: *Five years of air chemistry observations in the Arctic*, *Atmos. Environ.*, 19, 1995–2010, 1985.
3. Becagli, S., Scarchilli, C., Traversi, R., Dayan, U., Severi, M., Frosini, D., Vitale, V., Mazzola, M., Lupi, A., Nava, S., Udisti, R.: *Study of present-day sources and transport processes affecting oxidised sulphur compounds in atmospheric aerosols at Dome C (Antarctica) from year-round sampling campaigns*, *Atmos. Environ.*, 52, 98–108, 2012.
4. Bikkina, S., Sarin, M.M.: *Light absorbing organic aerosols (brown carbon) over the tropical Indian Ocean: impact of biomass burning emissions*, *Environ. Res. Lett.*, 8 (4), 044042, 2013.
5. Bond, T. C., Doherty, S. J., Fahey, D. W., Forster, P. M., Berntsen, T., Deangelo, B. J., Flanner, M. G., Ghan, S., Kärcher, B., Koch, D., Kinne, S., Kondo, Y. and Quinn, P. K.: *Bounding the role of black carbon in the climate system: A scientific assessment*, *J. Geophys. Res.*, 118, 1–173, doi:10.1002/jgrd.50171, 2013.
6. Brock, C. A., Radke, L.F., Lyons, J. H., and Hobbs, P. V. : *Arctic hazes in summer over Greenland and the North American Arctic, I, Incidence and origins*, *J. Atmos. Chem.* 9, 129–148, 1989.
7. Brock, C.A., J. Cozic, R. Bahreini, K.D. Froyd, A.M. Middlebrook, A. McComiskey, J. Brioude, O.R. Cooper, A. Stohl, K.C. Aikin, J.A. De Gouw, D.W. Fahey, R.A. Ferrare, R.-S. Gao, W. Gore, J. Holloway, G. Hubler, A. Jefferson, D.A. Lack, S. Lance, R.H. Moore, D.M. Murphy, A. Nenes, P.C. Novelli, J.B. Nowak, J.A. Ogren, J. Peischl, R.B. Pierce, P. Pilewski, P.K. Quinn, T.B. Ryerson, K.S. Schmidt, J.P. Schwarz, H. Sodemann, J.R. Spackman, H. Stark, D.S. Thomson, T. Thornberry, P. Veres, L.A. Watts, C. Warneke and A.G. Wollny.: *Characteristics, sources, and transport of aerosols measured in spring 2008 during the aerosol, radiation, and cloud processes affecting Arctic climate (ARCPAC) project*, *Atmospheric Chemistry and Physics*, 11:2423–2453, 2011.
8. Browse, J., Carslaw, K.S., Arnold, S., Pringle, K.J. and Boucher O.: *The scavenging processes controlling the seasonal cycle in Arctic sulphate and black carbon aerosol*, *Atmos. Chem. Phys.*, 12, 6775–6798, 2012.
9. Corbett, J. J., Lack, D. a., Winebrake, J. J., Harder, S., Silberman, J. a. and Gold, M.: *Arctic shipping emissions inventories and future scenarios*, *Atmospheric Chemistry and Physics*, 10(19), 9689–9704, doi:10.5194/acp-10-9689-2010, 2010.
10. Drinovec, L., Močnik, G., Zotter, P., Prévôt, A. S. H., Ruckstuhl, C., Coz, E., Rupakheti, M., Sciare, J., Müller, T., Wiedensohler, A., and Hansen, A. D. A.: *The "dual-spot" Aethalometer: an improved measurement of aerosol black carbon with real-time loading compensation*, *Atmos. Meas. Tech.*, 8, 1965–1979, doi: 10.5194/amt-8-1965-2015, 2015.
11. Eckhardt, S., Hermansen, O., Grythe, H., Fiebig, M., Stebel, K., Cassiani, M., Baecklund, a. and Stohl, a.: *The influence of cruise ship emissions on air pollution in Svalbard – a harbinger of a more polluted Arctic?*, *Atmospheric Chemistry and Physics*, 13(16), 8401–8409, doi:10.5194/acp-13-8401-2013, 2013.
12. Eleftheriadis, K., Vratolis, S. and Nyeki, S.: *Aerosol black carbon in the European Arctic: Measurements at Zeppelin station, Ny-Ålesund, Svalbard from 1998–2007*, *Geophysical Research Letters*, 36(2), doi:10.1029/2008GL035741, 2009.
13. Engvall, A.-C., Krejci, R., Ström, J., Minikin, A., Treffeisen, R., Stohl, A. and Herber, A.: *In-situ airborne observations of the microphysical properties of the Arctic tropospheric aerosol during late spring and summer*, *Tellus B*, 080414161623888–???, doi:10.1111/j.1600-0889.2008.00348.x, 2008b.
14. Ferrero, L., Mocnik, G., Ferrini, B. S., Perrone, M. G., Sangiorgi, G. and Bolzacchini, E.: *Vertical profiles of aerosol absorption coefficient from micro-Aethalometer data and Mie*

- calculation over Milan., *Sci. Total Environ.*, 409(14), 2824–37, doi:10.1016/j.scitotenv.2011.04.022, 2011.
15. Giardi, F., Becagli, S., Traversi, R., Frosini, D., Severi, M., Caiazzo, L., Ancillotti, C., Cappelletti, D., Moroni, B., Grotti, M., Bazzano, A., Lupi, A., Mazzola, M., Vitale, V., Malandrino, M., Ferrero, L., Bolzacchini, E., Viola, A., Udisti, R.: Size distribution and ion composition of aerosol collected at Ny Ålesund in the spring-summer field campaign 2013. *Rend. Lincei*, DOI 10.1007/s12210-016-0529-3, 2016.
 16. Gilardoni, S., Vignati, E., Wilson J.: Using measurements for evaluation of black carbon modeling, *Atmos. Chem. Phys.*, 11, 439–455, 2011.
 17. Hansen, A.D.A., and T. Novakov.: Aerosol black carbon measurements in the Arctic haze during AGASP-II, *J. Atmos. Chem.*, 9, 347–361, doi:10.1007/BF00052842, 1989.
 18. IPCC, 2013: *Climate Change 2013: The Physical Science Basis*. Cambridge University Press, Cambridge, United Kingdom and New York, USA, 2013.
 19. Jacob, D.J., Crawford, J.H., Maring, H., Clarke, A.D., Dibb, J.E., Emmons, L.K., Ferrare, R.A., Hostetler, C.A., Russell, P.B., Singh, H.B., Thompson, A.M., Shaw, G.E., McCauley, E., Pederson, J.R. and J. A. Fisher.: The Arctic Research of the Composition of the Troposphere from Aircraft and Satellites (ARCTAS) mission: design, execution, and first results, *Atmos. Chem. Phys.*, 10, 5191–5212, 2010.
 20. Kaufman, Y.J., Tanré, D., Boucher, O.: A satellite view of aerosols in the climate system. *Nature*, 419, 215–223, 2002.
 21. Koch, D., Schulz, M., Kinne, S., Mcnaughton, C., Spackman, J. R., Balkanski, Y., Bauer, S. and Berntsen, T, et al.: Evaluation of black carbon estimations in global aerosol models, *Atmos. Chem. Phys.*, 9, 9001–9026, 2009.
 22. Koren, I., Kaufman, Y.J., Remer, L.A., Martins, J.V.: Measurements of the effect of amazon smoke on inhibition of cloud formation. *Scienze*, 303, 1342–1345, 2004.
 23. Koren, I., Martins, J.V., Remer, L.A., Afargan, H.: Smoke invigoration versus inhibition of clouds over the amazon, *Science*, 321, 946–949, 2008.
 24. Kupiszewski, P., Leck, C., Tjernström, M., Sjogren, S., Sedlar, J., Graus, M., Müller, M., Brooks, B., Swietlicki, E., Norris, S. and Hansel, a.: Vertical profiling of aerosol particles and trace gases over the central Arctic Ocean during summer, *Atmospheric Chemistry and Physics*, 13(24), 12405–12431, doi:10.5194/acp-13-12405-2013, 2013.
 25. Massabò, D., Caponi, L., Bernardoni, V., Bove, M.C., Brotto, P., Calzolari, G., Cassola, F., Chiari, M., Fedi, M.E., Fermo, P., Giannoni, M., Lucarelli, F., Nava, S., Piazzalunga, A., Valli, G., Vecchi, R., Prati, P.: Multi-wavelength optical determination of black and brown carbon in atmospheric aerosols, *Atmos. Environ.*, 108, 1–12, 2015.
 26. Maturilli, M. and Kayser M.: Arctic Warming, Moisture Increase and Circulation Changes Observed in the Ny-Ålesund Homogenized Radiosonde Record. *Theor. Appl. Climatol.* doi: 10.1007/s00704-016-1864-0, 2016.
 27. Petzold, A., Ogren, J.A., Fiebig, M., Laj, P., Li, S.M., Baltensperger, U., Holzer-Popp, T., Kinne, S., Pappalardo, G., Sugimoto, N., Wehrli, C., Wiedensohler, A., Zhang, X.Y.: Recommendations for reporting “black carbon” measurements, *Atmos. Chem. Phys.*, 13, 8365–8379, 2013.
 28. Quinn, P. K., Bates, T. S., Baum, E., Doubleday, N., Fiore, a. M., Flanner, M., Fridlind, a., Garrett, T. J., Koch, D., Menon, S., Shindell, D., Stohl, a. and Warren, S. G.: Short-lived pollutants in the Arctic: their climate impact and possible mitigation strategies, *Atmospheric Chemistry and Physics*, 8(6), 1723–1735, doi:10.5194/acp-8-1723-2008, 2008.
 29. Radke, L. F., Lyons, J. H., Hegg, D. A., Hobbs, P. V., and Bailey, I. H.: Airborne observations of Arctic aerosols, I, Characteristics of Arctic haze, *Geophys. Res. Lett.*, 11, 393–396, 1984.

30. Ramanathan, V. and Feng, Y.: *Air pollution, greenhouse gases and climate change: Global and regional perspectives*, *Atmos. Environ.*, 43(1), 37–50, doi:10.1016/j.atmosenv.2008.09.063, 2009.
31. Ran, L., Deng, Z.Z., Xu, X.B., Yan, P., Lin, W.L., Wang, Y., Tian, P., Wang, P.C., Pan, W.L. and Lu, D.R.: *Vertical profiles of black carbon measured by a micro-aethalometer in summer in the North China Plain*, *Atmos. Chem. Phys. Discuss.*, doi:10.5194/acp-2016-219, 2016.
32. Riccobono, F., Schobesberger, S., Scott, C. E., Dommen, J., Ortega, I. K., Rondo, L., Almeida, J., Amorim, A., Bianchi, F., Breitenlechner, M., David, A., Downard, A., Dunne, E. M., Duplissy, J., Ehrhart, S., Flagan, R. C., Franchin, A., Hansel, A., Junninen, H., Kajos, M., Keskinen, H., Kupc, A., Kurten, A., Kvashin, A. N., Laaksonen, A., Lehtipalo, K., Makhmutov, V., Mathot, S., Nieminen, T., Onnela, A., Petaja, T., Praplan, A. P., Santos, F. D., Schallhart, S., Seinfeld, J. H., Sipila, M., Spracklen, D. V., Stozhkov, Y., Stratmann, F., Tome, A., Tsagkogeorgas, G., Vaattovaara, P., Viisanen, Y., Vrtala, A., Wagner, P. E., Weingartner, E., Wex, H., Wimmer, D., Carslaw, K. S., Curtius, J., Donahue, N. M., Kirkby, J., Kulmala, M., Worsnop, D. R. and Baltensperger, U.: (Suppl.) *Oxidation Products of Biogenic Emissions Contribute to Nucleation of Atmospheric Particles*, *Science*, 344(6185), 717–721, doi:10.1126/science.1243527, 2014.
33. Sandradewi, J., Prevot, A.H., Szidat, S., Perron, N., Rami Alfarra, M., Lanz, V., Weingartner, E., Baltensperger, U.: *Using aerosol light absorption measurements for the quantitative determination of Wood burning and traffic emission contributions to particulate matter*, *Environ. Sci. Technol.* 42, 3316–3323, 2008.
34. Schwarz, J. P., Spackman, J. R., Gao, R. S., Watts, L. a., Stier, P., Schulz, M., Davis, S. M., Wofsy, S. C. and Fahey, D. W.: *Global-scale black carbon profiles observed in the remote atmosphere and compared to models*, *Geophysical Research Letters*, 37(18), n/a–n/a, doi:10.1029/2010GL044372, 2010.
35. Schwarz, J. P., Spackman, J. R., Gao, R. S., Watts, L. a., Stier, P., Schulz, M., Davis, S. M., Wofsy, S. C. and Fahey, D. W.: *Global-scale black carbon profiles observed in the remote atmosphere and compared to models*, *Geophysical Research Letters*, 37(18), n/a–n/a, doi:10.1029/2010GL044372, 2010.
36. Schwarz, J.P., Samset, B.H., Perring, A.E., Spackman, J.R., Gao, R.S., Stier, P., Schultz, M.G., Moore, F.L., Ray, E.A. and Fahey, D.W.: *Global-scale seasonally resolved black carbon vertical profiles over the Pacific*, *Geophysical Research Letters*, 40, 5542–5547, 2013.
37. Shamjad, P.M., Tripathi, S.N., Pathak, R., Hallquist, M., Arola, A., and Bergin M.H.: *Contribution of Brown Carbon to Direct Radiative Forcing over the Indo-Gangetic Plain*, *Environ. Sci. Technol.*, 49, 10474–10481, 2015.
38. Shaw, G. E: *The Arctic haze phenomenon*, *BAMS*, 2403–2413, 1995.
39. Stohl, A., Klimont, Z., Eckhardt, S., Kupiainen, K., Shevchenko, V.P., Kopeikin, V.M. and Novigatsky, A.N.: *Black carbon in the Arctic: the underestimated role of gas flaring and residential combustion emissions*, *Atmos. Chem. Phys.*, 13, 8833–8855, 2013.
40. Stohl, A.: *Characteristics of atmospheric transport into the Arctic troposphere*, *J. Geophys. Res.*, 111, D11306, doi:10.1029/2005JD006888, 2006.
41. Stone, R.S., A. Herber, V. Vitale, M. Mazzola, A. Lupi, R.C. Schnell, E.G. Dutton, P.S.K. Liu, S.M. Li, K. Dethloff, A. Lampert, C. Ritter, M. Stock, R., Neuber and M. Maturilli.: *A three-dimensional characterization of Arctic aerosols from airborne Sun photometer observations: PAMARCMIP, April 2009*, *Journal of Geophysical Research: Atmospheres*, 115, doi 10.1029/2009jd013605, 2010.
42. Ström J., Umegard, J., Tørseth, K., Tunved, P., Hansson, H.C., Holmen, K., Wismann, V., Herber, A., König-Langlo, G.: *One year of particle size distribution and aerosol chemical*

- composition measurements at the Zeppelin Station, Svalbard, March 2000–March 2001, Phys. Chem. Earth, 28, 1181–1190, 2003.*
43. Ström, J., Engvall, A.-C., Delbart, F., Krejci, R. and Treffeisen, R.: *On small particles in the Arctic summer boundary layer: observations at two different heights near Ny-Ålesund, Svalbard, Tellus B, 61(2), 473–482, doi:10.1111/j.1600-0889.2008.00412.x, 2009.*
 44. Tunved, P., Ström, J. and Krejci, R.: *Arctic aerosol life cycle: linking aerosol size distributions observed between 2000 and 2010 with air mass transport and precipitation at Zeppelin station, Ny-Ålesund, Svalbard, Atmospheric Chemistry and Physics, 13(7), 3643–3660, doi:10.5194/acp-13-3643-2013, 2013.*
 45. Udisti R., Bazzano A., Becagli S., Bolzacchini E., Caiazza L., Cappelletti D., Ferrero L., Frosini D., Giardi F., Grotti M., Lupi A., Malandrino M., Mazzola M., Moroni B., Severi M., Traversi R., Viola A., Vitale V.: *Sulfate source apportionment in the Ny-Ålesund (Svalbard Islands) Arctic aerosol. Rendiconti Lincei. DOI 10.1007/s12210-016-0517-7, 2016.*
 46. Udisti, R., Dayan, U., Becagli, S., Busetto, M., Frosini, D., Legrand, M., Lucarelli, F., Preunkert, S., Severi, M., Traversi, R., Vitale, V.: *Sea-spray aerosol in central Antarctica. Present atmospheric behavior and implications for paleoclimatic reconstructions. Atmos. Environ., 52, 109–120, 2012.*
 47. Vihma, T., Kilpeläinen, T., Manninen, M., Sjöblom, A., Jakobson, E., Palo, T., Jaagus, J., Maturilli, M.: *Characteristics of temperature and humidity inversions and low-level jets over Svalbard fjords in spring, Adv. Met., 2011:ID486807, doi: 10.1155/2011/486807, 2011.*
 48. Weingartner, E., Saathoff, H., Schnaiter, M., Streit, N., Bitnar, B. and Baltensperger, U.: *Absorption of light by soot particles: determination of the absorption coefficient by means of aethalometers, J. Aerosol Sci., 34(10), 1445–1463, doi:10.1016/S0021-8502(03)00359-8, 2003.*
 49. Wofsy, S.C., et al.: *HIAPER Pole-to-Pole Observations (HIPPO): fine grained, global-scale measurements of climatically important atmospheric gases and aerosols. Philosophical Transactions of the Royal Society, 369, 2073–2086, 2011.*
 50. Zangrando, R., Barbaro, E., Zennaro, P., Rossi, S., Kehrwald, N. M., Gabrieli, J., Barbante, C. and Gambaro, A.: *Molecular markers of biomass burning in Arctic aerosols, Environmental Science and Technology, 47(15), 8565–8574, doi:10.1021/es400125r, 2013.*

Vertical profiles of aerosol and black carbon in the Arctic: a seasonal phenomenology along two years (2011-2012) of field campaigns

5 Luca Ferrero¹, David Cappelletti^{2,3}, Maurizio Busetto³, Mauro Mazzola³, Angelo Lupi³,
Christian Lanconelli⁴, Silvia Becagli⁵, Rita Traversi⁵, Laura Caiazzo⁵, Fabio Giardi⁵, Beatrice
Moroni², Stefano Crocchianti², Martin Fierz⁶, Griša Močnik^{7,8}, Giorgia Sangiorgi¹, Maria G.
Perrone¹, Marion Maturilli⁹ and Vito Vitale³, Roberto Udisti⁵, Ezio Bolzacchini¹

10 ¹Department of Earth and Environmental Sciences, University of Milano-Bicocca, Piazza della Scienza 1, 20126,
Milano, Italy

²Department of Chemistry, Biology and Biotechnology, University of Perugia, 06123 Perugia, Italy

³Institute of Atmospheric Sciences and Climate, CNR-ISAC, Via Gobetti 101, 40129, Bologna, Italy

⁴European Commission, Joint Research Centre (JRC), Institute for Environment & Sustainability, via E. Fermi,
2749 - 21027 Ispra (VA), Italy

15 ⁵University of Florence, Via della Lastruccia 3, 50019, Sesto Fiorentino, Florence Italy

⁶University of Applied Sciences Northwestern, Switzerland, Windisch, Switzerland

⁷Aerosol d.o.o., Kamniska 41, SI-1000 Ljubljana, Slovenia

⁸Condensed Matter Physics Department, Jozef Stefan Institute, Jamova 39, SI-1000 Ljubljana, Slovenia

20 ⁹Alfred Wegener Institute, Helmholtz Centre for Polar and Marine Research, Telegraphenberg 43A, 14473
Potsdam, Germany.

Correspondence to: Luca Ferrero (luca.ferrero@unimib.it)

25 **Abstract.** We present results from a systematic study of vertical profiles of aerosol number size distribution and
black carbon (BC) concentrations conducted in the Arctic, over Ny-Ålesund (Svalbard). The campaign lasted 2
years (2011-2012) and resulted in 200 vertical profiles measured **by means of a tethered balloon (up to 1200 m
AGL)** during the spring and summer seasons. In addition, chemical analysis of filter samples, aerosol size
distribution and a full set of meteorological parameters were determined at ground. The collected experimental
30 data allowed a classification of the vertical profiles into different typologies, which allowed us to describe the
seasonal phenomenology of vertical aerosol properties in the Arctic.

During spring, four main types of profiles were found and their behaviour was related to the main aerosol and
atmospheric dynamics occurring at the measuring site. Background conditions generated homogenous profiles.
Transport events caused an increase of aerosol concentration with altitude. High Arctic haze pollution trapped
below thermal inversions promoted a decrease of aerosol concentration with altitude. Finally, ground-based
35 plumes of locally formed secondary aerosol determined profiles with decreasing aerosol concentration located at
different altitude as a function of size.

During the summer season, the impact from shipping caused aerosol and BC pollution plumes constrained close to the ground, indicating that increasing shipping emissions in the Arctic could bring anthropogenic aerosol and BC in the summer Arctic affecting the climate.

5 1 Introduction

The Arctic is subject to an amplification of the global warming, as the observed temperature increase has been almost twice than the global average (IPCC, 2013; Serreze and Barry, 2011; Shindell and Faluvegi, 2009). This resulted in the first complete opening of the Northwest Passage in 2007 (Serreze et al., 2007) together with a greening of the coastal tundra (Bhatt et al., 2010) and altered wind patterns (Overland and Wang, 2010). The “Arctic amplification” is the result of complex global feedbacks (acting at different spatial and temporal scales): the impact of sea ice changes on the heat fluxes between the ocean and the atmosphere (Screen and Simmonds, 2010a and 2010b), the effect of changes in the cloud cover and water vapor on the longwave radiation fluxes (Francis and Hunter, 2006), the changes in atmospheric and oceanic heat transports (Yang et al., 2010), the black carbon (BC) deposition on the snow (Hansen and Nazarenko, 2004), and the changes in the atmospheric BC and aerosol concentrations themselves (Flanner, 2013; Serreze and Barry, 2011; Shindell and Faluvegi, 2009). Many of these processes depend on aerosol absorption and scattering of the solar radiation (direct effect). Additionally, indirect effects play an important role as the aerosols seed and modify the cloud properties. Lastly, light absorption by BC can alter the atmospheric thermal structure within, below, or above clouds consequently affecting cloud distributions (IPCC, 2013; Bond et al., 2013; Ramanathan and Feng, 2009; Koren et al. 2008; Koren et al., 2004; Kaufman et al., 2002). Shindell and Faluvegi (2009) estimated that globally the decreasing concentrations of sulfate aerosols and the increasing concentrations of BC contributed (during 1976–2007) with 1.09 ± 0.81 °C to the Arctic surface temperature increase of 1.48 ± 0.28 °C.

Aerosol particles are short-lived pollutants (~one-few weeks of residence time) and act as short-lived climate forcers; thus, their effect could be employed in short-term climate strategies (Ødemark et al., 2012; Shindell et al., 2012; Jacobson, 2010; Quinn et al., 2008). To adopt the right mitigation strategies, key scientific issues in the study of Arctic aerosols has to be solved. They include the identification of the relative importance of long-range advection with respect to local emissions (Flanner, 2013; Sand et al., 2013; Shindell and Faluvegi, 2009). Most important, the seasonal characterization of the aerosol vertical structure, a very poorly determined piece of information, is required.

Indeed, the aerosol properties (size distribution, chemical composition, optical properties) in the Arctic exhibit a pronounced seasonal variation due to an interplay of dominating sources (outside or inside the Arctic region) with meteorological conditions that allow or inhibit the transport from source regions (Quinn et al., 2008; Eckhardt et al., 2003). The spring period is characterized by the presence of the Arctic Haze dominated by the accumulation mode aerosol (enriched in BC). During the Arctic Haze, an inflow of pollution (aerosol and gases) from northern mid-latitudes (during winter-spring) results in a reduction in visibility (Jacob et al., 2010; Sthol et al., 2006; Radke et al., 1984; Barrie and Hoff, 1985; Brock et al., 1989; Shaw, 1995). The Arctic Haze occurs under meteorological conditions with stable stratifications and the frequent and persistent occurrences of surface-based inversions. According to Stohl et al. (2006), within these conditions, the air pollution can be transported into the Arctic at low-level (followed by ascent in the Arctic or low-level alone) or with an uplift outside the Arctic, followed by descent

in the Arctic itself. The summer period is dominated by fresh Aitken particles, locally formed, with a negligible BC content (Tunved et al., 2013; Spackman et al., 2010; Eleftheriadis et al., 2009; Ström et al., 2003 and 2009; Udisti et al., 2013; Viola et al., 2013).

In addition to the aforementioned seasonality, the same type of aerosol can produce different climatic effects (warming or cooling) and local feedbacks (snow/ice-albedo, clouds) depending on its vertical location (Flanner, 2013; Sand et al., 2013; Shindell and Faluvegi, 2009). For example, it is well known that BC aerosol absorbs solar radiation and heats the surrounding air (Ferrero et al., 2014 and 2011a; Samset et al., 2014; Samset et al., 2013; Ramana et al., 2007). The surface temperature response varies considerably with the altitude of the induced heating. BC may potentially warm the Arctic if it is located immediately above snow and ice while it has a cooling effect, if it is located in the free troposphere. In the latter case, BC may reduce the surface air temperature and promote the increase in the sea-ice fraction (Flanner, 2013; Brock et al., 2011; Seinfeld and Pandis, 2006; Hansen and Nazarenko, 2004). The latter phenomenon results from a combination of the weakening of the northward heat transport (due to a reduction in the meridional temperature gradient) and the increasing of atmospheric stability (caused by the contemporary dimming of the surface and heating aloft) which turns into a reduction of the downward sensible heat flux (Flanner, 2013; Sand et al., 2013; Shindell and Faluvegi, 2009).

In addition to the vertical distribution of BC, that of the total aerosol particles is important; it can influence the indirect effect and the related feedbacks. Changes in the cloud cover (especially low-level Arctic stratus) increase the downward longwave flux to the surface in function of the cloud base temperature and cloud phase (liquid, mixed or ice) (Serreze and Barry, 2011; Francis and Hunter, 2006). Low clouds mainly warm the surface in the Arctic (with the exception of a brief period in summer) (Vavrus et al., 2009; Intrieri et al., 2002) due to the stable stratified conditions that often prevail in the Arctic (Manabe and Wetherald, 1975). Because the highest number density of aerosol particles observed in the Arctic is due to a locally formed aerosol (mainly in summer as stated above) (Tunved et al., 2013; Engvall et al., 2008; Ström et al., 2003) it is important to assess the vertical behavior of the aerosol concentration in function of its size and the season.

It is therefore necessary to measure the vertical profiles in the Arctic.

At this purpose, several field campaigns have been performed in the Arctic in recent years with the aim to characterize aerosol properties along the vertical direction.

The ARCTAS mission (Jacob et al., 2010 and reference therein) showed highly-layered air pollution transport from North America and East Asia in spring, characterized by anthropogenic aerosol below 2 km and by biomass burning in the 2–4 km layer. The ARCPAC campaign (Brock et al. 2011) grouped the aerosol affecting the Arctic in spring in four categories: background troposphere (relatively diffuse, sulfate-rich aerosol); depleted aerosol within the surface inversion layer over sea-ice; layers of organic-rich biomass burning aerosol (above the top of the inversion layer) (see also Warneke et al., 2010) and layers dominated by fossil fuel combustion. The ASTAR campaign (Engvall et al., 2008), focussed on the spring to summer transition period in Svalbard, found Aitken and accumulation mode particles more concentrated in the free troposphere compared to the boundary layer. Kupiszewski et al. (2013), reported new particle formation events in the near-surface layer (possibly related to biological processes) during the summer ASCOS campaign.

Considering the BC, the springtime, PAM-ARCMIP (Stone et al., 2010) and HIPPO (Schwarz et al., 2010) campaigns showed high BC concentrations close to the ground, below the thermal inversion, but also dense pollution and BC at high altitudes over the Arctic (Wofsy et al., 2011). Interestingly, the PAM-ARCMIP results

show a decrease of BC compared to past measurements (i.e. AGASP, Hansen and Novakov, 1989). In addition, the HIPPO campaign revealed that in the lower troposphere the BC vertical gradient can change seasonally from positive to negative (Schwarz et al., 2013). In this respect, Spackman et al. (2010) and Koch et al. (2009) reported BC located mainly in the Arctic free troposphere with a positive gradient in the lower troposphere.

5 The aforementioned campaigns were conducted mainly using aircraft (or helicopters) that for their inner nature are limited to intensive observational periods (Kupiszewski et al., 2013; Bates et al., 2013; Spackman et al., 2010; Schwarz et al., 2010; Koch et al., 2009). Thus, aerosol vertical profiles in the Arctic appear scarce if compared with the number of available data collected at ground level (Samset et al., 2013; Koch et al., 2009). There is the need for regular vertical aerosol profiling campaigns to improve the description of a seasonally resolved aerosol and BC vertical behavior.

10 In addition to this, aerosol vertical distribution could be affected in the future by changes in the aerosol emissions within the Arctic itself. The increasing of shipping emission in the Arctic is a good example. Shipping emissions inject the BC directly into the Arctic planetary boundary layer (probably warming the surface and depositing on snow and ice). The importance of the increasing shipping emission in the Arctic has been recently underlined (Eckhardt et al., 2013; Corbett et al., 2010; Granier et al., 2006). Although the final impact is debated (Browse et al., 2013), the effective vertical distribution of these emissions has not yet been investigated.

Thus, there is a clear need to also improve the knowledge about aerosol vertical profiles in the Arctic during week-long campaigns along years to find common rules of behavior.

20 The Arctic site of Ny-Ålesund (Svalbard Islands) is particularly suitable for such measurements, featuring long term data series of ground based aerosol properties, lidar profiles, radiometric and meteorological data (Maturilli et al. 2015; Tunved et al., 2013; Di Liberto et al., 2012; Vihma et al., 2011; Hoffmann et al., 2009; Eleftheriadis et al., 2009; Eleftheriadis et al., 2004; Stock et al., 2012; Ström et al., 2003, 2009). Long-term upper-air observations by daily radiosondes provided an overview of the atmospheric vertical structure above Ny-Ålesund, including the Planetary Boundary Layer (PBL) altitude range (Maturilli and Kayser, 2016; Vihma et al., 2011). In this climatological approach, stable atmospheric conditions, radiative surface-based inversion were frequently found during polar night conditions, indicating stable atmospheric conditions with suppressed vertical exchange. Once the snowmelt leads to considerable sensible and latent heat fluxes at the surface, atmospheric stratification becomes neutral or instable, allowing convection and vertical mixing.

25 These observations point towards the need to understand how the aerosol is vertically layered in function of the meteorological changes along seasons. Despite this, as stated above, aerosol and BC measurements along vertical profiles are reported to be sparse, even recent UAVs applications could improve the available datasets (Bates et al., 2013).

30 Thus, this paper reports new data of aerosol and BC vertical profiles measured over Ny-Ålesund (Svalbard Islands) in two successive years (2011-2012) during an extensive field campaign (200 vertical profiles). Vertical profiles measurements were conducted in the framework of the PRIN2009 “ARCTICA” project. The main part of the scientific activities at Ny-Ålesund was aimed at studying the chemical and physical properties of the aerosols and the long-range transport processes relevant for the measurements of organic and inorganic species at the site and along vertical profiles (Moroni et al., 2015; Udisti et al., 2013).

35 We describe first the sampling sites and the vertical profile measurements (section 2). Results and discussion follow in section 3, with the conclusions in the final section 4.

2 Methodology

Tethered balloon soundings were carried out during spring 2011 and two summers 2011 and 2012 over Ny-Ålesund. The site is located at the Kongsfjorden, a fjord that develops in the north-west south-east direction. Northwards, Ny-Ålesund faces the sea, while a small chain of 400-500 m high mountains is located to the South (Figure 1a).

Vertical profiles were measured from two sampling sites: during spring, the vertical profiles were taken at the Italian CNR Gruvebadet sampling site (78°55'03"N 11°53'40"E; Figure 1b) to assure a large distance to the Ny-Ålesund village. During summer, the tethered balloon measurements were operated at the German-French AWIPEV research base (78°55'24" N 11°55'15"E) to lie in the proximity of the Ny-Ålesund harbour (600 m) allowing the measurement of ship plume diffusion (section 3.3). Table 1 lists the dates of the campaign (25 measurement days), the number of flights (197 measured profiles), the maximum altitudes (~700-1300 m), and the cloud base height (clouds present for 48% of campaign). The aerosol and meteorological measurements were carried out both at ground and along the profiles as described in the following sections.

2.1 Ground-based measurements

Ground-based measurements were carried out at the Gruvebadet laboratory (Figure 1b) where the distance (1.2 km southern Ny-Ålesund) and the limitations established for snow mobile traffic and other potentially contaminant activities limits the impact from local emissions.

The Gruvebadet laboratory is equipped with a series of instruments aimed at measuring aerosol physical and optical properties, and to collect samples for chemical analysis (section 2.1.1). The aerosol size distribution was measured using a Scanning Mobility Particle Sizer (TSI-SMPS 3034, 54 size classes, 10–487 nm) coupled with an Aerodynamic Particle Sizer (TSI-APS 3321, 52 classes, 0.5–20 μm). The two coupled systems measure one size spectrum every 10 minutes (Giardi et al, 2016). PM samples were collected by high-volume and low-volume samplers. For the purpose of the present paper, PM₁₀ samples collected using two TECORA SkyPost low-volume sampler (EN 12341; PM₁₀ sampling head, flow 2.3 m³ h⁻¹; PTFE and quartz microfiber filters, Ø=47 mm) were considered. Sampling was carried out in ambient conditions: pressure and temperature were continuously monitored in order to maintain the constant flow rate of 2.3 m³ h⁻¹. The first sampler collected PM₁₀ for 24 h on Teflon filters (Pall R2PJ047) to determine the ionic fraction, while the second one collected PM₁₀ for 96 h on pre-fired Quartz microfiber filters (chm QF1 grade) to determine organic and elemental carbon (section 2.1.1). The Teflon filters were conditioned for 48 hours (25°C and 50% relative humidity) before and after the sampling, then weighted by a 5-digit microbalance (Sartorius ME235P). The reproducibility error for filter weighing was lower than 5% (experimentally evaluated). After sampling, filters were individually sealed in pre-washed (with Milli-Q water, 18.3 MΩ cm) polystyrene filter containers and stored at –20°C until analysis.

2.1.1 Aerosol chemistry measurements at ground level

PM₁₀ samples collected at ground-level at Gruvebadet were analyzed to determine first the water-soluble ionic fraction. Half of each PM₁₀ Teflon filter was extracted in 10 ml of ultrapure water (Milli-Q, 18.3 MΩ cm resistivity) by ultrasonic bath for 20 min. Filters manipulation was carried out under a class-100 laminar-flow hood, in order to minimize contamination risks. Inorganic cations and anions together with organic anions, were simultaneously

measured by a triple Dionex ion-chromatography system, equipped with electrochemical-suppressed conductivity detectors. Cations (Na^+ , NH_4^+ , K^+ , Mg^{2+} and Ca^{2+}) have been determined by a Dionex CS12A-4 mm analytical column with 20 mM H_2SO_4 eluent. Anions (Cl^- , NO_3^- , SO_4^{2-} and $\text{C}_2\text{O}_4^{2-}$) were measured by a Dionex AS4A-4 mm analytical column with a 1.8 mM Na_2CO_3 / 1.7 mM NaHCO_3 eluent, while F^- and some organic anions (acetate, glycolate, formate and methanesulfonate) were determined by a Dionex AS11 separation column by a gradient elution (0.075 mM to 2.5 mM $\text{Na}_2\text{B}_4\text{O}_7$ eluent) (Udisti et al., 2004; Becagli et al., 2011).

The detection limit (ng m^{-3}) of each analyzed chemical component is reported in the supplemental material (Table S1) together with the measured ambient ion concentrations. All the analyzed chemical components were largely above the detection limit.

The contribution of sea salt and crustal components in Ny-Ålesund is not-negligible (Udisti et al., 2016; Giardi et al., 2016; Moroni et al., 2015). Thus, Na^+ , Ca^{2+} and SO_4^{2-} (which originate from both these sources) were apportioned between sea-salt (ss-) and non-sea-salt (nss-) fractions on the basis of known w/w (weight/weight) ratios in sea water and Earth crust (Udisti et al., 2016; Giardi et al., 2016; Becagli et al., 2012; Udisti et al., 2012):

$$\text{tot-Na}^+ = \text{ss-Na}^+ + \text{nss-Na}^+ \quad (1)$$

$$\text{tot-Ca}^{2+} = \text{ss-Ca}^{2+} + \text{nss-Ca}^{2+} \quad (2)$$

$$\text{ss-Na}^+ = \text{tot-Na}^+ - 0.562 \text{nss-Ca}^{2+} \quad (3)$$

$$\text{nss-Ca}^{2+} = \text{tot-Ca}^{2+} - 0.038 \text{ss-Na}^+ \quad (4)$$

where 0.562 represents the w/w $\text{Na}^+/\text{Ca}^{2+}$ ratio in the crust (Bowen, 1979) and 0.038 is the $\text{Ca}^{2+}/\text{Na}^+$ w/w ratio in seawater (Nozaki, 1997). Similarly, the ss- SO_4^{2-} fraction was calculated from the ss- Na^+ using the 0.253 $\text{SO}_4^{2-}/\text{Na}^+$ w/w ratio in seawater (Bowen, 1979). The crustal fraction of sulfate (cr- SO_4^{2-}) was determined from the nss- Ca^{2+} using the 0.59 $\text{SO}_4^{2-}/\text{Ca}^{2+}$ w/w ratio in the uppermost Earth crust (Wagenbach et al., 1996). Finally, the nss-nc- SO_4^{2-} fraction, which can be due to anthropogenic or secondary formed aerosol, was calculated by subtracting the ss- SO_4^{2-} and cr- SO_4^{2-} contributions from the total SO_4^{2-} concentrations.

The Organic Carbon (OC) and Elemental Carbon (EC) fractions were determined in PM_{10} samples using a Thermo-Optical Transmission (TOT) method following the NIOSH protocol. The organic matter (OM) was calculated by multiplying the OC fraction by 2.1 (Turpin and Lim, 2001) typical for remote sites with a large fraction of secondary aerosols. Table S1 in supplemental material also reports the detection limit for EC and OC.

2.1.2 Meteorological Context

Meteorological parameters are currently measured at different sites in Ny-Alesund. The German-French AWIPEV research base operates surface meteorology measurements with 1-minute time resolution, including temperature and relative humidity at 2 m height, wind speed and direction at 10 m height, and pressure at station level close to the summer campaign balloon launch site (Maturilli et al., 2013). The cloud base height above the station is retrieved using a Vaisala LD-40 ceilometer. Daily radiosoundings (1100 UTC) by the AWIPEV observatory provide auxiliary data for the aerosol profile analysis.

The Italian National Research Council (CNR) operates since 2009 the Amundsen-Nobile Climate Change Tower (CCT), providing meteorological, micro-meteorological, radiation and snow measurements continuously all year-long (Mazzola et al. 2016). Conventional and micro-meteorological parameters are measured at different heights (4 and 3 levels, respectively) in order to investigate their vertical variations in different conditions. Dai et al. (2011) and Mazzola et al. (2015) found that both in the Adventfjorden and in Kongsfjorden, where Ny-Ålesund is located,

the atmosphere is stable for about 50% of the time along the year, by analyzing micro-meteorological data. The term stability refers to the propensity of air masses to move vertically: stable air resists any vertical motion, while unstable air masses are prone to vertical movements. A parcel of air results to be stable/unstable if the temperature lapse rate is lower/higher than the adiabatic one, i.e. if the potential temperature is increasing/decreasing with height, respectively. In stable stratification, turbulence and vertical mixing is suppressed, leading to trapping of pollutants near ground level. On the above grounds, the spring 2011, summer 2011, and summer 2012 campaign periods can be put into a climatological context.

2.2 Vertical profile measurements

Vertical profile measurements have been carried out by means of a kytoon-shape helium-filled tethered balloon (length 8 m, $\varnothing=3$ m, volume 55.0 m³, payload 25 kg, Figure 1c). The tethered balloon was designed to fly in severe wind conditions. However, the presence of the payload limits the balloon flights from low to moderate wind conditions (< 10 m s⁻¹).

The tethered balloon was equipped with an instrumental package consisting of:

- 1) an Optical Particle Counter (OPC GRIMM 1.107; 31 size classes between 0.25 to 32 μ m, 6 sec sampling time) for the particle number size distribution determination;
- 2) a miniaturized electrical particle detector (miniDiSC, Matter Aerosol) to measure the total particle number concentration (1 sec sampling time);
- 3) two micro-Aethalometers: the microAeth[®] AE51 and a prototype (1-60 sec sampling time);
- 4) a meteorological station (LSI-Lastem: pressure, temperature and relative humidity, 6 sec sampling time).

During the period 11/04/2011-30/04/2011, the Vaisala tethersonde TTS111 (pressure, temperature, relative humidity, wind speed and wind direction; 1 sec sampling time) was also used.

The maximum height reached during each flight depended on atmospheric conditions and, for the majority of the profiles, was between 0.7 and 1.3 km. An electric winch controlled the ascent/descent rates that were set at 40.0 ± 0.1 m/min.

A deeper description of each instrument is reported here below.

2.2.1 Size distribution data

In this study, the total aerosol concentration and the number size-distribution along height were measured using a coupled miniDiSC –OPC ($\lambda=655$ nm) system.

The miniDiSC is a miniature Diffusion Size Classifier, a small and portable instrument (4×9×18 cm, 670 g, 8h of battery supply) (Fierz et al., 2011). The aerosol is first charged in a standard positive unipolar diffusion charger (the average charge is approximately proportional to the particle diameter). The charged particles flow through a diffusion stage (an electrically insulated stack of stainless steel screens connected to a sensitive electrometer that collect the finest particles) and into a second stage (equipped with a HEPA filter) where the current of larger particles is measured with an electrometer. The miniDiSC has a d_{50} cutoff at 14 nm. Thus, the instrument underestimates particle number concentrations for particles smaller than 20 nm (Nucleation Mode). As a result, the miniDiSC counts only partially the Nucleation Mode, while it allows a whole determination of Aitken and

Accumulation Mode particles. As demonstrated by Fierz et al. (2011), a bimodal lognormal aerosol size distribution with a fixed accumulation mode at 100 nm and a varying nucleation mode at 20 nm introduces an underestimation of about -2% – -10% of the total aerosol concentration in the miniDiSC response. The particle number determination is robust, and the error never exceeds 20%.

5 The OPC used in the campaign was the model the Grimm *I.107* that counts and classifies the aerosol in 31 size classes between 250 nm and 32 μm . As reported in literature (Ferrero et al., 2014; Howell et al., 2006; Heyder and Gebhart, 1979), OPCs size classification of the aerosol particles is a function of their ability to scatter the laser light under the assumption of spherical particles. The aerosol particles are classified in terms of their optical equivalent diameter, which is defined as “the diameter of a sphere of known refractive index (that of polystyrene latex spheres used for of calibration) that scatters light as efficiently as the real particle in question”. This effect usually results in an “undersizing” of the size classification, due to the higher refractive index of the polystyrene latex spheres (PSL spheres, $m=1.58$ at 655 nm; Ma et al., 2003) used in the OPC calibration compared to ambient aerosol (Guyon et al., 2003; Liu and Daum, 2008; Schumann, 1990). In order to derive a proper size classification of the aerosol over Svalbard, the “undersizing” issue was solved by correcting the OPC size channels to account for the ambient aerosol refractive index m . The OPC response function (S : the partial light scattering cross section of the particle related to the specific optical design of the OPC) was computed at 655 nm as follows (Baron and Willeke, 2005; Heyder and Gebhart, 1979):

$$S(\theta_0, \Delta\Omega, x, m) = \frac{\lambda^2}{4\pi^2} \iint_{\Delta\Omega} i(\theta, \phi, x, m) \sin\theta d\theta d\phi \quad (5)$$

where θ_0 represents the mean scattering angle of the optical arrangement, $\Delta\Omega$ the receiver aperture, x the dimensionless size parameter, m the refractive index and $i(\theta, \phi, x, m)$ the Mie scattering function composed by the perpendicular and parallel components $i_1(\theta, x, m)$ and $i_2(\theta, x, m)$, respectively. The optical arrangement of the OPC 1.107 consists of: 1) a wide angle parabolic mirror (121°, from 29.5° to 150.5°, $\theta_0=90^\circ$) that focuses scattered light on the photodetector located on the opposite side; 2) 18° of direct collected scattered light on the photodetector (from 81° to 99°, $\theta_0=90^\circ$) (Heim et al., 2008).

25 The response function was calculated both for PSL spheres (S_{PSL}) and for ambient aerosol (S_{AMB}). The refractive indexes of ambient aerosol used in S_{AMB} calculations were obtained from the **closest** AERONET site (Horsund site, 77°00'04" N 15°33'37" E) for spring 2011 and summer 2011-2012: 1.544+0.013i and 1.535+0.015i, respectively. These refractive indexes were determined at 674 nm (the closest AERONET wavelength to the OPC laser wavelength of 655 nm) and were close to those determined at 530 nm at Gruvebadet site (range 1.4-1.8 during 2010 and 2011; Lanconelli et al., 2013). Table S2 shows the new size corrected channels in comparison with the PSL spheres equivalent ones. The new channels were used to define three broad-size ranges (detailed here below) to evaluate the vertical behavior of aerosol.

The coupled miniDiSC–OPC ($\lambda=655$ nm) system measurement range covers the relevant region of the aerosol number size-distribution. In order to study the behavior of different size classes along height, three aerosol number concentration size ranges were selected:

1) the number concentration of aerosol between 14 nm (d_{50} of miniDiSC) and 260 nm (cfr Table S2) obtained as the difference between the total number concentration measured by the miniDiSC and that measured by the OPC, hereinafter indicated as N_{14-260} ;

2) the number concentration of aerosol between 260 nm (lower limit of OPC) and 1200 nm hereinafter indicated as $N_{260-1200}$;

3) the number concentration of aerosol above 1200 nm, hereinafter indicated as $N_{>1200}$.

The mode N_{14-260} includes a small fraction of the Nucleation mode (from 14 to 20 nm), the totality of the Aitken mode (20-100 nm) and a fraction of the Accumulation mode (from 100 to 260 nm). The mode $N_{260-1200}$ includes most of the Accumulation mode particles. Finally, mode $N_{>1200}$ covers the totality of Giant Nuclei mode.

The accuracy of both miniDiSC and OPC measurements was investigated comparing the lowermost portion of their measurements along vertical profile with SMPS+APS data collected at ground-level at Gruebadet. This comparison was performed during spring 2011 to avoid any contamination from ship plumes arriving from Ny-Ålesund harbor towards Gruebadet in summer (balloon sounding were conducted from the Koldeway station instead that from Gruebadet; section 2.1). The comparison of N_{14-260} (miniDiSC vs. SMPS) and of $N_{>260}$ (OPC vs. SMPS+APS) was characterized by an excellent correlation ($R^2 > 0.9$; linear best fit close to the ideal one) with an average error of 7% and 16% for both N_{14-260} and $N_{>260}$, respectively (supplemental material, Figure S1a-b). These results highlight the reliability of measurements carried out along the vertical profiles, an important feature considering the low aerosol concentration values and their variation, which are present within the Arctic (section 1).

Number concentration data were also used in section 3.2.4 to estimate the contribution of locally formed aerosol. The method is based on the N/BC ratio, developed by Rodríguez and Cuevas (2007) and successfully applied in Europe by Reche et al. (2011). The basic concept of this method is that highest values of N/BC ratios (i.e. the lowest BC fraction values) occur during secondary aerosol formation in the atmosphere (Reche et al., 2011; Dall'Osto et al., 2013 and 2011). The methodology is as follows:

$$N_2 = N - N_1 \quad (6)$$

$$N_1 = S_1 \times BC \quad (7)$$

where N_2 represents the secondary aerosol concentration locally formed in the atmosphere, N is the measured aerosol number concentration and N_1 is the aerosol number concentration already present in the background air. S_1 represents a reference value for the N/BC ratio (expressed as particles $\text{cm}^{-3}/\text{ng m}^{-3}$ of BC) in the background air. The parameter N_1 is calculated from the parameter S_1 multiplied by the measured BC concentration (see next section 2.2.2). S_1 can vary from ~ 2 to ~ 9 , while the N/BC ratio during secondary aerosol formation reaches values higher than $\sim 15-20$ and up to $\sim 100-200$ (Reche et al., 2011; Dall'Osto et al., 2013 and 2011). The differences in S_1 values determined in different sites can be caused by: 1) the use of different particle counters (with different d_{50} cutoff), as lowest S_1 values are usually observed when devices with largest d_{50} cutoff are used; 2) the influence of the ambient air conditions on the secondary aerosol formation. Thus, S_1 is site-instrument specific and has to be determined on-site depending on the used particle counter. If the Rodríguez and Cuevas (2007) method is applied to ground-based temporal data series, S_1 can be obtained as the minimum N vs. BC slope observed during the day (Reche et al., 2011). However, in the case of measured vertical profiles, the values of S_1 were taken as that of background aerosol above the aerosol stratifications described in section 3.2.4.

2.2.2 Black Carbon

BC have been determined using two micro-Aethalometers: the microAeth[®] AE51 and a prototype (Magee Scientific; 250 g, 117x66x38 mm³). Adopting the nomenclature recommended by Petzold et al. (2013), by Andreae

and Gelencser (2006) and by other authors (Gilardoni et al., 2010; Hoffman et al., 2011; Sthol et al., 2013; Eckhardt et al., 2013), we refer to the measured parameter as “equivalent black carbon” (eBC) due to the absence of an overall agreed reference material, linking light absorption to the empirically defined BC mass concentration. In agreement with the above cited literature, we also report the absorption coefficient values.

5 AE51 and the prototype were identical with the exception that the prototype measured at 2- λ (370 and 880 nm) while AE51 only at 880 nm. At the time of campaign the prototype was just yet developed and was used instead the AE51 on the balloon platform during the spring 2011 campaign only when necessary (i.e. AE51 in charge) to ensure the continuity of measurements during the campaign.

10 In both the Aethalometers the aerosol containing BC was continuously sampled onto a PTFE-coated borosilicate glass fiber filter (Fiberfilm™ Filters, Pall Corporation) where the light attenuation (ATN) was measured at 880 nm relative to a clean part of the filter. ATN was calculated as:

$$ATN=100*\ln(I_0/I) \quad (8)$$

where I_0 and I are the light intensities transmitted throughout a reference blank spot and the aerosol-laden 3 mm diameter sample spot of the filter, respectively.

15 The attenuation coefficient of the particles collected on the filters, b_{ATN} , was derived from ATN as follows (Weingartner et al., 2003):

$$b_{ATN} = \frac{A}{100Q} \frac{\Delta ATN}{\Delta t} \quad (9)$$

where ΔATN indicates the ATN variation during the time period Δt , A is the sample spot area ($7.1 \cdot 10^{-6} \text{ m}^2$) and Q is the volumetric flow rate ($2.5 \cdot 10^{-6} \text{ m}^3 \text{ sec}^{-1}$ for the AE51 and $4.42 \cdot 10^{-6} \text{ m}^3 \text{ sec}^{-1}$ for the prototype).

20 Finally, to determine the eBC ambient concentration the apparent mass attenuation cross-section ($\sigma_{ATN} = 12.5 \text{ m}^2 \text{ g}^{-1}$) is needed; it is defined for the eBC collected on the PTFE-coated borosilicate glass fiber filter. The σ_{ATN} value ($12.5 \text{ m}^2 \text{ g}^{-1}$) was obtained by comparing the eBC values measured with the microAeth® Model AE51, with an AE31 Aethalometer (880 nm wavelength) operating in a test chamber with different eBC concentrations at low attenuation values. The comparison was then repeated using ambient air (Ferrero et al., 2011a). This value is not far from the σ_{ATN} values of $15.2 \text{ m}^2 \text{ g}^{-1}$ and $15.9 \text{ m}^2 \text{ g}^{-1}$ reported in Eleftheriadis et al. (2009) when reported ten years of eBC measurements in Ny-Ålesund at the Zeppelin station with the Aethalometers AE9 and AE31. The difference between these values results from the use of different filter materials to collect the sample in the different Aethalometers, which was quantified in Ferrero et al. (2011a) and Drinovec et al. (2015).

The eBC concentrations were determined as follows:

30
$$eBC = \frac{b_{ATN}}{\sigma_{ATN}} \quad (10)$$

The accuracy of eBC measurement was investigated. The AE51 and the prototype measurements carried out simultaneously agreed very well ($R^2=0.852$; slope=0.976; Figure S1c supplemental material). This result was important as obtained with two different flowrates ($2.5 \cdot 10^{-6} \text{ m}^3 \text{ sec}^{-1}$ for the AE51, and $4.42 \cdot 10^{-6} \text{ m}^3 \text{ sec}^{-1}$ for the prototype).

35 However, a large scatter is present at low eBC concentrations (i.e. $10\text{-}20 \text{ ng m}^{-3}$; see Figure S2c). Thus, the absolute error (in percentage) of each eBC value (considering the average of the two Aethalometers) was calculated for intervals of 5 ng m^{-3} of concentrations. At low concentrations, the error can reach up to 90% and more (Figure S2a, supplemental material). This error decreases with increasing concentration, dropping below 20 ng m^{-3} for eBC concentrations above 5 ng m^{-3} . The relative error lies below 20% for both the average and the 90th Percentile

at eBC concentrations above 20 ng m^{-3} . Thus, it is possible to consider this value as the limit above which a single eBC measurement point is not affected by instrumental noise. Nevertheless, this limit is close to the BC concentrations that have been previously measured in the Arctic (Eleftheriadis et al., 2009). In this respect, we note that the BC profiles presented in the manuscript are an average of many measurements, hence the effect of the noise on the reported eBC concentrations is further reduced. The aim of this paper is to determine the seasonal phenomenology of the aerosol behavior along vertical profiles classifying the collected experimental data, according to their shape and averaging them for each season. This is very important as, even the error in percentage of each data point can reach high values (especially at low concentrations), the average of the data stabilizes the instrumental fluctuations. This effect is demonstrated by Figure S2b (supplemental material) which reports the correlation between the BC concentrations (AE51 and prototype) averaged on the same intervals of 5 ng m^{-3} used in Figure S2a ($R^2=0.986$; slope=1.017).

The above reported analysis underlines a critical situation for summer because, as reported in Eleftheriadis et al. (2009), the eBC concentration range expected in summer is $\sim 0\text{-}10 \text{ ng m}^{-3}$. Therefore, summer eBC data were used here only to highlight the impact of shipping emissions on the Arctic background concentrations along the atmospheric column. Due to high ship impact (section 3.4), the performance of the micro-Aethalometers was suitable and reliable for the purpose of this application.

In addition to eBC, the micro-Aethalometers allows also the determination of the aerosol absorption coefficient, b_{abs} , that was calculated as follows:

$$b_{abs} = \frac{b_{ATN}}{C \cdot R(ATN)} \quad (11)$$

where C and $R(ATN)$ are the multiple scattering optical enhancement factor and the aerosol loading factor, respectively. Briefly, the constant optical enhancement factor C compensates for the enhanced optical path through the filter caused by multiple scattering induced by the filter fibers themselves (Schmid et al., 2006; Arnott et al., 2005; Weingartner et al., 2003). The parameter $R(ATN)$ compensates for the nonlinearity – the loading effect due to reduction of the measurement sensitivity due to the saturation caused by the collected sample on the filter. The compensation with the parameter $R(ATN)$ is needed only when ATN becomes higher than 20 (Schmid et al., 2006; Arnott et al., 2005; Weingartner et al., 2003). In this study, the experimental design allowed us to neglect the use of $R(ATN)$: all eBC vertical profiles were conducted in the clean Arctic environment and the filter tickets were changed regularly to always keep ATN lower than 20 as recommended by Weingartner et al. (2003). For the AE51, and the prototype, the only parameter C available in the literature is 2.05 ± 0.03 (at $\lambda = 880 \text{ nm}$) (Ferrero et al., 2011a), even though recently Ran et al. (2016) proposed a C value of 2.52 for ground-based measurements in China.

The C value of 2.05 ± 0.03 was determined over Milan in Ferrero et al. (2011a) and thus a brief description is necessary to determine its applicability in the Arctic area. The parameter C was determined using data collected both below the mixing layer and above it, in a cleaner atmosphere, along the vertical profiles (Ferrero et al., 2011a). During the C determination, a new filter ticket was used for each profile. As a result, ATN never reached values higher than 20 (average ATN was 5 ± 1) and the total amount of aerosol collected on each filter during the C determination was negligible. Therefore, the determined C was exclusively dependent on the filter material and the AE51 instrumental geometry. This ensures the negligible influence of the particles in the filter matrix on the

C value. The reliability of the obtained C (2.05 ± 0.03) was demonstrated in Ferrero et al. (2014) below the mixing layer and in free troposphere.

Finally, it should be noted that absorbing non-BC particles may contribute to the signal in Aethalometers (i.e. Brown Carbon, dust). However, BrC is characterized by negligible absorption in the infrared (Andreae and Gelencsér, 2006), the wavelength range of the eBC measurements (micro-Aeth AE51 uses 880 nm). In this respect, Massabò et al. (2013) showed the potential contribution of BrC to the determination of eBC to be below 10%.

To estimate the possible influence of BrC on eBC measurements carried out during the spring 2011 campaign, the data collected with the micro-Aeth prototype at 370 and 880 nm were considered. They highlighted a BrC positive artifact on eBC measurements less than 10% during the campaign. Details are reported in supplemental material.

2.2.3 Meteorological data and aerosol stratifications

Meteorological data along height allowed the determination of the absolute height of the balloon using the hypsometric equation; due to change during April 2011 in the measuring system (section 2.2), a comparison of the altitude obtained by the LSI-Lastem and Vaisala tethersonde was conducted during several target flights. The result ($R^2=0.997$; slope=0.999; Figure S1d, supplemental material) demonstrated the accuracy of the height determination. The measurement of altitude is fundamental in the study of the vertical aerosol properties in relationship with meteorological parameters. In fact, vertical aerosol profiles allows the determination of the height of aerosol stratifications by means of a gradient method, applied to aerosol concentration profiles, as suggested by Seibert et al. (2000).

The gradient method is based on the determination of the minimum value of the vertical derivative of the aerosol concentration. The use of gradient method to determine the aerosol mixing height has been demonstrated at lower latitudes in previous works (Ferrero et al., 2012, 2011a, 2011b and 2007; Sangiorgi et al., 2011; Di Liberto et al., 2012). However, in remote areas, such as the Arctic, several processes other than dispersion can shape the aerosol profiles. The two most important ones are: 1) differential advection (Tunved et al., 2013) and 2) a lack of emission of aerosol from ground. These processes should generate a vertical structure not directly related to the PBL height. Therefore, in the present work the gradient method has been limited to individuate aerosol stratification heights (AS_h), even if these related to the behaviour of meteorological variables governing the behaviour of the PBL as will be addressed in section 3.1.

The AS_h will be used in the next sections to calculate averaged aerosol and eBC profiles (sections 3.2 and 3.3). In fact, in order to investigate the variation of aerosol properties with height, vertical profiles were statistically averaged. As reported in previous works (Ferrero et al., 2011a, 2012 and 2014), a way to average vertical profile data by taking their main gradients (AS_h) into account, is to consider the relative position of each measured data point in respect to the AS_h . Thus, vertical profiles were first normalized, introducing a standardized height (H_s) calculated as follows:

$$H_s = \frac{z - AS_h}{AS_h} \quad (12)$$

where z is the height above ground. H_s assumes a value of 0 at the AS_h , and values of -1 and 1 at ground-level and at twice the AS_h , respectively.

Examples of AS_h , accompanied with the corresponding potential temperature (θ) and RH profiles, are presented in Figure 2a-d. The presented data, accurately describe the vertical distribution of the aerosol and its properties in the first kilometer above Ny-Ålesund. Moreover, they allowed to obtain different piece of information.

The absence or the presence of marked aerosol stratifications (AS) is notable. When present, the altitude at which they occur (AS_h) was determined by the gradient method, described above. This is the first obtainable information.

A second piece of information was the size dependent vertical behavior of aerosol concentrations. Figures 2b and 2c highlight a similar behavior for both N_{14-260} and $N_{260-1200}$, while, Figure 2d shows different behavior for $N_{260-1200}$ due to a concentration change located at a different altitude. Finally, we obtained the magnitude of the observed concentration change at each AS_h for each size range (N_{14-260} , $N_{260-1200}$ and $N_{>1200}$) and season.

The analysis and combination of these three types of information allowed to classify, as a function of seasonality, the altitude, magnitude and frequency of aerosol stratifications. Furthermore, it has been possible to shed some light on the dynamics underlying the seasonal phenomenology found during the field campaigns. A detailed discussion on these points is reported in the following section.

3 Results and Discussion

Vertical profiles of aerosol number size distribution and eBC concentrations were measured to assess changes in aerosol properties within the vertical column in the Arctic region. The results obtained along vertical profiles are discussed in order to highlight first the vertical behavior of the AS_h in relation to the main atmospheric meteorological parameters (section 3.1). Then, vertical aerosol properties are discussed in details for springtime (section 3.2) and summertime (section 3.3). All averaged data are reported hereinafter as mean \pm mean standard deviation.

3.1 Aerosol stratifications: seasonal vertical frequency distribution and relationship with meteorology

As reported in Table 1, about 200 profiles were measured during 3 campaigns in spring 2011, summer 2011 and summer 2012. Here below, the ambient conditions under which the vertical profiles were measured are briefly described.

First of all, the observational periods (spring 2011, summer 2011 and summer 2012) were addressed in a climatological context. In this respect, the temperature measured in spring 2011 was within the standard deviation range of the long-term observations, while a 10-day period at the end of April 2011 was slightly warmer than the climatological mean (Figure S3a). The temperatures during the summer seasons 2011 and 2012 were mostly within the range of the long-term observations (Figure S3b). Neither of the campaign periods was conducted under exceptional meteorological conditions, so the vertical profile measurements can be considered to have been obtained under typical meteorological conditions representative for the Ny-Ålesund environment.

We note, however, that the tethered balloon measurements have limitations with respect to its launch conditions (section 2.2). Particularly, balloon profiles were measured in low wind conditions, as it is very difficult to launch the balloons during high winds. This introduces a bias in respect to average meteorological conditions above the launch site. The maximum wind speed measured at the Amundsen-Nobile Climate Change Tower (section 2.1.2) during balloon flights was lower than that during the whole period of the campaign (April 2011, June and July 2011-2012): 4.9 m s^{-1} and 10.7 m s^{-1} (springtime and summertime balloon profiles) compared to 27.9 m s^{-1} and 16.3 m s^{-1} (full spring 2011 and summer 2011-2012). Table 1 resumes the conditions for all the measured profiles.

The majority of vertical profile measurements was conducted under clear sky conditions (no clouds) or with clouds with base height above the balloon payload.

Thus, it is possible to assert that the measured profiles, and the seasonal phenomenology described hereinafter, are representative of typical Arctic springtime and summertime periods mainly for low wind and clear sky conditions.

5 Figure 2a-d highlights different atmospheric dispersal conditions upon Ny-Ålesund. Although these four case studies are not illustrative and comprehensive of the whole data set, their discussion helps to illustrate the seasonal and size-dependent behavior of the frequency distribution of the AS_h with altitude.

An example for homogeneous dispersion of aerosol (independent from its size) in the lower troposphere is shown in Figure 2a. Decreasing potential temperature with height indicates atmospheric instability, allowing the vertical mixing of air masses by convection. Homogeneous aerosol profiles with convective conditions were found in 15% of the profiles in spring and 37% of the profiles in summer, respectively. Convective conditions generally are observed more frequent during summer in Ny-Alesund related to the different level of radiation energy at disposal and surface properties. In summer homogenous profiles were observed often (37%) than in spring (15%), due to a synergy of the higher solar power density at disposal ($186.4 \pm 71.2 \text{ W m}^{-2}$ in summer and $109.2 \pm 35.9 \text{ W m}^{-2}$ in spring) together with a lower albedo (0.15 ± 0.01 in summer and 0.87 ± 0.04 in spring) induced by the summer snowmelt in Svalbard (Mazzola et al. 2015). The resulting change in surface energy balance affects the atmospheric stability, from the more stable conditions and inversion situations with snow-cover to the unstable conditions favoring mixing within the boundary layer once the snow cover has disappeared.

In spring, the presence of different layers of aerosol, separated by abrupt changes in the aerosol properties (i.e. concentration) along height were observed more frequently than the homogeneous mixing conditions (Figure 2b-d). The presence of aerosol stratification was complementary to the homogenous profiles and thus occurred for 85% and 63% of cases during spring and summer, respectively.

Within stratified conditions it was possible to determine the AS_h for each aerosol size and season together with the altitude of sharp changes observed also for θ and RH. For example, Figure 2c shows AS_h at 630 m in agreement with the vertical gradients of θ and RH. On the other hand, Figure 2d shows a first AS_h at 134 m only for N_{14-260} , while $N_{260-1200}$ appeared homogeneously distributed until a second AS_h located at 674 m. The first AS_h detected for the smallest particles was related to a ground-based θ inversion, while the second AS_h , detected for the accumulation mode particles, was related to an elevated θ inversion.

The aforementioned case studies helped us to introduce the description of the AS_h frequency distribution with altitude and season. The AS_h were used independently from the sign of the aerosol concentration change (either positive or negative; Figure 2b-c) and were computed separately for each broad size range (i.e. Figure 2d). The resulting frequency distribution with altitude of the first AS_h is reported in Figures 3a-d and Figures 3e-h for spring and summer, respectively. It has to be underlined that sometimes it was possible to detect up to two AS_h for each profile. This situation was observed for ~30% of profiles (characterized by the presence of aerosol gradients) in spring and summer, due to the limited maximum altitude reached by the balloon during the flight (usually between 0.7 and 1.3 km). The behavior of the second AS_h is shown in the supplemental material (Figure S4) to support the description of the behavior of the first aerosol stratification with altitude.

Focusing on each season and considering first the springtime AS_h vertical frequency distributions (Figure 3a-d) a common behavior can be first observed for both the three size ranges (N_{14-260} , $N_{260-1200}$ and $N_{>1200}$) and meteorological parameters (θ and RH): all of them showed a bimodal distribution characterized by a minimum

within the ~400-500 m height range. Maturilli and Kayser (2016) identified a frequent occurrence of a temperature inversion layer in the shear zone above the mountain ridges; this phenomenon is typically present throughout the year, leading to a decoupling of the lowermost kilometer of the atmosphere from the free troposphere above. In between the mountains, the atmosphere is characterized by wind channeling along the fjord axis, disturbed by e.g.

5 glacier outflow or land-sea breeze. Thus, the observed separation of AS_h most likely relates to the separation of the atmospheric flow.

Moving forward, some differences were then found in the behavior of each aerosol size range below and above the minimum at 400-500 m. While $N_{260-1200}$ and $N_{>1200}$ (Figure 3b-c) appeared equally distributed below and above the minimum at 400-500 m, N_{14-260} showed highest frequencies of AS_h below 400 m (Figure 3a). Particularly, the
10 82% of AS_h for N_{14-260} were located below 400 m and showed a clear maximum peak close to the ground (0-100 m) with a frequency of 38%. Moreover, the average values of AS_h for N_{14-260} below and above the minimum at 400-500 m were 143 ± 13 m and 669 ± 32 m, respectively. Conversely, AS_h for $N_{260-1200}$ and $N_{>1200}$ occurred for 52% and 51% below 400 m peaking in the 100-200 m range (22% and 21%, respectively) with average values of 208 ± 19 m and 177 ± 14 m, respectively. Above 400 m the AS_h for $N_{260-1200}$ and $N_{>1200}$ peaked in the 600-700 m range (22% and 19%, respectively) with average values of 672 ± 16 m and 652 ± 20 m.

The observed lack of symmetry between N_{14-260} and $N_{260-1200} - N_{>1200}$ is explained in Figure 2d, where a decoupled trend for N_{14-260} and $N_{260-1200}$ is shown. As stated above, the behavior of smallest particles was in that case related to a ground-based θ inversion. Considering the whole data set, the behavior of the vertical frequency distribution of the first gradient of both θ and RH was in agreement with that of AS_h for N_{14-260} . In this respect, a maximum
20 peak for both θ and RH was found close to the ground (0-100 m), with a frequency of 49% and 38%, respectively (average values below the minimum at 400-500 m for gradients for θ and RH of 117 ± 12 m and 669 ± 32 m). Interestingly, the frequency of ground-based θ inversions (49%) was higher than that of AS_h for N_{14-260} (38%). This feature is due to vertical profile along which, even in the presence of a ground-based θ inversion, N_{14-260} did not show any variation of concentration; an example is reported in Figure 2b. Thus, the presence of a ground-based
25 θ inversion appears as a necessary but not sufficient condition to observe the aforementioned behavior (resumed by Figure 2d, Figure 3a and 3d). The phenomenology and the aerosol dynamic responsible of this behavior (together with that of $N_{260-1200} - N_{>1200}$) will be addressed and discussed in the following section 3.3.

We describe below the summer AS_h behavior. Figure 3e-h (and Figure S4) show that even in summer, the multi-layered structure persisted and was also characterized by a bimodal distribution, as in spring, but with a higher
30 minimum (than in spring) that ranged approximately between 500 m and 600 m. The summer AS_h for all size ranges and the gradient for θ and RH peaked between 100 and 300 m: 78% (N_{14-260} ; average value 276 ± 19 m), 71% ($N_{260-1200}$; average value 269 ± 18 m), 76% ($N_{>1200}$; average value 272 ± 18 m), 83% (θ ; average value 262 ± 18 m) and 79% (RH; average value 268 ± 18 m). Figure 3e-h, and the aforementioned data, highlight that the vertical frequency distribution for AS_h of all sizes and gradients for θ and RH behave similarly. This phenomenon, different
35 from that observed in spring, will be addressed and discussed in section 3.3. As a final conclusion, a multi-layered structure was found over Ny-Ålesund both in spring and summer (see also Figure S4), and the most important atmospheric thermodynamic parameters (θ and RH) indicated the role of meteorology in shaping the aerosol vertical profiles. This result is of great importance as the majority of the aerosol measurements conducted in the Arctic area is ground-based and thus, it is necessary to understand their validity with altitude.

40

3.2 Springtime phenomenology

The previous section introduced the vertical behavior of sized aerosol in terms of frequency distribution of AS_h . However, it is also necessary to describe the intensity of the aerosol concentration changes at the AS_h , and the possible dynamics underlying these changes. Thus in this section, the springtime vertical aerosol phenomenology will be investigated. All the profiles measured in spring 2011 were classified based on their vertical behavior (i.e. shape) and averaged considering the relative position of each measured data point with respect to the AS_h . The obtained averaged vertical profiles were referred to a standardized height (H_s , Eq. 12) as described in section 2.2.3. As the size classes can behave differently with height, $H_s=0$ was referred to that observed for the intermediate $N_{260-1200}$ size class. The result of the classification and averaging procedure is reported in Figure 4a-m (all profile data are reported in Figure S5, supplemental material). Four main typologies of vertical profile were found. According to their shape they were named as follows:

- 1) Type 1, homogeneous profiles (hereinafter addressed as HO), Figure 4a-c
- 2) Type 2, profiles characterized by a positive gradient at $H_s=0$ (hereinafter addressed as PG), Figure 4d-f
- 3) Type 3, profiles characterized by a negative gradient at $H_s=0$ (hereinafter addressed as NG), Figure 4g-i
- 4) Type 4, profiles characterized by negative gradients located at different altitude in function of size (hereinafter addressed as decoupled negative gradient, DNG), Figure 4l-m.

Average concentrations of aerosol (N_{14-260} , $N_{260-1200}$, $N_{>1200}$) and eBC below and above $H_s=0$ for each profile class are summarized in Table 3.

We first report here the columnar averages of both total aerosol number and eBC concentrations obtained by averaging all the aforementioned profile classes: $236.1 \pm 23.9 \text{ cm}^{-3}$ (N_{14-260}), $21.1 \pm 1.3 \text{ cm}^{-3}$ ($N_{260-1200}$), $0.2 \pm 4 \cdot 10^{-2} \text{ cm}^{-3}$ ($N_{>1200}$) and $52 \pm 8 \text{ ng m}^{-3}$ (eBC). They perfectly agree with long-term data series collected over Ny-Ålesund at the Zeppelin observatory (Eleftheriadis et al., 2009; Tunved et al., 2013) during Spring ($\sim 100\text{-}250 \text{ cm}^{-3}$ and $50\text{--}70 \text{ ng m}^{-3}$ of eBC during April). This agreement indicates that all the profile classes discussed below can be considered to be characteristic (with their occurring frequencies and altitudes) for the background Arctic aerosols measured by Arctic observatories within GAW, AMAP and EMEP observation programs. Moreover, the eBC data also agreed with results from PAM-ARCMIP (Stone et al., 2010) which showed a $40\text{--}90 \text{ ng m}^{-3}$ range of eBC within the surface inversion layer and $30\text{--}50 \text{ ng m}^{-3}$ above.

All the CCT wind data were used to compute wind rose graphs timely coincident with each profile typology (Figure 5a-d) and will be used in the following sections. The fjord direction into which the wind is often channeled is NW-SE. Here we underline that Figure 5a-d shows the absence of wind from north during the profile measurements, thus any influence from the Ny-Ålesund village is negligible. In addition, Figure 6 shows the ground-based number size distribution measured at Gruebadet (section 2.1) for HO, PG, NG and DNG profiles, respectively.

Finally, a brief discussion of the air masses origin for the four categories is summarized in the supplemental material (see also Figure S6).

3.2.1 Homogeneous Profiles (HO)

HO profiles (Type1, Figure 4a-c) were observed in 15% of cases (during 7 days) and were characterized by a homogenous vertical distribution of aerosol and eBC upon Ny-Ålesund. HO profiles are reported with an absolute

height AGL, because they did not show any AS_h to calculate H_s . They appear in some way analogous to the relatively diffuse background aerosol reported in the springtime ARCPAC campaign (Brock et al. 2011). During HO profiles, local wind (Figure 5a) was blowing mainly from the SW direction, from the glaciers behind Ny-Ålesund (Figure 1a) and not along the predominant NW-SE direction. Moreover, HO profiles featured the lowest wind speed (range 0-2 m s⁻¹, average of 0.6±0.1 m s⁻¹ at 33 m; Table 2).

At the same time, as shown in Figure 4c, a slightly positive θ profiles characterized, on average, the HO profiles. To this average contributed θ profiles with both positive and negative (as shown in Figure 2a) vertical gradients. Negative θ gradients allowed vertical mixing. Positive θ gradients instead favored stable conditions. However, they are not in contrast with the absence of an aerosol stratification. In fact, just the presence of an important aerosol source (either local or transported) allow the formation of a distinct aerosol layer. This process is detailed in section 3.2.3.

The number concentrations in HO profiles were 80.2±16.4 cm⁻³ (81.9±16.8% of the total aerosol concentration), 17.5±2.0 cm⁻³ (17.9±2.0% of the total aerosol concentration) and 0.2±0.1 cm⁻³ (0.2±0.1% of the total aerosol concentration) for N_{14-260} , $N_{260-1200}$, $N_{>1200}$, respectively. The aerosol number concentration was thus dominated by the N_{14-260} size fraction along the whole profile. eBC and the related b_{abs} (section 2.2.2, eq. 4) reached values of 35±21 ng m⁻³ and 0.22±0.13 Mm⁻¹.

Aerosol number concentration in HO profiles lies close to the lower values registered at Zeppelin in April (Tunved et al., 2013) and were characterized by a ground-based size distribution dominated by the accumulation mode particles (Figure 6). eBC was close to the 25°-50° percentiles reported in Eleftheriadis et al. (2009a) for April and to the lower troposphere value of refractory BC (rBC) measured in spring during the HIPPO campaign (Schwarz et al., 2013).

Within HO profiles the aerosol pollution, previously transported from mid-latitudes, affected the first km of the atmosphere. The observed homogenous mixing conditions, allowed us to assume that the aerosol properties measured at ground-level in Ny-Ålesund were representative for the lower troposphere.

3.2.2 Positive Gradient Profiles (PG)

PG profiles (Type 2, Figure 4d-f) occurred in 17% of cases (during 6 days) and were characterized by an increase of aerosol number concentrations above $H_s=0$ and moderate eBC concentrations (24±3 ng m⁻³; b_{abs} was 0.15±0.02 Mm⁻¹). The average value of AS_h (corresponding to $H_s=0$) was 417±266 m. During PG profiles local wind (Figure 5b) was blowing mainly from the SE along the predominant NW-SE direction. This situation is common in Kongsfjorden (Vihma et al., 2011). PG profiles featured the highest wind speed (range 0-5 m s⁻¹, average of 2.3±0.1 m s⁻¹ at 33 m; Table 2). At the same time, as shown in Figure 4f, a positive θ profiles was present with a +1.5±0.4 K increase from $H_s=0$. A stable atmosphere was present and the aerosol was brought to the site by long-range transport in this stable situation. The increment of aerosol number concentrations with altitude was particularly evident for N_{14-260} that increased by +171.5±25.4% (going from 205.4±12.5 cm⁻³ below the AS_h to 557.6±45.9 cm⁻³ above it) while, $N_{260-1200}$ experienced a more modest increase of 11.8±7.0% (going from 19.9±0.2 cm⁻³ below the AS_h to 22.3±1.4 cm⁻³ above it). Conversely, the coarse fraction ($N_{>1200}$) decreased with altitude of -38.1±10.0% (going from 0.26±0.02 cm⁻³ below the AS_h to 0.16±0.02 cm⁻³ above it). The observed increase of Aitken and Accumulation mode fractions (N_{14-260} plus $N_{260-1200}$), and the corresponding decrease of the coarse fraction ($N_{>1200}$), appear to be in agreement with the observation that during transport events wet removal processes

and dry deposition decrease the coarse particle concentration by scavenging and, at the same time, establish conditions that favor secondary aerosol formation due to the lowering of the condensational sink (Tunved et al., 2013).

The aerosol number concentration values above $H_s=0$ were close to those reported in Engvall et al. (2008) for the Arctic free troposphere during ASTAR. The ground-based size distribution, not influenced by the pollution layer at high altitude, was dominated by accumulation mode particles as in HO profiles (Figure 6).

The PG profile data suggested that high altitude transport events could be the origin of this type of profiles during springtime. An example of this process is the interesting case study of 23th April 2011 (1200-1330 UTC), when an intense plume of aerosol was transported over Ny-Ålesund. Figure 7a-b shows this event with the associated air mass back trajectories, and the time evolution of the event obtained through the interpolation of 6 vertical profiles, each of which lasted ~15 min and was removed about 1 min from the following profile.

Altitude layers of pollution were documented in Brock et al. (2011) and in Kupiszewski et al. (2013) and Wofsy et al. (2011). Jacob et al. (2010) reported that transport from North America and East Asia takes place mainly at higher altitudes, as also documented in Stohl et al. (2006). In this respect, the back-trajectories reported in Figure 6a described high altitude air from North America and Asia that descended in the Arctic. High aerosol concentrations at high altitude are important because aerosols can act as CCN and thus impact on climate via the indirect aerosol effects.

3.2.3 Negative Gradient Profiles (NG)

NG profiles (Figure 4g-i) were observed in 48% of all cases (during 9 days) making the NG the dominant typology of profiles. The average value of AS_h (corresponding to $H_s=0$) was 506 ± 212 m. The predominant wind direction was the same as in PG profiles (SE-E direction) with a component also from SW (Figure 5c). Figure 4i shows that a strong, positive θ profile ($+4.1\pm 0.3$ K increase from $H_s=0$) characterized NG profiles.

Within this condition, the case study reported in figure 7b showed the origin of NG profiles. Figure 7b shows first a transport event that generated PG profiles (section 3.2.2). Afterwards, the transported aerosol was mixed downward within the PBL until ground. Most important, at the end of the process (1330 UTC) a negative concentration gradient with altitude was established generating a NG profile.

As now shown, NG profiles might be originated from the entrance of Arctic Haze into the PBL after a transport process. In the Arctic, in absence of an important local aerosol source (i.e. nucleation which acts mainly in summer; Tunved et al., 2013), only transported aerosol trapped within a thermal inversion made possible the presence of this typology of profiles. The presence of an intense θ inversion stabilizes the situation maintaining a NG typology of profile since vertical mixing is prevented (see also Figure 2c). It has to be noticed that an intense θ inversion is just a necessary condition to promote the formation of NG profiles, not a sufficient one. This result explains the presence of HO profiles even in a stable atmosphere (section 3.2.1) and is in agreement with the observation (reported in section 3.1.1) that the frequency of ground-based θ inversions (49%, Figure 3d) reached values higher than those for any AS_h for any aerosol size (Figure 3a-c).

NG profiles were characterized by high pollution levels below $H_s=0$ where an intense decrease of both aerosol and eBC was observed. Crossing the AS_h , aerosol concentrations decreased by $-52.9\pm 8.7\%$ (from $252.3\pm 17.5\text{cm}^{-3}$ to $118.9\pm 9.3\text{cm}^{-3}$) for N_{14-260} , by $-57.9\pm 2.6\%$ (from $23.1\pm 0.4\text{cm}^{-3}$ to $9.7\pm 0.3\text{cm}^{-3}$) for $N_{260-1200}$ and by $-66.5\pm 11.5\%$ (from $0.53\pm 0.05\text{cm}^{-3}$ to $0.18\pm 0.02\text{cm}^{-3}$) for $N_{>1200}$. eBC behaved similarly, decreasing by $-50.4\pm 6.8\%$ (from 71 ± 4

ng m⁻³ to 35±2 ng m⁻³), with the same phenomenology for b_{abs} (from 0.43±0.02Mm⁻¹ to 0.21±0.01Mm⁻¹). The last finding is very important because the altitude of eBC occurrence in the atmosphere modulates its influence on the climate in the Arctic.

5 NG profiles exhibited characteristics in agreement with literature data. Focusing on eBC, the vertical behavior and the observed concentrations agreed with those found in the PAM-ARCMIP campaign. Stone et al. (2010) reported rBC concentrations of 40-90 ng m⁻³ within the surface-based temperature inversion layer, decreasing to 30–50 ng m⁻³ above it. Results reported in Schwarz et al. (2013) for the HIPPO campaign in January agree with our measurements. Aerosol number concentration and eBC are also close to the higher values registered at the Zeppelin station in April (Tunved et al., 2013; Eleftheriadis et al., 2009a). In fact, NG profiles represent the most polluted
10 situation affecting the whole boundary layer, quite the opposite to HO profiles.

3.2.4 Decoupled Negative Gradient Profiles (DNG)

A particular kind of profiles characterized by a decrease in concentration with altitude is the DNG typology. Within this class, observed in 20% of cases (during 5 days), a lack of symmetry between N_{14-260} and $N_{260-1200}$ – $N_{>1200}$ was
15 observed (Figure 4l-n). The average value of AS_h (corresponding to $H_s=0$) was 585±90 m. The main wind direction was the same as in PG profiles (SE-E direction; Figure 5d) but with a lower wind speed (close to that of HO profiles; 0-2 m s⁻¹; average of 0.7±0.1 m s⁻¹ at 33 m).

Figure 4n shows two strong, positive θ inversions. The first one, ground based, resulted in +1.3±0.4 K increase from ground; the second one characterized by +1.1±0.2 K increase from $H_s=0$.

20 Within this condition, N_{14-260} showed a concentration peak close to the ground of 601.3±19.9 cm⁻³ that was not present for $N_{260-1200}$ and $N_{>1200}$. N_{14-260} quickly decreased above the ground-based peak (-56.7±4.4%) to a concentration value of 260.6±13.1 cm⁻³ analogous to that observed in standard NG profiles (252.3±17.5 cm⁻³) below the AS_h (before reaching $H_s=0$). $N_{260-1200}$ and $N_{>1200}$ instead remained quite constant (32.4±0.8 cm⁻³ and 0.17±0.01 cm⁻³, respectively) from ground until $H_s=0$ where decreased by -31.1±2.9% (to 22.3±0.8 cm⁻³) and by -
25 54.2±4.7% (to 0.08±0.01 cm⁻³), respectively.

Interestingly, eBC concentrations behave contrary to the N_{14-260} aerosol fraction. Lowest eBC concentrations were found close to the ground (36±11 ng m⁻³; b_{abs} was 0.22±0.06 Mm⁻¹) in correspondence of the N_{14-260} concentration peak. Above this peak, eBC concentrations were higher (121±5 ng m⁻³; b_{abs} was 0.74±0.03 Mm⁻¹).

All the aforementioned observations suggest that a particular process could have influenced ground-level
30 concentrations for this size class only. In order to shed light on this process several parameters will be here below considered, namely: meteorological parameters, the aerosol chemical composition and the aerosol number size distribution. Starting with meteorological parameters, and recalling first Figure 2d, we see that the behavior of smallest particles in the proximity of the ground can be observed concomitantly to the presence of ground-based θ inversions, a necessary condition (or a concurrent cause) to promote the presence of ground-based concentration
35 peaks for N_{14-260} . The crucial point to unravel this phenomenon is to understand the possible origin of this particles. Thus, ground-based aerosol and meteorological measurements, collected at Gruebadet laboratory and at the CCT (section 2.1) and temporally coincident with the observation of DNG profile, were considered.

Figure 8a-d shows the ground-level PM₁₀ chemical composition determined for the four categories (HO, PG, NG, DNG) of profiles.

The nss-nc-SO₄²⁻ in DNG profiles (1349.9±354.7 ng m⁻³) was 3.0±0.7 times higher than that observed in the other profile classes (389.9±113.2 ng m⁻³, 410.5±104.3 ng m⁻³ and 622.1±210.0 ng m⁻³, for HO, PG and NG). At the same time, the ss-SO₄²⁻ was 0.6±0.2 times lower compared to the other profile classes while the cr-SO₄²⁻ remained quite constant (ratio 1.1±0.4). The same pattern can be observed considering the aforementioned sulfate fractions in the PM₁₀ samples (Figure S7, supplemental material).

These observations, coupled with the lowering of eBC fraction in proximity of the ground (Figure 4l) point towards the hypothesis that the ground-based N₁₄₋₂₆₀ concentration peak was secondary in origin. The nss-nc-SO₄²⁻ fraction during DNG profiles appeared in acidic form, as it was just poorly neutralized by the ammonium. Particularly, the w/w (weight/weight) nss-nc-SO₄²⁻/NH₄⁺ ratio was 1.6±0.4 times higher for DNG profiles (10.3±1.5) than that observed in the other profile classes: 6.1±1.9, 5.8±2.1 and 7.0±2.2 for HO, PG and NG, respectively. As reported in literature (Udisti et al., 2016; Becagli et al., 2012; Udisti et al., 2012) these values for DNG profiles feature the presence of sulfate in acidic form (H₂SO₄). This is in agreement with the finding that “springtime submicron aerosol in the Arctic surface sites is composed predominantly of partially neutralized sulfate and sea-salt, with lesser contributions from nitrate, BC, soil and trace elements” as reported in Quinn et al. (2002).

This information is very important when coupled with meteorological data measured at the CCT (Table 2). Focusing first on the air temperature, it can be observed that, during DNG profiles, the temperature close to the ground (-17.2±0.3 °C) was lower than that observed in the other profile classes: -9.7±0.5 °C, -5.9±0.3 °C and -9.9±0.2 for HO, PG and NG, respectively. In addition, the RH was 18.0±2.0% higher (73.6±0.3%) for DNG profiles, compared to that observed in the other profile classes. Finally, also the wind speed during DNG profiles was half than during the other profile classes and was not affected by north direction, avoiding the influence of Ny-Ålesund (Figure 5d). All the aforementioned conditions, featured during DNG profiles, can be resumed in: higher acidic sulfate fraction, lower eBC fraction, lower temperature, higher relative humidity and lower wind speed during DNG profiles.

As reported in literature (Kirkby et al., 2011; Reddington et al., 2011; Lovejoy et al., 2004) these conditions decrease the height of the barrier for new particle formation just considering the very simplified binary H₂SO₄-H₂O system. Under these conditions, the secondary aerosol formation can proceed at ambient acid concentrations in the cooler mid-troposphere and at lower altitude in polar regions. However, it has to be underlined that, as recently reported (Riccobono et al., 2014), organics plays a fundamental role for secondary aerosol formation. They were found in Ny-Ålesund even in spring (Zangrando et al., 2013). These figures, coupled with the aforementioned data indicated the N₁₄₋₂₆₀ concentration peaks at ground as locally formed secondary aerosol.

The ground-based aerosol number size distribution (Figure 6) shows a huge Aitken mode for DNG profiles, while it is negligible for the other profile classes. This mode was characterized by a geometric mean diameter D_g of 0.032±0.001 μm and by a geometric standard deviation σ_g of 1.790±0.006 that were in agreement with ten-year average values reported in Tunved et al. (2013) at the Zeppelin observatory during the month of April. The presence of a clearly visible Aitken mode in DNG profiles supports the aforementioned hypothesis of the presence of a ground-based plume of locally newly formed aerosol particles.

In order to estimate (meaning the order of magnitude) the contribution of locally formed aerosol, the method based on the N/eBC ratio (section 2.2.1), developed by Rodríguez and Cuevas (2007) was used. The value of S₁ (2.4±0.2) was taken as that of background aerosol above the the ground N₁₄₋₂₆₀ plume in DNG profiles. This value was very similar to that measured during homogeneous profiles (2.5±0.1) when a pure background aerosol was measured.

These S_1 values, obtained over Ny-Ålesund, are close to the lowest values reported in literature (Reche et al., 2011; Dall'Osto et al., 2013), a fact resulting from the d_{50} cutoff size of the miniDiSC (14 nm; section 2.2.1), which is higher than d_{50} cutoff sizes (~2-7 nm) usually present in the widely used condensation particle counters. Using this reference S_1 value, N_1 (background number concentration) and N_2 (locally formed secondary aerosol) were computed as reported in section 2.2.1. Their vertical behavior is reported in Figure 9. The total amount of secondary aerosol close to the ground is clearly visible and accounted on average for $63.7 \pm 5.6\%$ (up to 95% at ground) of the total N_{14-260} plume. In fact, within these plumes, the N_{14-260}/eBC ratio reached an average value of 22.5 ± 5.4 (maximum value of 54.8 at ground) clearly indicating the presence of a secondary formed aerosol (Reche et al., 2011; Dall'Osto et al., 2013). In addition to this, Figure 10 shows the temporal behavior of SMPS+APS data collected at Gruebadet during April 2011 together with the percentiles (25°, 50°, 75°, 90°) of the measured number size distribution. It is clearly evident the presence of nanoparticles (below 100 nm) even in Spring in the Arctic.

Interestingly, all the aforementioned results are analogous to data reported in ARCPAC by Brock et al. (2011). Within the surface inversion layer over sea-ice, they found a region of depleted BC and organic mass concentrations (lower than in the background case), while sulfate concentrations were similar or higher. However, under this condition, Brock et al. (2011), did not feature an increase in particle number concentration. Surprisingly, DNG profiles are more similar to vertical aerosol profiles discussed by Kupiszewski et al. (2013) during the summertime ASCOS campaign. In fact, they found a plume of nanoparticles within near-surface layer (not related with the behavior of accumulation mode particles) during new particle formation events. They hypothesize that the origin of ultrafine particles was related to biological processes. This observation becomes important when considering again the number size distribution reported in Figure 10. The 75° and 90° percentile exhibited a summer-like behavior when compared with Zeppelin data reported in Engvall et al. (2008) and in Tunved et al. (2013). These findings point towards the importance of measuring the frequencies of these episodes, present in the surface layer of Ny-Ålesund, together with their vertical development (i.e. vertical mixing), to understand their importance of CCN influencing the Arctic climate.

3.3 Summer phenomenology

Vertical profiles measured during summers 2011-2012 were also classified according to their vertical behavior (i.e. shape). They were averaged considering the relative position of each measured data point with respect to the AS_h . The obtained averaged vertical profiles were referred to the standardized height H_s . The result of the classification and averaging procedure is reported in Figure 11a-f (all profile data are reported in Figure S8, supplemental material). In summer, two main categories were observed:

- 1) Type 1, homogeneous profiles (HO), Figure 11a-c
- 2) Type 2, profiles characterized by the presence of shipping emissions (hereinafter addressed as SP), Figure 11d-f.

Average concentrations of aerosol (N_{14-260} , $N_{260-1200}$, $N_{>1200}$) and eBC below and above $H_s=0$ for each profile class are summarized in Table 3.

3.3.1 HO profiles

HO profiles (Type1, Figure 11a-c) were observed in 37% of cases due to the summer higher solar power density at disposal together with the low albedo as discussed in section 3.2. As already reported for springtime results, these are the only averaged profiles referred to an absolute height AGL because they did not show any AS_h to calculate H_s . During HO profiles, local wind (Figure 5e) was interestingly blowing from the same direction as in the case of HO springtime profiles: SW direction, from the glaciers behind Ny-Ålesund (Figure 1a) and not along the predominant NW-SE direction of the Kongsfjord. However, summertime HO profiles featured higher wind speed than in spring (range 0-11 $m s^{-1}$, average of $4.1 \pm 0.1 m s^{-1}$ at 33 m; Table 2). At the same time, as shown in Figure 11c, a slightly positive θ profiles characterized, on average, the HO profiles.

The aerosol number concentrations were found to be $435.9 \pm 5.8 cm^{-3}$ for N_{14-260} , $2.1 \pm 0.1 cm^{-3}$ for $N_{260-1200}$, and $4 \cdot 10^{-2} \pm 4 \cdot 10^{-3} cm^{-3}$ for $N_{>1200}$, respectively. Thus, N_{14-260} accounted for $99.5 \pm 1.9\%$ of the total aerosol number concentration, which is considerably higher than $81.9 \pm 16.8\%$ observed in springtime HO profiles. This is in agreement with the observations, reported in literature, that the sunlit summer period is dominated by small locally formed Aitken particles (Giardi et al., 2016; Tunved et al., 2013; Ström et al., 2009 and 2003; Udisti et al., 2013; Viola et al., 2013). eBC and the related b_{abs} were negligible, as also reported by Eleftheriadis et al. (2009). HO profiles were observed in the absence of ships anchoring in the Ny-Ålesund harbor.

3.3.2 Ship impact along vertical profiles

Summer vertical profiles showed a considerable impact of ship emissions. The number of ships and the number of passengers (a useful proxy of the ship dimension) was registered by the Kings-Bay Kull Company and it is reported in Figure S9 for summer 2011 and 2012, respectively. Particularly, 57 days with a total of 103 ship arrivals were registered during JJA of 2011 (62% of days; Figure S9a) while 78 days (85% of days) with 138 ships (Figure S9b) were registered during JJA of 2012.

Figure 12a-e reports the case study of 6th July 2011, when four ships anchored (not simultaneously) in the harbor of Ny-Ålesund from 0700 UTC to 1900 UTC. The largest ship arrived in the morning with approx. 1000 passengers. Figure 12a-d shows four profiles (0740 UTC, 0901 UTC, 0932 UTC and 1340 UTC) together with ground SMPS data collected at Gruvebadet (Figure 12e). The ship impact in the Kongsfjord, distant about 1.200 m as the crow flies, is clearly evident. N_{14-260} concentrations reached values up to $2-3 \cdot 10^4 cm^{-3}$ and the eBC concentrations reached the maximum value of $2000 ng m^{-3}$ (at 0932 UTC).

To highlight the impact of ship emission along the two years, average vertical profiles were calculated. The result is shown in Figure 11d-f. During SP, wind blew mainly from the N-NE direction (where the harbor is located; Figure 5f). The average wind speed was $2.6 \pm 0.1 m s^{-1}$. Once a ship plume arrived, SP profiles were characterized by high pollution levels below $H_s=0$. Figure 11f also shows a positive gradient of θ ($+1.4 \pm 0.2 K$ increase from $H_s=0$). This gradient constrains the ship plume above ground to an altitude variable with time as shown in Figure 12a-d (from 103 m to 592 m). Particularly, N_{14-260} showed a concentration peak close to the ground of $9.0 \cdot 10^3 \pm 2.5 \cdot 10^2 cm^{-3}$, $N_{260-1200}$ of $7.0 \pm 0.7 cm^{-3}$ and $N_{>1200}$ of $6 \cdot 10^{-2} \pm 4 \cdot 10^{-3} cm^{-3}$. eBC concentrations behave similarly reaching concentrations of $319 \pm 14 ng m^{-3}$. These concentration values were higher by a factor of 13.9 ± 0.7 (N_{14-260}), 5.1 ± 0.5 ($N_{260-1200}$), 4.8 ± 0.4 ($N_{>1200}$) and 13.4 ± 1.0 (eBC) than those observed above $H_s=0$ where an intense decrease of both aerosol and eBC is observed. Crossing the AS_h , aerosol concentrations decreased to $648.1 \pm 27.3 cm^{-3}$ for N_{14-260} , to $1.4 \pm 0.1 cm^{-3}$ for $N_{260-1200}$ and to $1 \cdot 10^{-2} \pm 1 \cdot 10^{-3} cm^{-3}$ for $N_{>1200}$. These values were close to the

background values observed during summer HO profiles. eBC behave similarly decreasing to $24 \pm 1 \text{ ng m}^{-3}$. As the ship plume of eBC is located close to the ground, it may exert positive forcing (Flanner, 2013; Brock et al., 2011; Seinfeld and Pandis, 2006; Hansen and Nazarenko, 2004). In fact, the b_{abs} reached values of $1.95 \pm 0.09 \text{ Mm}^{-1}$ below $H_s=0$.

5 It is important to note that SP profiles were observed in summer. In summer the long-range transport of aerosol from mid-latitudes is minor (Browse et al., 2012; Quinn et al., 2008; Stohl et al., 2006) and the locally formed aerosol becomes dominant (Giardi et al., 2015; Tunved et al., 2013; Ström et al., 2009 and 2003). Within this context, the SP profiles show that the rising shipping emissions in the Arctic (Corbett et al., 2010; Granier et al., 2006) could affect the concentrations and the vertical distribution of aerosol, resulting in a positive forcing, induced
10 by a positive feedback through the local anthropogenic impact on climate.

4 Conclusions

Vertical profiles of in situ aerosol number size distribution and black carbon measurements were conducted by tethered balloon in the atmosphere over Ny-Ålesund. The balloon payload was equipped with an Optical Particle Counter (31 size classes, 0.25 to 32 μm), an electrical particle detector ($d_{50}=14 \text{ nm}$), two micro-Aethalometers and meteorological sensors. Moreover, chemical analysis of filter samples, aerosol size distribution and a full set of meteorological parameters at ground were available. A systematic study of vertical profiles of aerosol number size distribution (14 nm – 32 μm) and equivalent black carbon concentrations was conducted. 200 vertical profiles were measured during spring and summer along 2 years (2011-2012). Vertical aerosol profiles were classified for
15 each season according to their shape allowing to obtain a description of the seasonal phenomenology of vertical aerosol properties in the Arctic.

Focusing on spring, four main types of profiles were found.

The first one was the homogeneous profiles class (HO), characterized by constant aerosol and eBC concentration with altitude, and representative of Arctic background conditions.

25 The second class was that of positive gradient profiles (PG) characterized by an increase of aerosol concentration with altitude. The importance of this class is related to the fact that aerosols can act as CCN influencing the cloud cover and thus the longwave fluxes.

The third class was characterized by negative gradient profiles (NG) with a decrease of aerosol concentration with altitude and thus high pollution level close to the ground. This finding is very important because a eBC layer
30 located immediately above snow and ice may induce a positive forcing.

The fourth class of profiles was characterized by negative gradients located at different altitude in function of size (DNG). These profiles were observed during ground-based events of locally formed secondary aerosol. It is important as locally formed aerosol can act as CCN. As low clouds play a particular role in the sensitive Arctic climate system, the aerosol-cloud interactions will be one focus of future research activities within the Ny-Ålesund research community, manifested in the Ny-Ålesund Atmospheric Flagship program.

35 The four categories described above are important when considering the large amount of ground-based data available for comparisons with modelling results. Particularly, for HO profiles, ground measurements were fully representative of the vertical column (up until $\sim 1 \text{ km}$, vertical limit of experimental activity). During NG and PG profiles, the ground-based measurements were representative of the air column up to the planetary boundary layer.
40 Finally, DNG profiles showed that ground-based measurements differ from those conducted aloft. However, the

last case was influenced by secondary aerosol formation that can be easily detected by an SMPS (or similar experimental devices). Thus, ground-based measurements (coupled with a proper PBL determination) are fundamental and very useful for model comparison. In addition to these, vertical profiles shed light on the phenomenology and dynamics of the vertical distribution of aerosols in the Arctic.

5 During summer, two main types of profiles were observed. The first class was characterized by homogeneous background condition profiles while the second class reflected the impact of shipping emissions. The ship impact resulted in a plume of aerosol and eBC pollution constrained close to the ground. In summer, atmospheric transport from mid-latitudes is minor. Increasing shipping emissions in the Arctic could significantly increase anthropogenic aerosol and eBC concentrations in the summer Arctic, enhancing the climate change that this region is already
10 experiencing.

Acknowledgements

The scientific activity in Ny Alesund was carried out in the framework of the CNR Polar Program. We thank the PRIN2009 “ARCTICA” project for financial support. We thank the Alfred Wegener Institute and the CICCI
15 project for logistical support. We thank both Brent Holben and Piotr Sobolewski for their effort in establishing and maintaining the AERONET Hornsund site. Finally, we thank LSI-Lastem and Federico Pasquini for the cooperation concerning meteorological instruments.

References

- 20 Andreae, M.O and Gelencsér A.: Black carbon or brown carbon? The nature of light-absorbing carbonaceous aerosols, *Atmos. Chem. Phys.*, 6, 3131–3148, 2006.
- Arnett, W. P., Hamasha, K., Moosmüller, H., Sheridan, P. J. and Ogren, J. a.: Towards Aerosol Light-Absorption Measurements with a 7-Wavelength Aethalometer: Evaluation with a Photoacoustic Instrument and 3-Wavelength Nephelometer, *Aerosol Sci. Tech.*, 39(1), 17–29, doi:10.1080/027868290901972, 2005.
- 25 Ban-Weiss, G. a., Cao, L., Bala, G. and Caldeira, K.: Dependence of climate forcing and response on the altitude of black carbon aerosols, *Climate Dynamics*, 38(5-6), 897–911, doi:10.1007/s00382-011-1052-y, 2011.
- Baron, P.A., and Willeke, K.: *Aerosol measurements. Principles, Techniques and Applications*. Wiley-Interscience, Second edition, 2005.
- Barrie, L. A., and Hoff, R. M: Five years of air chemistry observations in the Arctic, *Atmos. Environ.*, 19, 1995–
30 2010, 1985.
- Bates, T. S., Quinn, P. K., Johnson, J. E., Corless, a., Brechtel, F. J., Stalin, S. E., Meinig, C. and Burkhardt, J. F.: Measurements of atmospheric aerosol vertical distributions above Svalbard, Norway, using unmanned aerial systems (UAS), *Atmospheric Measurement Techniques*, 6(8), 2115–2120, doi:10.5194/amt-6-2115-2013, 2013.
- 35 Becagli S., Ghedini, C., Peeters, S., Rottiers, A., Traversi, R., Udisti, R., Chiari, M., Jalba, A., Despiu, S., Dayan, U., Temara, A.: MBAS (Methylene Blue Active Substances) and LAS (Linear Alkylbenzene Sulphonates) in Mediterranean coastal aerosols: sources and transport processes. *Atmos. Environ.*, 45, 6788-6801, 2011.
- Becagli, S., Scarchilli, C., Traversi, R., Dayan, U., Severi, M., Frosini, D., Vitale, V., Mazzola, M., Lupi, A., Nava, S., Udisti, R.: Study of present-day sources and transport processes affecting oxidised sulphur compounds in atmospheric aerosols at Dome C (Antarctica) from year-round sampling campaigns. *Atmos. Environ.*, 52, 98-108,
40 2012.

- Bhatt, U.S., Walker, D.A., Raynolds, M.K., Comiso, J.C., Epstein, H.E., Gia, G.-S., Gens, R., Pinzon, J.E., Tucker, C.J., Tweediw, C.E., Webber, P.J.: Circumpolar Arctic tundra vegetative change is linked to sea ice decline. *Earth Interact.* 14, 1–20, 2010.
- Bond, T. C., Doherty, S. J., Fahey, D. W., Forster, P. M., Berntsen, T., Deangelo, B. J., Flanner, M. G., Ghan, S., Kärcher, B., Koch, D., Kinne, S., Kondo, Y. and Quinn, P. K.: Bounding the role of black carbon in the climate system : A scientific assessment, *J. Geophys. Res.*, 118, 1–173, doi:10.1002/jgrd.50171, 2013.
- Bowen, H.J.M.: *Environmental Chemistry of the Elements*. Academic Press, London, 1979.
- Brock, C. A., Radke, L.F., Lyons, J. H., and Hobbs, P. V. : Arctic hazes in summer over Greenland and the North American Arctic, I, Incidence and origins, *J. Atmos. Chem.* 9, 129–148, 1989.
- 10 Brock, C. a., Cozic, J., Bahreini, R., Froyd, K. D., Middlebrook, a. M., McComiskey, a., Brioude, J., Cooper, O. R., Stohl, a., Aikin, K. C., de Gouw, J. a., Fahey, D. W., Ferrare, R. a., Gao, R.-S., Gore, W., Holloway, J. S., Hübler, G., Jefferson, a., Lack, D. a., Lance, S., Moore, R. H., Murphy, D. M., Nenes, a., Novelli, P. C., Nowak, J. B., Ogren, J. a., Peischl, J., Pierce, R. B., Pilewskie, P., Quinn, P. K., Ryerson, T. B., Schmidt, K. S., Schwarz, J. P., Sodemann, H., Spackman, J. R., Stark, H., Thomson, D. S., Thornberry, T., Veres, P., Watts, L. a., Warneke, C. and Wollny, a. G.: Characteristics, sources, and transport of aerosols measured in spring 2008 during the aerosol, radiation, and cloud processes affecting Arctic Climate (ARCPAC) Project, *Atmospheric Chemistry and Physics*, 11(6), 2423–2453, doi:10.5194/acp-11-2423-2011, 2011.
- 15 Browse, J., Carslaw, K.S., Arnold, S., Pringle, K.J. and Boucher O.: The scavenging processes controlling the seasonal cycle in Arctic sulphate and black carbon aerosol, *Atmos. Chem. Phys.*, 12, 6775-6798, 2012.
- 20 Browse, J., Carslaw, K. S., Schmidt, a. and Corbett, J. J.: Impact of future Arctic shipping on high-latitude black carbon deposition, *Geophysical Research Letters*, 40(16), 4459–4463, doi:10.1002/grl.50876, 2013.
- Corbett, J. J., Lack, D. a., Winebrake, J. J., Harder, S., Silberman, J. a. and Gold, M.: Arctic shipping emissions inventories and future scenarios, *Atmospheric Chemistry and Physics*, 10(19), 9689–9704, doi:10.5194/acp-10-9689-2010, 2010.
- 25 Dai C.Y., Gao Z.Q., Wang Q., Cheng G. : Analysis of atmospheric boundary layer height characteristics over the Arctic Ocean using the aircraft and GPS soundings. *Atmos. Oceanic Sci. Lett.* 4: 124, 2011.
- Dall’Osto, M., Thorpe, A., Beddows, D. C. S., Harrison, R. M., Barlow, J. F., Dunbar, T., Williams, P. I., and Coe, H.: Remark- able dynamics of nanoparticles in the urban atmosphere, *At- mos. Chem. Phys.*, 11, 6623–6637, doi:10.5194/acp-11-6623- 2011, 2011.
- 30 Dall’Osto, M., Querol, X., Alastuey, A., O’Dowd, C., Harrison, R. M., Wenger, J. and Gómez-Moreno, F. J.: On the spatial distribution and evolution of ultrafine particles in Barcelona, *Atmospheric Chemistry and Physics*, 13(2), 741–759, doi:10.5194/acp-13-741-2013, 2013.
- Di Liberto, L., Angelini, F., Pietroni, I., Cairo, F., Di Donfrancesco, G., Viola, A., Argentini, S., Fierli, F., Gobbi, G., Maturilli, M., Neuber, R. and Snels, M.: Estimate of the Arctic Convective Boundary Layer Height from Lidar Observations: A Case Study, *Adv. Met.*, 2012:ID851927,1-9, doi:10.1155/2012/851927, 2012.
- 35 Drinovec, L., Močnik, G., Zotter, P., Prévôt, A. S. H., Ruckstuhl, C., Coz, E., Rupakheti, M., Sciare, J., Müller, T., Wiedensohler, A., and Hansen, A. D. A.: The "dual-spot" Aethalometer: an improved measurement of aerosol black carbon with real-time loading compensation, *Atmos. Meas. Tech.*, 8, 1965-1979, doi: 10.5194/amt-8-1965-2015, 2015.
- 40 Eckhardt, S., Stohl, a., Beirle, S., Spichtinger, N., James, P., Forster, C., Junker, C., Wagner, T., Platt, U. and

- Jennings, S. G.: The North Atlantic Oscillation controls air pollution transport to the Arctic, *Atmospheric Chemistry and Physics Discussions*, 3(3), 3222–3240, doi:10.5194/acpd-3-3222-2003, 2003.
- Eckhardt, S., Hermansen, O., Grythe, H., Fiebig, M., Stebel, K., Cassiani, M., Baecklund, a. and Stohl, a.: The influence of cruise ship emissions on air pollution in Svalbard – a harbinger of a more polluted Arctic?, *Atmospheric Chemistry and Physics*, 13(16), 8401–8409, doi:10.5194/acp-13-8401-2013, 2013.
- 5 Eleftheriadis, K., Vratolis, S. and Nyeki, S.: Aerosol black carbon in the European Arctic: Measurements at Zeppelin station, Ny-Ålesund, Svalbard from 1998-2007, *Geophysical Research Letters*, 36(2), doi:10.1029/2008GL035741, 2009.
- Engvall, A., Krejci, R. and Str, J.: and Physics Changes in aerosol properties during spring-summer period in the Arctic troposphere, , 445–462, 2008a.
- 10 Engvall, A.-C., Krejci, R., Ström, J., Minikin, A., Treffeisen, R., Stohl, A. and Herber, A.: In-situ airborne observations of the microphysical properties of the Arctic tropospheric aerosol during late spring and summer, *Tellus B*, 080414161623888–???, doi:10.1111/j.1600-0889.2008.00348.x, 2008b.
- Ferrero, L., Bolzacchini, E., Petraccone S., Perrone, M. G., Sangiorgi, G., Lo Porto, C., Lazzati, Z., and Ferrini, B.: Vertical profiles of particulate matter over Milan during winter 2005/2006, *Fresen. Environ. Bull.*, 16(6), 697–700, 2007.
- 15 Ferrero, L., Mocnik, G., Ferrini, B. S., Perrone, M. G., Sangiorgi, G. and Bolzacchini, E.: Vertical profiles of aerosol absorption coefficient from micro-Aethalometer data and Mie calculation over Milan., *Sci. Total Environ.*, 409(14), 2824–37, doi:10.1016/j.scitotenv.2011.04.022, 2011a.
- 20 Ferrero, L., Riccio, a., Perrone, M. G., Sangiorgi, G., Ferrini, B. S. and Bolzacchini, E.: Mixing height determination by tethered balloon-based particle soundings and modeling simulations, *Atmos. Res*, 102(1-2), 145–156, doi:10.1016/j.atmosres.2011.06.016, 2011b.
- Ferrero, L., Cappelletti, D., Moroni, B., Sangiorgi, G., Perrone, M. G., Crocchianti, S. and Bolzacchini, E.: Wintertime aerosol dynamics and chemical composition across the mixing layer over basin valleys, *Atmos. Environ.*, 56, 143–153, doi:10.1016/j.atmosenv.2012.03.071, 2012.
- 25 Ferrero, L., Castelli, M., Ferrini, B.S., Moscatelli, M., Perrone, M.G., Sangiorgi, G., Rovelli, G., D’Angelo, L., Moroni, B., Scardazza, F., Mocnik, G., Bolzacchini, E., Petitta, M., Cappelletti, D.: Impact of Black Carbon Aerosol over Italian basin valleys: high resolution measurements along vertical profiles, radiative forcing and heating rate. *Atmos. Chem. Phys.*, 14, 9641–9664, 2014.
- 30 Fierz, M., Houle, C., Steigmeier, P. and Burtscher, H.: Design, Calibration, and Field Performance of a Miniature Diffusion Size Classifier, *Aerosol Science and Technology*, 45(1), 1–10, doi:10.1080/02786826.2010.516283, 2011.
- Flanner, M. G.: Arctic climate sensitivity to local black carbon, *Journal of Geophysical Research: Atmospheres*, 118(4), 1840–1851, doi:10.1002/jgrd.50176, 2013.
- 35 Francis, J.A., Hunter, E.: New insight into the disappearing Arctic sea ice. *EOS Trans. Am. Geophys. Union* 87, 509–511, 2006.
- Giardi, F., Becagli, S., Traversi, R., Frosini, D., Severi, M., Caiazza, L., Ancillotti, C., Cappelletti, D., Moroni, B., Grotti, M., Bazzano, A., Lupi, A., Mazzola, M., Vitale, V., Malandrino, M., Ferrero, L., Bolzacchini, E., Viola, A., Udisti, R.: Size distribution and ion composition of aerosol collected at Ny Ålesund in the spring-summer field campaign 2013. *Rend. Lincei*, DOI 10.1007/s12210-016-0529-3, 2016.
- 40

- Gilardoni, S., Vignati, E., Wilson, J.: Using measurements for evaluation of black carbon modeling, *Atmos. Chem. Phys.*, 11, 439–455, 2011.
- Granier, C., Niemeier, U., Jungclaus, J. H., Emmons, L., Hess, P., Lamarque, J.-F., Walters, S. and Brasseur, G. P.: Ozone pollution from future ship traffic in the Arctic northern passages, *Geophysical Research Letters*, 33(13), L13807, doi:10.1029/2006GL026180, 2006.
- Guyon, P., Boucher, O., Graham, B., Beck, J., Mayol-Bracero, O. L., Roberts, G. C., Maenhaut, W., Artaxo, P. and Andreae, M. O.: Refractive index of aerosol particles over the Amazon tropical forest during LBA-EUSTACH 1999, *J. Aerosol Sci.*, 34(7), 883–907, doi:10.1016/S0021-8502(03)00052-1, 2003.
- Hansen, A.D.A., and T. Novakov.: Aerosol black carbon measurements in the Arctic haze during AGASP-II, *J. Atmos. Chem.*, 9, 347–361, doi:10.1007/BF00052842, 1989.
- Hansen, J., Nazarenko, L.: Soot Climate Forcing via Snow and Ice Albedo. *Proc. Natl. Acad. Sci.* 101, 423–428. www.pnas.org/doi/10.1073/pnas.2237157100, 2004.
- Heim, M., Mullins, B. J., Umhauer, H. and Kasper, G.: Performance evaluation of three optical particle counters with an efficient “multimodal” calibration method, *Journal of Aerosol Science*, 39(12), 1019–1031, doi:10.1016/j.jaerosci.2008.07.006, 2008.
- Heyder, J. and Gebhart, J.: Optimization of response functions of light scattering instruments for size evaluation of aerosol particles, *Appl. Optics*, 18(5), 705–11, 1979.
- Hoffmann, A., Ritter, C., Stock, M., Shiobara, M., Lampert, A., Maturilli, M., Orgis, T. and Neuber, R.: Ground-based lidar measurements from Ny- Alesund during ASTAR, , 9059–9081, 2009.
- Howell, S.G., Clarke, A.D., Shinzuka, Y., Kapustin, V., McNaughton, C.S., Huebert, B.J.: Influence of relative humidity upon pollution and dust during ACE-Asia: Size distributions and implications for optical properties, *J. Geophys. Res.*, 111, D06205, doi:10.1029/2004JD005759, 2006.
- Intrieri, J.M., Fairall, C.W., Shupe, M.D., Persson, P.O.G., Andreas, E.L., Guest, P.S., Moritz, R.E.: Annual cycle of Arctic surface cloud forcing at SHEBA. *J. Geophys. Res.*, 107 (C10), doi:10.1029/2000JC000439, 2002.
- IPCC, 2013: *Climate Change 2013: The Physical Science Basis*. Cambridge University Press, Cambridge, United Kingdom and New York, USA, 2013.
- Jacob, D.J., Crawford, J.H., Maring, H., Clarke, A.D., Dibb, J.E., Emmons, L.K., Ferrare, R.A., Hostetler, C.A., Russell, P.B., Singh, H.B., Thompson, A.M., Shaw, G.E., McCauley, E., Pederson, J.R. and J. A. Fisher.: The Arctic Research of the Composition of the Troposphere from Aircraft and Satellites (ARCTAS) mission: design, execution, and first results, *Atmos. Chem. Phys.*, 10, 5191–5212, 2010.
- Jacobson, M.Z.: Short-term effects of controlling fossil-fuel soot, biofuel soot and gases, and methane on climate, arctic ice, and air pollution health, *J. Geophys. Res.*, 115, D14209, doi:10.1029/2009JD013795, 2010.
- Kaufman, Y.J., Tanré, D., Boucher, O.: A satellite view of aerosols in the climate system. *Nature*, 419, 215–223, 2002.
- Kirkby, J., Curtius, J., Almeida, J., Dunne, E., Duplissy, J., Ehrhart, S., Franchin, A., Gagné, S., Ickes, L., Kürten, A., Kupc, A., Metzger, A., Riccobono, F., Rondo, L., Schobesberger, S., Tsagkogeorgas, G., Wimmer, D., Amorim, A., Bianchi, F., Breitenlechner, M., David, A., Dommen, J., Downard, A., Ehn, M., Flagan, R. C., Haider, S., Hansel, A., Hauser, D., Jud, W., Junninen, H., Kreissl, F., Kvashin, A., Laaksonen, A., Lehtipalo, K., Lima, J., Lovejoy, E. R., Makhmutov, V., Mathot, S., Mikkilä, J., Minginette, P., Mogo, S., Nieminen, T., Onnela, A., Pereira, P., Petäjä, T., Schnitzhofer, R., Seinfeld, J. H., Sipilä, M., Stozhkov, Y., Stratmann, F., Tomé, A.,

- Vanhanen, J., Viisanen, Y., Vrtala, A., Wagner, P. E., Walther, H., Weingartner, E., Wex, H., Winkler, P. M., Carslaw, K. S., Worsnop, D. R., Baltensperger, U. and Kulmala, M.: Role of sulphuric acid, ammonia and galactic cosmic rays in atmospheric aerosol nucleation., *Nature*, 476(7361), 429–33, doi:10.1038/nature10343, 2011.
- Koch, D., Schulz, M., Kinne, S., McNaughton, C., Spackman, J. R., Balkanski, Y., Bauer, S. and Berntsen, T.: and
5 Physics Evaluation of black carbon estimations in global aerosol models, 9, 9001–9026, 2009.
- Koren, I., Kaufman, Y.J., Remer, L.A., Martins, J.V.: Measurements of the effect of amazon smoke on inhibition of cloud formation. *Science*, 303, 1342-1345, 2004.
- Koren, I., Martins, J.V., Remer, L.A., Afargan, H.: Smoke invigoration versus inhibition of clouds over the amazon, *Science*, 321, 946-949, 2008.
- 10 Kupiszewski, P., Leck, C., Tjernström, M., Sjogren, S., Sedlar, J., Graus, M., Müller, M., Brooks, B., Swietlicki, E., Norris, S. and Hansel, a.: Vertical profiling of aerosol particles and trace gases over the central Arctic Ocean during summer, *Atmospheric Chemistry and Physics*, 13(24), 12405–12431, doi:10.5194/acp-13-12405-2013, 2013.
- Lanconelli, C., Busetto, M., Mazzola, M., Lupi, A., Becagli, S., Frosini, D., Virkkula, A., Vitale, V.: Physical,
15 Chemical and Optical Properties of Aerosol at Ny Ålesund, 189 Svalbard: a Closure Study. Proceeding at the 1st Iberian Meeting on Aerosol Science and Technology, July 1-3, 2013, ISBN: 978-989-20-3962-6, pages 189-192, 2013.
- Lawson, R. P., Stamnes, K., Stamnes, J., Zmarzly, P., Koskuliks, J., Roden, C., Mo, Q., Carrithers, M. and Bland, G. L.: Deployment of a Tethered-Balloon System for Microphysics and Radiative Measurements in Mixed-Phase
20 Clouds at Ny-Ålesund and South Pole, *Journal of Atmospheric and Oceanic Technology*, 28(5), 656–670, doi:10.1175/2010JTECHA1439.1, 2011.
- Liu, Y. and Daum, P. H.: Relationship of refractive index to mass density and self-consistency of mixing rules for multicomponent mixtures like ambient aerosols, *J. Aerosol Sci.*, 39(11), 974–986, doi:10.1016/j.jaerosci.2008.06.006, 2008.
- 25 Lovejoy, E. R.: Atmospheric ion-induced nucleation of sulfuric acid and water, *Journal of Geophysical Research*, 109(D8), D08204, doi:10.1029/2003JD004460, 2004.
- Ma, X., Lu, J. Q., Brock, R. S., Jacobs, K. M., Yang, P. and Hu, X.-H.: Determination of complex refractive index of polystyrene microspheres from 370 to 1610 nm., *Physics in medicine and biology*, 48(24), 4165–72 [online] Available from: <http://www.ncbi.nlm.nih.gov/pubmed/14727759>, 2003.
- 30 Manabe, S., Wetherald, R.T.: The effect of doubling the CO₂ concentration on the climate of a general circulation model. *J. Atmos. Sci.* 32, 3–15, 1975.
- Massabò, D., Caponi, L., Bernardoni, V., Bove, M.C., Brotto, P., Calzolari, G., Cassola, F., Chiari, M., Fedi, M.E., Fermo, P., Giannoni, M., Lucarelli, F., Nava, S., Piazzalunga, A., Valli, G., Vecchi, R., Prati, P.: Multi-wavelength optical determination of black and brown carbon in atmospheric aerosols, *Atmos. Environ.*, 108, 1-12, 2015.
- 35 Maturilli, M. and Kayser M.: Arctic Warming, Moisture Increase and Circulation Changes Observed in the Ny-Ålesund Homogenized Radiosonde Record. *Theor. Appl. Climatol.* doi: 10.1007/s00704-016-1864-0, 2016.
- Mazzola M., Viola A.P., Lanconelli C., and Vitale V: Atmospheric observations at the Amundsen-Nobile Climate Change Tower in Ny-Alesund, Svalbard. *Rend. Lincei*, DOI 10.1007/s12210-016-0514-x, 2016.

- Mazzola, M., Tampieri, F., Viola, A.P., Lanconelli, C. and Choi, T.: Stable boundary layer vertical scales in the Arctic: observations and analyses at Ny-Ålesund, Svalbard. *Quarterly Journal of the Royal Meteorological Society*, *in press*, doi: 10.1002/qj.2727, 2015.
- Moroni, B., Becagli, S., Bolzacchini, E., Busetto, M., Cappelletti, D., Crocchianti, S., Ferrero, L., Frosini, D.,
5 Lanconelli, C., Lupi, A., Maturilli, M., Mazzola, M., Perrone, G., Sangiorgi, G., Traversi, R., Udisti, R., Viola A., Vitale, V.: Sources and properties of aerosol particles upon Ny-Ålesund (Svalbard Islands): results of integrated vertical profile measurements and electron microscopy analyses. *Advances in Meteorology*, 2015, 292081, 1-11, 2015.
- Nozaki, Y.: A Fresh Look at Element Distribution in the North Pacific. http://www.agu.org/eos_elec/97025e.html,
10 1997.
- Ødemark, K., Dalsøren, S. B., Samset, B. H., Berntsen, T. K., Fuglestad, J. S. and Myhre, G.: Short-lived climate forcers from current shipping and petroleum activities in the Arctic, *Atmospheric Chemistry and Physics*, 12(4), 1979–1993, doi:10.5194/acp-12-1979-2012, 2012.
- Overland, J.E., Wang, M.: Large-scale atmospheric circulation changes are associated with the recent loss of Arctic
15 sea ice. *Tellus* 62A, 1–9, 2010.
- Petzold, A., Ogren, J.A., Fiebig, M., Laj, P., Li, S.M., Baltensperger, U., Holzer-Popp, T., Kinne, S., Pappalardo, G., Sugimoto, N., Wehrli, C., Wiedensohler, A., Zhang, X.Y.: Recommendations for reporting “black carbon” measurements, *Atmos. Chem. Phys.*, 13, 8365-8379, 2013.
- Quinn, P. K., Bates, T. S., Baum, E., Doubleday, N., Fiore, a. M., Flanner, M., Fridlind, a., Garrett, T. J., Koch,
20 D., Menon, S., Shindell, D., Stohl, a. and Warren, S. G.: Short-lived pollutants in the Arctic: their climate impact and possible mitigation strategies, *Atmospheric Chemistry and Physics*, 8(6), 1723–1735, doi:10.5194/acp-8-1723-2008, 2008.
- Radke, L. F., Lyons, J. H., Hegg, D. A., Hobbs, P. V., and Bailey, I. H.: Airborne observations of Arctic aerosols, I, Characteristics of Arctic haze, *Geophys. Res. Lett.*, 11, 393–396, 1984.
- 25 Ramana, M. V., Ramanathan, V., Kim, D., Roberts, G. C. and Corrigan, C. E.: Albedo , atmospheric solar absorption and heating rate measurements with stacked UAVs, , 1931, 1913–1931, doi:10.1002/qj, 2007.
- Ramanathan, V. and Feng, Y.: Air pollution, greenhouse gases and climate change: Global and regional perspectives, *Atmos. Environ.*, 43(1), 37–50, doi:10.1016/j.atmosenv.2008.09.063, 2009.
- Ran, L., Deng, Z.Z., Xu, X.B., Yan, P., Lin, W.L., Wang, Y., Tian, P., Wang, P.C., Pan, W.L. and Lu, D.R.:
30 Vertical profiles of black carbon measured by a micro-aethalometer in summer in the North China Plain, *Atmos. Chem. Phys. Discuss.*, doi:10.5194/acp-2016-219, 2016.
- Reche, C., Querol, X., Alastuey, A., Viana, M., Pey, J., Moreno, T., Rodríguez, S., González, Y., Fernández-Camacho, R., de la Rosa, J., Dall’Osto, M., Prévôt, A. S. H., Hueglin, C., Harrison, R. M. and Quincey, P.: New considerations for PM, Black Carbon and particle number concentration for air quality monitoring across different
35 European cities, *Atmospheric Chemistry and Physics*, 11(13), 6207–6227, doi:10.5194/acp-11-6207-2011, 2011.
- Reddington, C. L., Carslaw, K. S., Spracklen, D. V., Frontoso, M. G., Collins, L., Merikanto, J., Minikin, a., Hamburger, T., Coe, H., Kulmala, M., Aalto, P., Flentje, H., Plass-Dülmer, C., Birmili, W., Wiedensohler, a., Wehner, B., Tuch, T., Sonntag, a., O’Dowd, C. D., Jennings, S. G., Dupuy, R., Baltensperger, U., Weingartner, E., Hansson, H. C., Tunved, P., Laj, P., Sellegri, K., Boulon, J., Putaud, J. P., Gruening, C., Swietlicki, E., Roldin,
40 P., Henzing, J. S., Moerman, M., Mihalopoulos, N., Kouvarakis, G., Ždímal, V., Zíková, N., Marinoni, a.,

- Bonasoni, P. and Duchi, R.: Primary versus secondary contributions to particle number concentrations in the European boundary layer, *Atmospheric Chemistry and Physics*, 11(23), 12007–12036, doi:10.5194/acp-11-12007-2011, 2011.
- Riccobono, F., Schobesberger, S., Scott, C. E., Dommen, J., Ortega, I. K., Rondo, L., Almeida, J., Amorim, A., Bianchi, F., Breitenlechner, M., David, A., Downard, A., Dunne, E. M., Duplissy, J., Ehrhart, S., Flagan, R. C., Franchin, A., Hansel, A., Junninen, H., Kajos, M., Keskinen, H., Kupc, A., Kurten, A., Kvashin, A. N., Laaksonen, A., Lehtipalo, K., Makhmutov, V., Mathot, S., Nieminen, T., Onnela, A., Petaja, T., Praplan, A. P., Santos, F. D., Schallhart, S., Seinfeld, J. H., Sipila, M., Spracklen, D. V., Stozhkov, Y., Stratmann, F., Tome, A., Tsagkogeorgas, G., Vaattovaara, P., Viisanen, Y., Vrtala, A., Wagner, P. E., Weingartner, E., Wex, H., Wimmer, D., Carslaw, K. S., Curtius, J., Donahue, N. M., Kirkby, J., Kulmala, M., Worsnop, D. R. and Baltensperger, U.: (Suppl.) Oxidation Products of Biogenic Emissions Contribute to Nucleation of Atmospheric Particles, *Science*, 344(6185), 717–721, doi:10.1126/science.1243527, 2014.
- Rodríguez, S. and Cuevas, E.: The contributions of “minimum primary emissions” and “new particle formation enhancements” to the particle number concentration in urban air, *J. Aerosol Sci.*, 38, 1207–1219, doi:10.1016/j.jaerosci.2007.09.001, 2007.
- Samset, B. H., Myhre, G., Schulz, M., Balkanski, Y., Bauer, S., Berntsen, T. K., Bian, H., Bellouin, N., Diehl, T., Easter, R. C., Ghan, S. J., Iversen, T., Kinne, S., Kirkevåg, a., Lamarque, J.-F., Lin, G., Liu, X., Penner, J. E., Seland, Ø., Skeie, R. B., Stier, P., Takemura, T., Tsigaridis, K. and Zhang, K.: Black carbon vertical profiles strongly affect its radiative forcing uncertainty, *Atmospheric Chemistry and Physics*, 13(5), 2423–2434, doi:10.5194/acp-13-2423-2013, 2013.
- Samset, B. H., Myhre, G., Herber, a., Kondo, Y., Li, S.-M., Moteki, N., Koike, M., Oshima, N., Schwarz, J. P., Balkanski, Y., Bauer, S. E., Bellouin, N., Berntsen, T. K., Bian, H., Chin, M., Diehl, T., Easter, R. C., Ghan, S. J., Iversen, T., Kirkevåg, a., Lamarque, J.-F., Lin, G., Liu, X., Penner, J. E., Schulz, M., Seland, Ø., Skeie, R. B., Stier, P., Takemura, T., Tsigaridis, K. and Zhang, K.: Modeled black carbon radiative forcing and atmospheric lifetime in AeroCom Phase II constrained by aircraft observations., 2014a.
- Samset, B. H., Myhre, G., Herber, a., Kondo, Y., Li, S.-M., Moteki, N., Koike, M., Oshima, N., Schwarz, J. P., Balkanski, Y., Bauer, S. E., Bellouin, N., Berntsen, T. K., Bian, H., Chin, M., Diehl, T., Easter, R. C., Ghan, S. J., Iversen, T., Kirkevåg, a., Lamarque, J.-F., Lin, G., Liu, X., Penner, J. E., Schulz, M., Seland, Ø., Skeie, R. B., Stier, P., Takemura, T., Tsigaridis, K. and Zhang, K.: Modelled black carbon radiative forcing and atmospheric lifetime in AeroCom Phase II constrained by aircraft observations, *Atmospheric Chemistry and Physics*, 14(22), 12465–12477, doi:10.5194/acp-14-12465-2014, 2014b.
- Sangiorgi, G., Ferrero, L., Perrone, M. G., Bolzacchini, E., Duane, M. and Larsen, B. R.: Vertical distribution of hydrocarbons in the low troposphere below and above the mixing height : Tethered balloon measurements in Milan, Italy, *Environ. Pollut.*, 159(12), 3545–3552, doi:10.1016/j.envpol.2011.08.012, 2011.
- Sand, M., Berntsen, T. K., Kay, J. E., Lamarque, J. F., Seland, Ø. and Kirkevåg, a.: The Arctic response to remote and local forcing of black carbon, *Atmospheric Chemistry and Physics*, 13(1), 211–224, doi:10.5194/acp-13-211-2013, 2013.
- Schmid, O., Artaxo, P., Arnott, W. P., Chand, D., Gatti, L. V., Frank, G. P., Hoffer, a., Schnaiter, M. and Andreae, M. O.: Spectral light absorption by ambient aerosols influenced by biomass burning in the Amazon Basin. I: Comparison and field calibration of absorption measurement techniques, *Atmospheric Chemistry and Physics*,

- 6(11), 3443–3462, doi:10.5194/acp-6-3443-2006, 2006.
- Schmid, O., Artaxo, P., Arnott, W. P., Chand, D., Gatti, L. V., Frank, G. P., Hoffer, a., Schnaiter, M. and Andreae, M. O.: Spectral light absorption by ambient aerosols influenced by biomass burning in the Amazon Basin. I: Comparison and field calibration of absorption measurement techniques, *Atmos. Chem. Phys.*, 6(11), 3443–3462, doi:10.5194/acp-6-3443-2006, 2006.
- Schumann, T.: On the use of a modified clean-room optical particle counter for atmospheric aerosols at high relative humidity, *Atmospheric Research*, 25(6), 499–520, doi:10.1016/0169-8095(90)90035-B, 1990.
- Schwarz, J. P., Spackman, J. R., Gao, R. S., Watts, L. a., Stier, P., Schulz, M., Davis, S. M., Wofsy, S. C. and Fahey, D. W.: Global-scale black carbon profiles observed in the remote atmosphere and compared to models, *Geophys. Res. Lett.*, 37(18), n/a–n/a, doi:10.1029/2010GL044372, 2010.
- Schwarz, J.P., Samset, B.H., Perring, A.E., Spackman, J.R., Gao, R.S., Stier, P., Schultz, M.G., Moore, F.L., Ray, E.A. and Fahey, D.W.: Global-scale seasonally resolved black carbon vertical profiles over the Pacific, *Geophys. Res. Lett.*, 40, 5542-5547, 2013.
- Screen, J.A., Simmonds, I.: The central role of diminishing sea ice in recent Arctic temperature amplification. *Nature* 464, 1334–1337, 2010a.
- Screen, J.A., Simmonds, I.: Increasing fall-winter energy loss from the Arctic Ocean and its role in Arctic temperature amplification. *Geophys. Res. Lett.* 37, L16707. doi:10.1029/2010GL044136, 2010b.
- Seibert, P., Beyrich, F., Gryning, S., Jo, S., Rasmussen, A. and Tercier, P.: Review and intercomparison of operational methods for the determination of the mixing height, *Atmospheric Environment*, 34, 1001–1027, doi:10.1016/S1352-2310(99)00349-0 2000.
- Seinfeld, J.H., Pandis, S.N.; *Atmos. Chem. Phys. – From air pollution to climate change*. Wiley-Interscience edition, 2006.
- Serreze, M. C. and Barry, R. G.: Processes and impacts of Arctic amplification: A research synthesis, *Global and Planetary Change*, 77(1-2), 85–96, doi:10.1016/j.gloplacha.2011.03.004, 2011.
- Serreze, M. C., Barrett, A. P., Slater, A. G., Steele, M., Zhang, J. and Trenberth, K. E.: The large-scale energy budget of the Arctic, *Journal of Geophysical Research*, 112(D11), D11122, doi:10.1029/2006JD008230, 2007.
- Shaw, G. E: The Arctic haze phenomenon, *BAMS*, 2403–2413, 1995.
- Shindell, D. and Faluvegi, G.: Climate response to regional radiative forcing during the twentieth century, *Nature Geoscience*, 2(4), 294–300, doi:10.1038/ngeo473, 2009.
- Shindell, D., Kuylenstierna, J.C.I., Vignati, E., Van Dingenen, R., Amann, M., Klimont, Z., Anenberg, S.C., Muller, N., et al.: Simultaneously mitigating near-term climate change and improving human health and food security, *Science*, 335 (6065), 183–189, doi:10.1126/science.1210026, 2012.
- Spackman, J. R., Gao, R. S., Neff, W. D., Schwarz, J. P., Watts, L. a., Fahey, D. W., Holloway, J. S., Ryerson, T. B., Peischl, J. and Brock, C. a.: Aircraft observations of enhancement and depletion of black carbon mass in the springtime Arctic, *Atmospheric Chemistry and Physics*, 10(19), 9667–9680, doi:10.5194/acp-10-9667-2010, 2010.
- Stock, M., Ritter, C., Herber, a., von Hoyningen-Huene, W., Baibakov, K., Gräser, J., Orgis, T., Treffeisen, R., Zinoviev, N., Makshtas, a. and Dethloff, K.: Springtime Arctic aerosol: Smoke versus haze, a case study for March 2008, *Atmospheric Environment*, 52(March 2008), 48–55, doi:10.1016/j.atmosenv.2011.06.051, 2012.
- Stohl, A.: Characteristics of atmospheric transport into the Arctic troposphere, *J. Geophys. Res.*, 111, D11306,

- doi:10.1029/2005JD006888, 2006.
- Stohl, A., Klimont, Z., Eckhardt, S., Kupiainen, K., Shevchenko, V.P., Kopeikin, V.M. and Novigatsky, A.N.: Black carbon in the Arctic: the underestimated role of gas flaring and residential combustion emissions, *Atmos. Chem. Phys.*, 13, 8833–8855, 2013.
- 5 Stone, R.S., A. Herber, V. Vitale, M. Mazzola, A. Lupi, R.C. Schnell, E.G. Dutton, P.S.K. Liu, S.M. Li, K. Dethloff, A. Lampert, C. Ritter, M. Stock, R., Neuber and M. Maturilli.: A three-dimensional characterization of Arctic aerosols from airborne Sun photometer observations: PAMARCMIP, April 2009, *Journal of Geophysical Research: Atmospheres*, 115, doi 10.1029/2009jd013605, 2010.
- 10 Ström, J., Umegård, J., Tørseth, K., Tunved, P., Hansson, H.-C., Holmén, K., Wismann, V., Herber, a. and König-Langlo, G.: One year of particle size distribution and aerosol chemical composition measurements at the Zeppelin Station, Svalbard, March 2000–March 2001, *Physics and Chemistry of the Earth, Parts A/B/C*, 28(28-32), 1181–1190, doi:10.1016/j.pce.2003.08.058, 2003.
- 15 Ström, J., Engvall, A.-C., Delbart, F., Krejci, R. and Treffeisen, R.: On small particles in the Arctic summer boundary layer: observations at two different heights near Ny-Ålesund, Svalbard, *Tellus B*, 61(2), 473–482, doi:10.1111/j.1600-0889.2008.00412.x, 2009.
- Tunved, P., Ström, J. and Krejci, R.: Arctic aerosol life cycle: linking aerosol size distributions observed between 2000 and 2010 with air mass transport and precipitation at Zeppelin station, Ny-Ålesund, Svalbard, *Atmospheric Chemistry and Physics*, 13(7), 3643–3660, doi:10.5194/acp-13-3643-2013, 2013.
- 20 Turpin, B.J., Lim, H.J.: Species contributions to PM_{2.5} mass concentrations: revisiting common assumptions for estimating organic mass. *Aerosol Sci Technol.*, 35, 602–10, 2001.
- Udisti, R., Becagli, S., Benassai, S., Castellano, E., Fattori, I., Innocenti, M., Migliori, A., Traversi, R.: Atmosphere-snow interaction by a comparison between aerosol and uppermost snow layers composition at Dome C (East Antarctica). *Ann. Glaciol.*, 39, 53-61, 2004.
- 25 Udisti, R., Dayan, U., Becagli, S., Busetto, M., Frosini, D., Legrand, M., Lucarelli, F., Preunkert, S., Severi, M., Traversi, R., Vitale, V.: Sea-spray aerosol in central Antarctica. Present atmospheric behavior and implications for paleoclimatic reconstructions. *Atmos. Environ.*, 52, 109-120, 2012.
- Udisti, R., Becagli, S., Frosini, D., Ghedini, C., Rugi, F., Severi, M., Traversi, R., Zanini, R., Calzolari, G., Chiari, M., Lucarelli, F., Nava, S., Ardini F, Grotti M, Vione D, Malandrino M, Bolzacchini E, Ferrero, L., Perrone, M.G., Sangiorgi, G., Francesconi, S., Giannarelli, S., Cappelletti, D., Moroni, B., Ceccato, D., Mittner, P., Sartori, P.: 30 Activity and preliminary results from the 2011-2012 field seasons at Ny-Ålesund. vol. DTA 14/2013, p. 53-68, CNR Edizioni, ISSN 2239-5172, 2013.
- Udisti, R., Bazzano, A., Becagli, S., Bolzacchini, E., Caiazzo, L., Cappelletti, D., Ferrero, L., Frosini, D., Giardi, F., Grotti, M., Lupi, A., Malandrino, M., Mazzola, M., Moroni, B., Severi, M., Traversi, R., Viola, A., Vitale, V.: 35 Sulfate source apportionment in the Ny Ålesund (Svalbard Islands) Arctic aerosol. *Rend. Lincei*, DOI 10.1007/s12210-016-0517-7, 2016.
- Vavrus, S., Waliser, D., Schweiger, A., Francis, J.A.: Simulations of 20th and 21st century Arctic cloud amount in the global climate models assessed in the IPCC AR4. *Climate Dyn.* 33, 1099–1115. doi:10.1007/s00382-008-0475-6, 2009.

- Vihma, T., Kilpeläinen, T., Manninen, M., Sjöblom, A., Jakobson, E., Palo, T., Jaagus, J., Maturilli, M.: Characteristics of temperature and humidity inversions and low-level jets over Svalbard fjords in spring, *Adv. Met.*, 2011:ID486807, doi: 10.1155/2011/486807, 2011.
- 5 Viola, A., Vitale, V., Petroni, I., Tampieri, F., Mazzola, M., Lanconelli, C., Busetto, M., Lupi, A., Di Liberto, L., Conidi, A., Ianniello, A., Salvatori, R., Esposito, G., Spataro, F., Udisti, R., Becagli, S., Frosini, D., Ghedini, C., Traversi, R., Cappelletti, D., Valt, M., Turetta, C.: Atmospheric studies at “Dirigibile Italia”. vol. DTA 14/2013, p. 35-52, CNR Edizioni, ISSN 2239-5172, 2013.
- 10 Wagenbach, D., Preunkert, S., Schäfer, J., Jung, W., and Tomadin, L.: Northward transport of Saharan dust recorded in a deep alpine ice core, in: *The Impact of Desert Dust Across the Mediterranean*, edited by: Guerzoni, S. and Chester, R., Environmental Science and Technology Library, vol. 11, Springer, the Netherlands, 291–300, 1996.
- 15 Warneke, C., Froyd, K.D., Brioude, J., Bahreini, R., Brock, C.A., Cozic, J., De Gouw, J.A., Fahey, D.W., Ferrare, R., Holloway, J.S., Middlebrook, A.M., Miller, L., Montzka, S., Schwarz, J.P., Sodemann, H., Spackman, J.R., and A.Stohl, A.: An important contribution to springtime Arctic aerosol from biomass burning in Russia. *Geophys. Res. Letters*, 37:L01801, doi:10.1029/2009GL041816, 2010.
- Weingartner, E., Saathoff, H., Schnaiter, M., Streit, N., Bitnar, B. and Baltensperger, U.: Absorption of light by soot particles: determination of the absorption coefficient by means of aethalometers, *J. Aerosol Sci.*, 34(10), 1445–1463, doi:10.1016/S0021-8502(03)00359-8, 2003.
- 20 Wofsy, S.C., et al.: HIAPER Pole-to-Pole Observations (HIPPO): fine grained, global-scale measurements of climatically important atmospheric gases and aerosols. *Philosophical Transactions of the Royal Society*, 369, 2073-2086, 2011.
- Yang, X.-Y., Fyfe, J.C., Flato, G.M.: The role of poleward energy transport in Arctic temperature evolution. *Geophys. Res. Lett.* 37, L14803. doi:10.1029/2010GL042487, 2010.
- 25 Zangrando, R., Barbaro, E., Zennaro, P., Rossi, S., Kehrwald, N. M., Gabrieli, J., Barbante, C. and Gambaro, A.: Molecular markers of biomass burning in Arctic aerosols, *Environmental Science and Technology*, 47(15), 8565–8574, doi:10.1021/es400125r, 2013.

30

35

Date	UTC Time	N° profiles	max altitude (m)	Cloud base (m)
<u>Spring 2011</u>				
30-03-2011	1240-1518	6	741	No clouds
01-04-2011	0630-1725	10	788	No clouds
04-04-2011	1817-2018	6	748	1152
06-04-2011	1642-1922	8	716	No clouds
07-04-2011	1251-1923	10	712	No clouds
08-04-2011	0825-1944	14	740	No clouds/1534 ⁽¹⁾
10-04-2011	1245-1438	6	300	No clouds/984 ⁽²⁾
14-04-2011	1502-1558	5	738	No clouds
22-04-2011	1917-2009	4	846	No clouds
23-04-2011	1210-1334	6	1008	2414
26-04-2011	1607-2200	8	1152	No clouds
30-04-2011	0946-1048	6	855	4018
<u>Summer 2011</u>				
06-07-2011	0740-1755	10	1143	No clouds/2813 ⁽³⁾
08-07-2011	1643-2053	2	1208	1787
12-07-2011	0819-1001	6	724	506
<u>Summer 2012</u>				
21-06-2012	1512-1611	2	980	No clouds
23-06-2012	0555-1107	12	1024	622
24-06-2012	1102-1516	8	1076	No clouds
26-06-2012	0743-1300	10	948	No clouds
29-06-2012	0758-1319	10	1144	No clouds
30-06-2012	0920-2030	8	1100	No clouds/821 ⁽⁴⁾
01-07-2012	0835-2140	10	1212	No clouds
04-07-2012	1330-1805	8	1192	654
10-07-2012	0844-2107	8	1268	No clouds
11-07-2012	0837-2320	14	1196	No clouds/722 ⁽⁵⁾

Table 1. Dates, UTC time, number of profiles, maximum altitude and sky conditions reached during the 2011-2012 Spring-Summer campaign in Ny-Ålesund; ⁽¹⁾from 1600 UTC (last 6 profiles), ⁽²⁾variable for half of the time, ⁽³⁾variable for half of the time, ⁽⁴⁾clouds until 1130 UTC, ⁽⁵⁾from 2219 UTC (last 2 profiles).

5

Season	Profile Type		T (°C)				RH (%)				WS (m/s)				P (hPa)
			33 m	10 m	5 m	2 m	33 m	10 m	5 m	2 m	33 m	10 m	5 m	2 m	Ground
Spring	HO	mean	-8.5	-8.9	-9.7	-9.7	61.0	61.2	61.8	62.7	0.6	0.7	0.6	0.6	997.4
		σ_m	0.5	0.5	0.5	0.5	1.0	1.0	0.9	0.9	0.1	0.1	0.1	0.1	0.4
	PG	mean	-4.7	-5.2	-5.8	-5.9	64.8	65.0	65.9	67.3	2.3	2.1	1.8	1.7	996.2
		σ_m	0.2	0.3	0.3	0.3	0.4	0.4	0.4	0.4	0.1	0.1	0.1	0.1	0.5
	NG	mean	-8.9	-9.3	-9.9	-9.9	57.2	58.5	59.1	60.1	1.3	1.1	1.0	0.9	992.8
		σ_m	0.2	0.2	0.2	0.2	0.4	0.3	0.3	0.3	0.1	0.1	0.1	0.1	0.2
	DNG	mean	-15.8	-16.5	-17.2	-17.2	72.6	73.2	72.9	73.6	0.7	0.9	1.0	0.9	994.8
		σ_m	0.3	0.3	0.3	0.3	0.5	0.3	0.3	0.3	0.1	0.1	0.1	0.1	0.4
Summer	HO	mean	5.7	5.8	5.5	6.0	76.5	75.3	74.7	74.9	4.1	3.8	3.6	3.4	1004.1
		σ_m	0.1	0.1	0.1	0.1	0.2	0.2	0.2	0.2	0.1	0.1	0.1	0.1	0.2
	SP	mean	5.8	5.9	5.6	6.1	78.0	76.4	75.6	75.8	2.6	2.6	2.5	2.4	1001.9
		σ_m	0.1	0.1	0.1	0.1	0.2	0.2	0.2	0.2	0.1	0.1	0.1	0.1	0.1

Table 2. Meteorological parameters (temperature, relative humidity, wind speed, pressure) measured at the CCT at different levels (33, 20, 5 and 2 m) and averaged (timely coincident) for each profile class.

Season	Profile Type		N_{14-260} (cm^{-3})	$N_{260-1200}$ (cm^{-3})	$N_{>1200}$ (cm^{-3})	eBC (ng m^{-3})	b_{abs} (Mm^{-1})
Spring	HO (Column)	mean	80.2	17.5	0.20	35	0.22
		σ_m	16.4	2	0.10	21	0.13
	PG (Hs<0)	mean	205.4	19.9	0.26	24	0.14
		σ_m	12.5	0.2	0.02	3	0.02
	PG (Hs>0)	mean	557.6	22.3	0.16	26	0.16
		σ_m	45.9	1.4	0.02	4	0.02
	NG (Hs<0)	mean	252.3	23.1	0.53	71	0.43
		σ_m	17.5	0.4	0.05	4	0.02
	NG (Hs>0)	mean	118.9	9.7	0.18	39	0.24
		σ_m	9.3	0.3	0.02	2	0.01
	DNG (Hs<0, Ground Aitken Plume)	mean	601.3	32.4	0.17	36	0.22
		σ_m	19.9	0.8	0.01	11	0.06
	DNG (Hs<0, Above Ground Plume)	mean	260.6	32.4	0.17	121	0.74
		σ_m	13.1	0.8	0.01	5	0.03
	DNG (Hs>0)	mean	187.8	22.3	0.08	102	0.62
		σ_m	17.8	0.5	0.01	11	0.07
Summer	HO (Column)	mean	435.9	2.1	0.04	--	--
		σ_m	5.8	0.1	0.004	--	--
	SP (Hs<0)	mean	9000	7.0	0.06	319	1.95
		σ_m	250	0.7	0.004	14	0.09
	SP (Hs>0)	mean	648.1	1.4	0.01	24	0.15
		σ_m	27.3	0.1	0.001	1	0.01

10 Table 3. Average concentrations of N_{14-260} , $N_{260-1200}$, $N_{>1200}$, eBC and b_{abs} along height over Ny-Ålesund for the
11 springtime and summertime typologies of vertical profiles.

12 .

13



Figure 1. a) Ny-Ålesund, the Kongsfjorden and the surrounding orography; b) Gruvebadet sampling site; c) the tethered balloon in Ny-Ålesund.

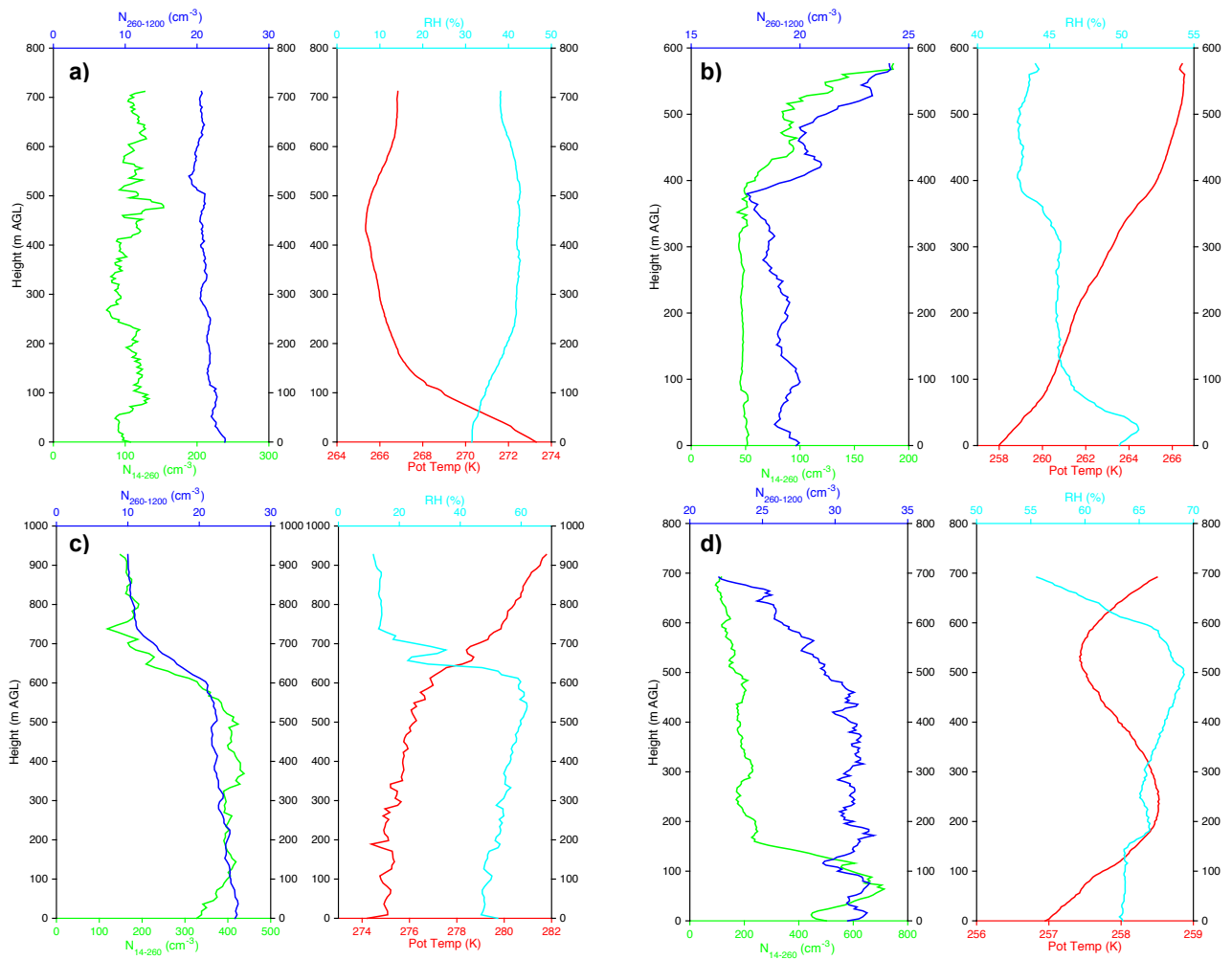


Figure 2. Vertical profiles of N_{14-260} (green line), $N_{260-1200}$ (blue line), potential temperature (red line) and relative humidity (light blue line) measured over Ny-Ålesund on: a) 7th April 2011 (1251-1310 UTC); b) 1st April 2011 (0630-0657 UTC); c) 23th April 2011 (1321-1334 UTC); d) 6th April 2011 (1803-1822 UTC).

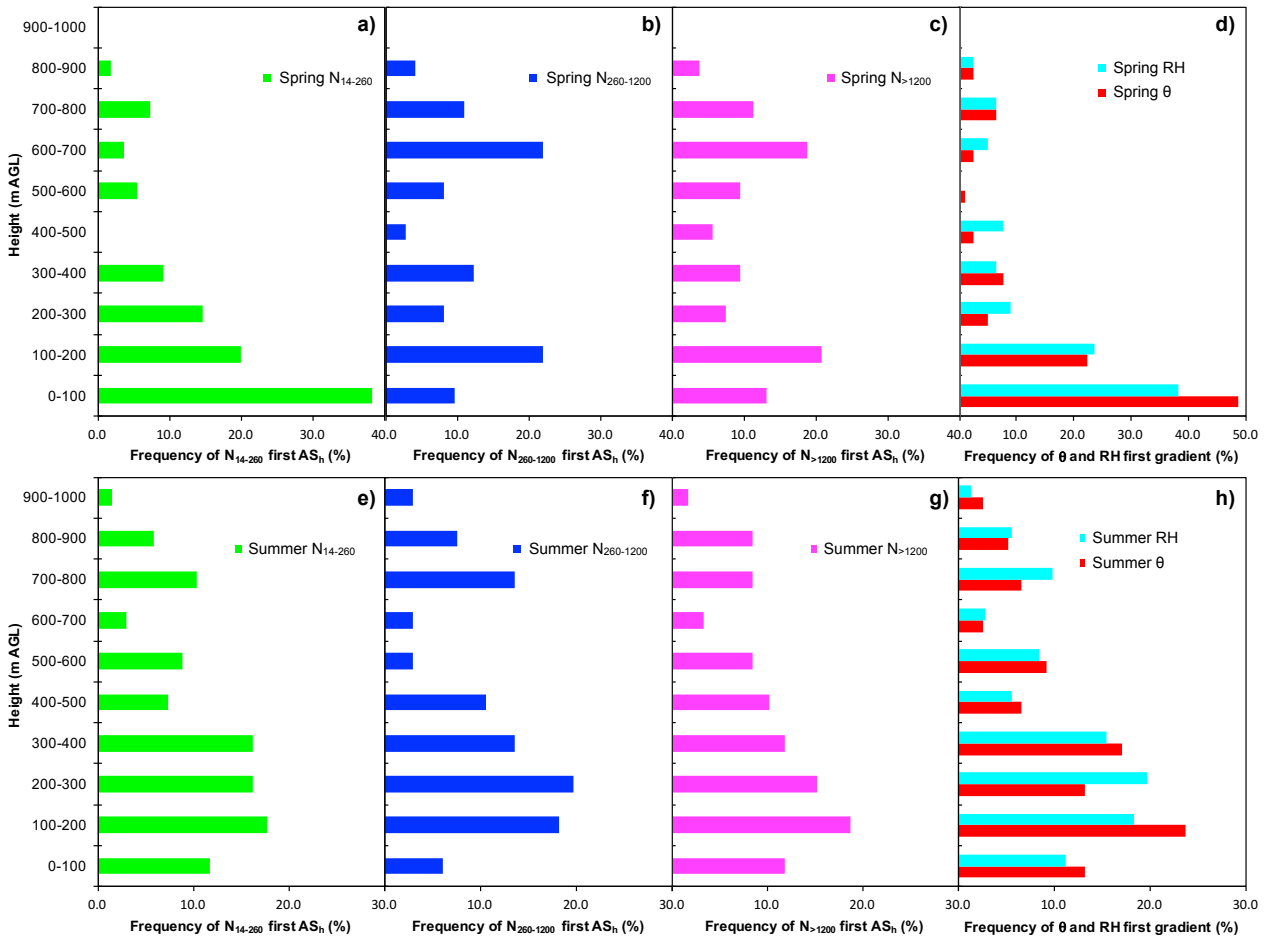


Figure 3. Vertical frequency distribution of the AS_h for N₁₄₋₂₆₀, N₂₆₀₋₁₂₀₀, N_{>1200}, θ and RH during spring in panels from a) to d) and in summer in panels from e) to h).

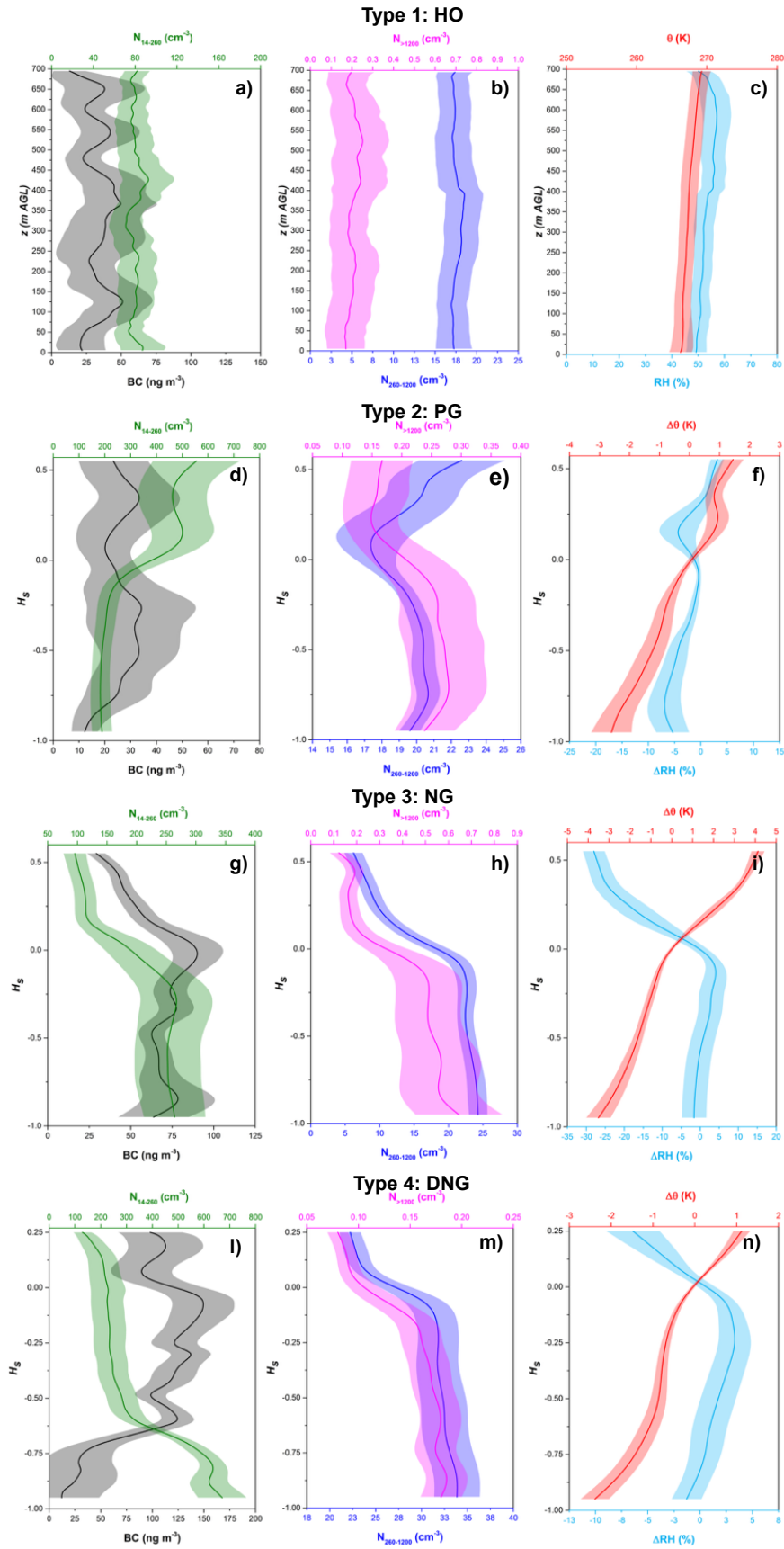
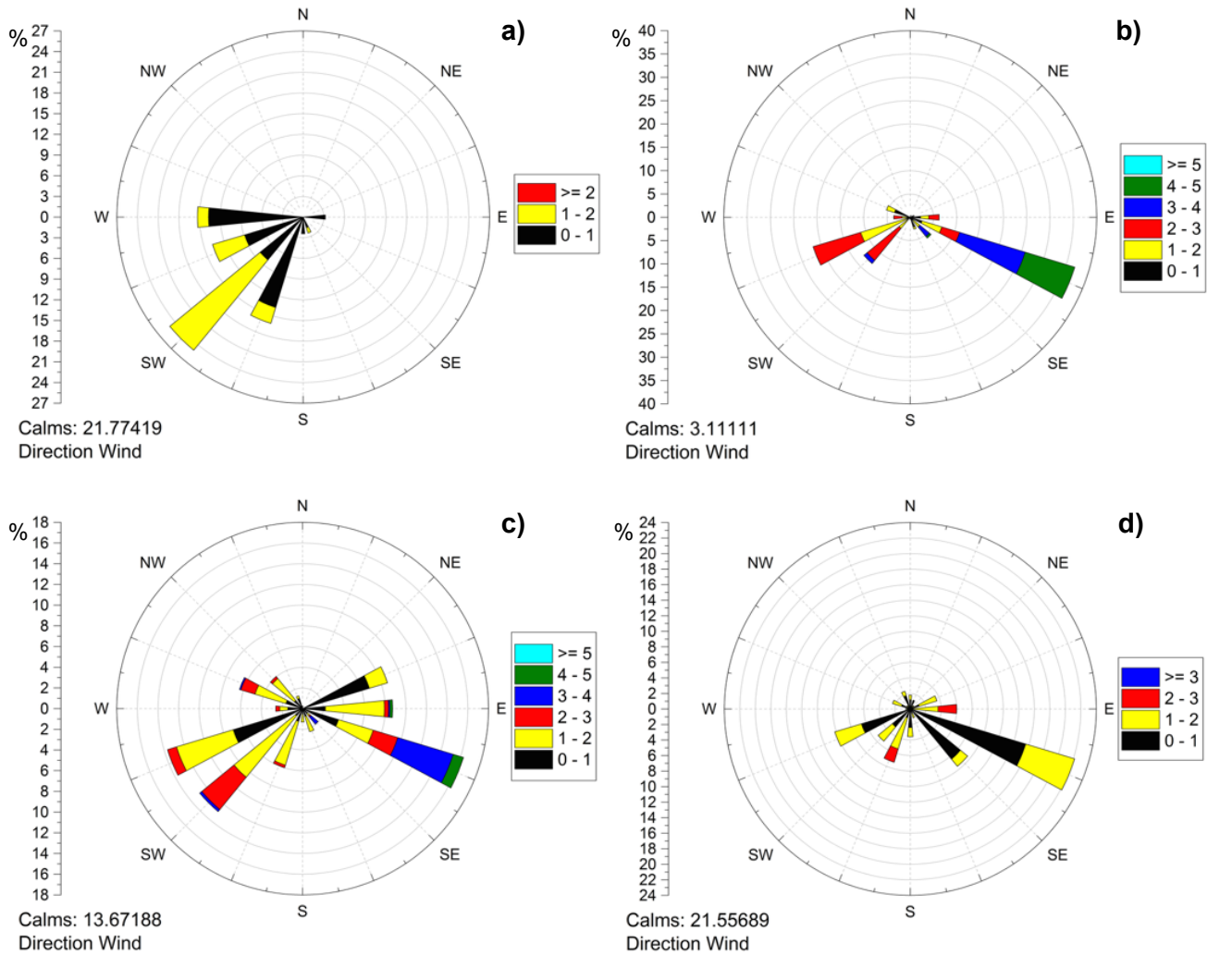


Figure 4. Springtime statistical mean profiles of N_{14-260} (green line), BC (black line), $N_{260-1200}$ (blue line), $N_{>1200}$ (magenta line), θ (red line) and RH (light blue line) along height over Ny-Ålesund for the four typologies of vertical profiles: a-c) homogeneous profiles (HO); d-f) positive gradient profiles (PG); g-i) negative gradient profiles (NG); l-n) decoupled negative gradient profiles (DNG).

Spring



Summer

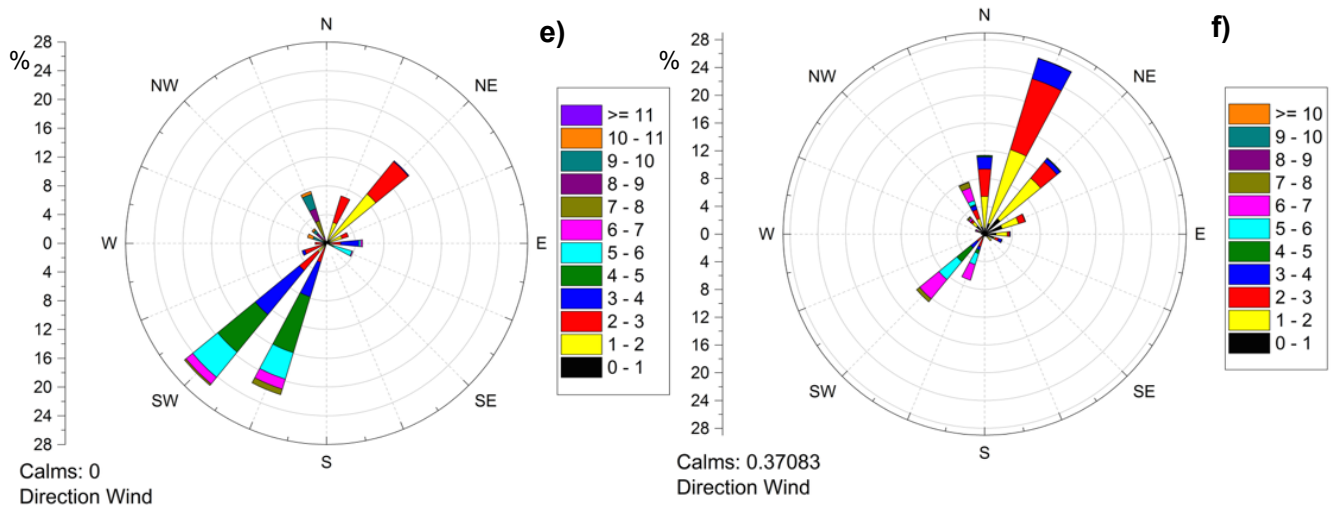


Figure 5. Wind rose obtained from the measured wind speed and direction at the CCT (33 m). Springtime wind rose timely coincident with: a) homogeneous profiles (HO); b) positive gradient profiles (PG); c) negative gradient profiles (NG); d) decoupled negative gradient profiles (DNG). Summertime wind rose timely coincident with: e) homogeneous profiles (HO); f) profiles impacted by shipping emissions (SP).

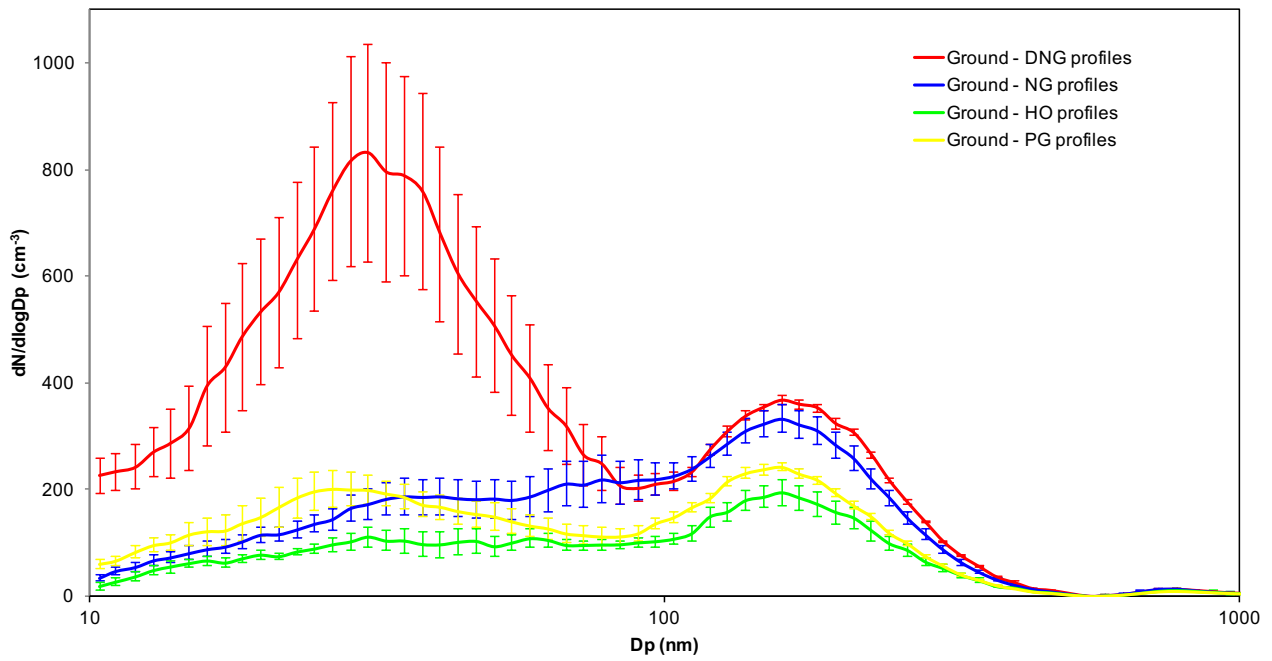


Figure 6. Springtime aerosol number size distribution measured at ground and timely coincident with: homogeneous profiles (HO), positive gradient profiles (PG), negative gradient profiles (NG) and decoupled negative gradient profiles (DNG).

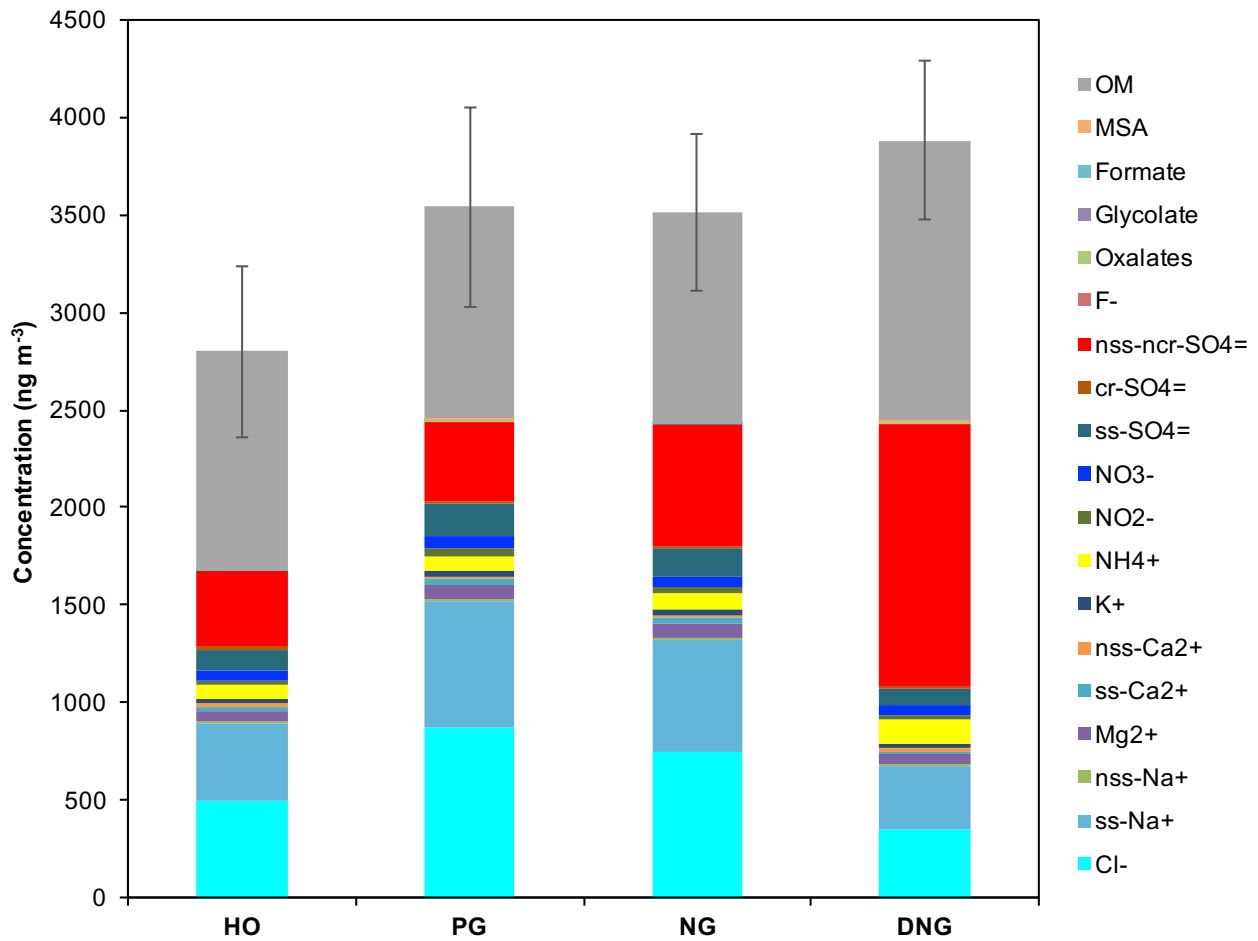


Figure 8. Springtime aerosol chemical composition determined at ground during: a) homogeneous profiles (HO); b) positive gradient profiles (PG); c) negative gradient profiles (NG); d) decoupled negative gradient profiles (DNG). Data shown are the ambient concentrations of each individual aerosol species.

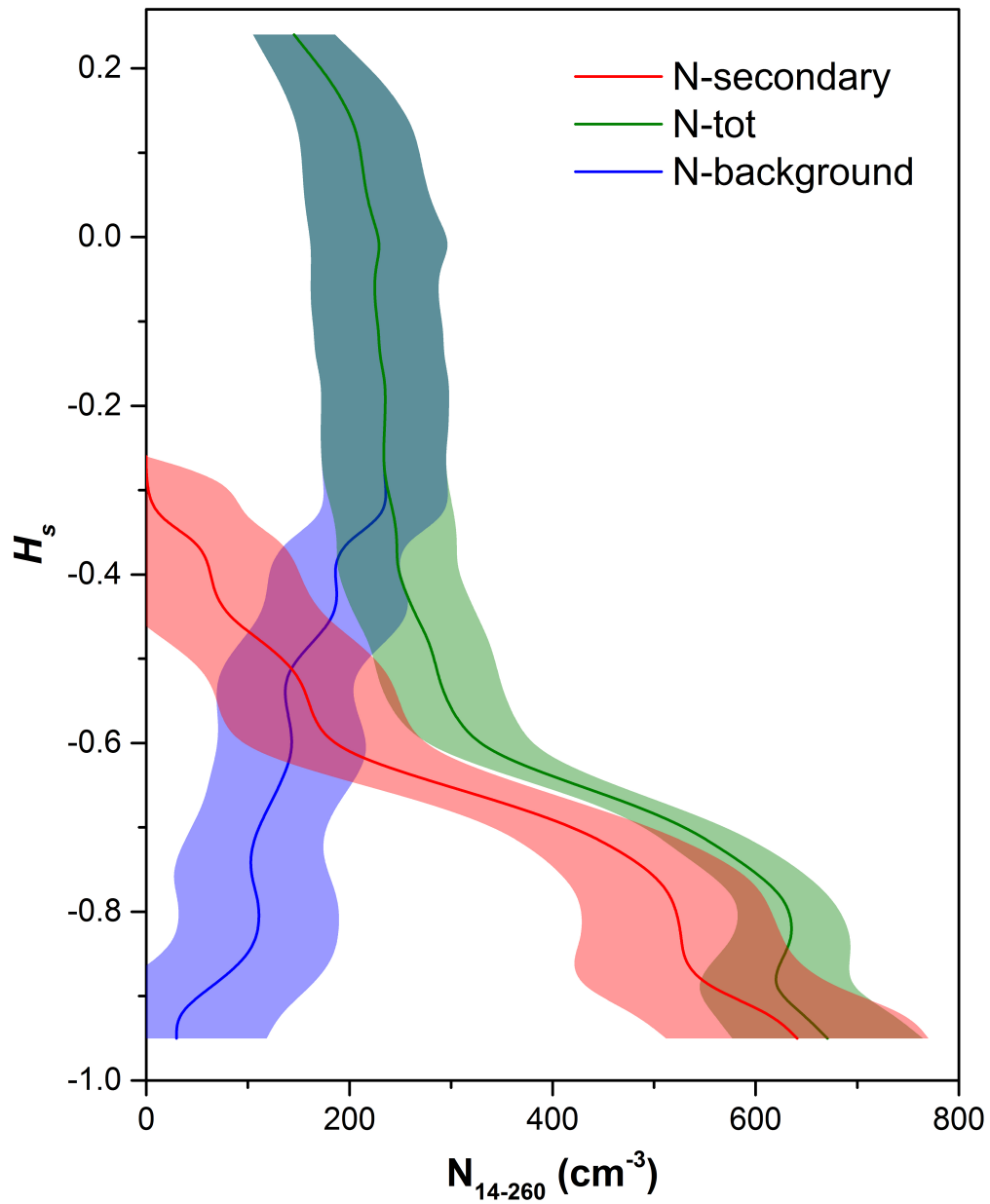


Figure 9. Springtime statistical mean profiles of N_{14-260} (green line) apportioned along height for the contribution of background N_{14-260} aerosol (blue line) and of secondary locally formed N_{14-260} aerosol (red line) for the decoupled negative gradient profiles (DNG) category.

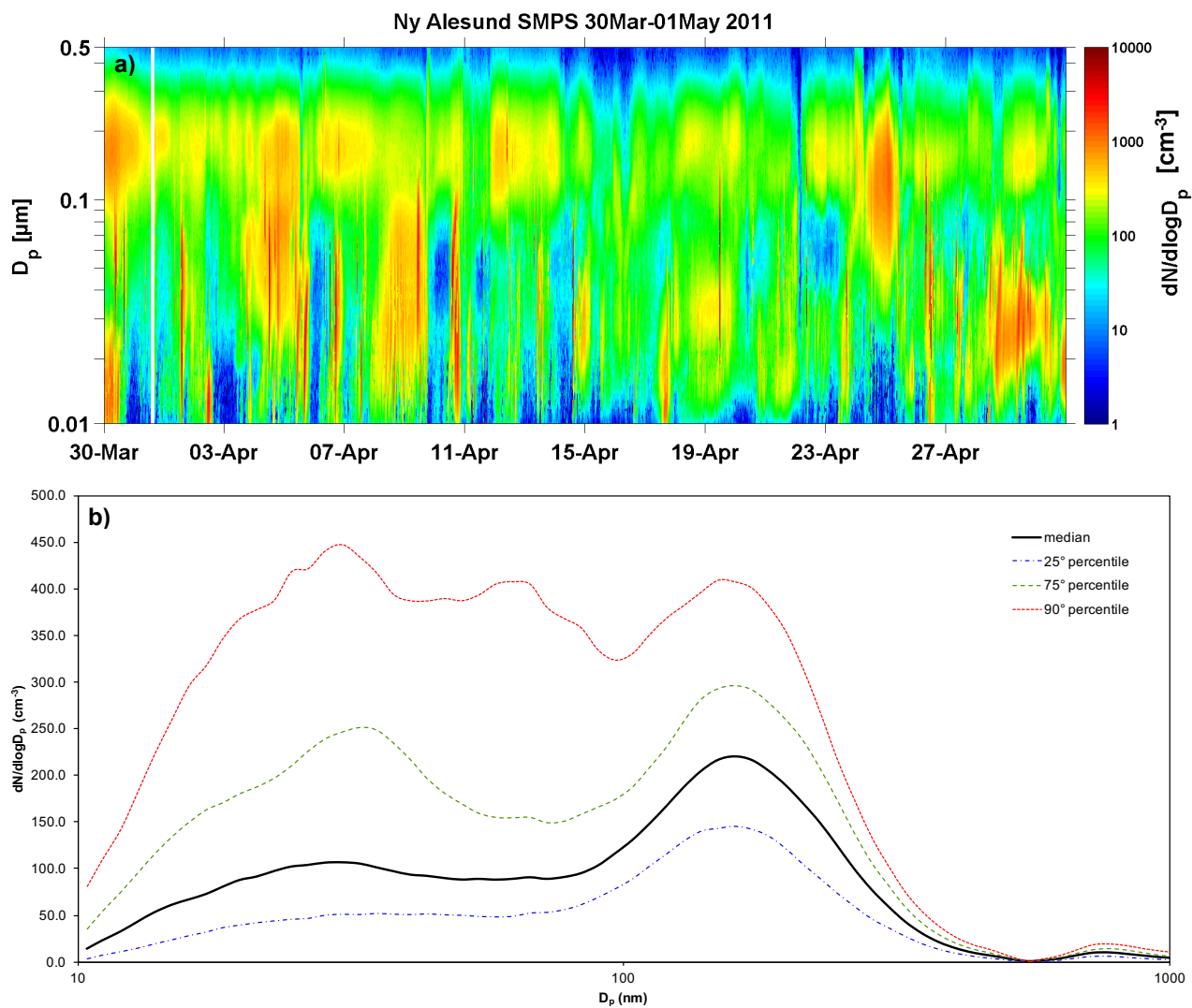


Figure 10. a) aerosol number size distribution measured at ground during April 2011; b) 25th, 50th, 75th and 90th percentiles of the measured number size distribution.

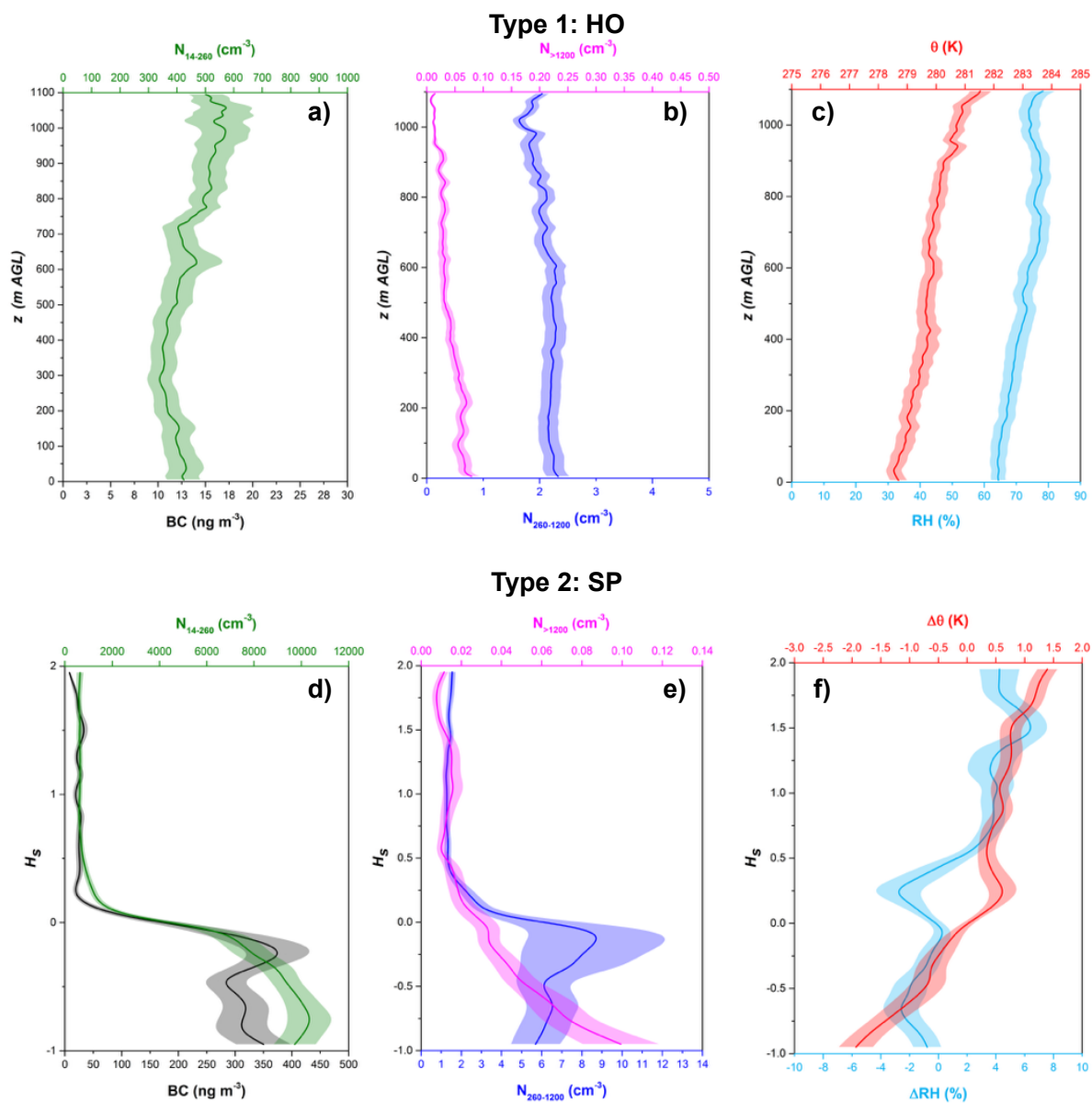


Figure 11. Summertime statistical mean profiles of N_{14-260} (green line), BC (black line), $N_{260-1200}$ (blue line), $N_{>1200}$ (magenta line), θ (red line) and RH (light blue line) along height over Ny-Ålesund for the two typologies of vertical profiles: a-c) homogeneous profiles (HO); d-f) profiles impacted by shipping emissions (SP).

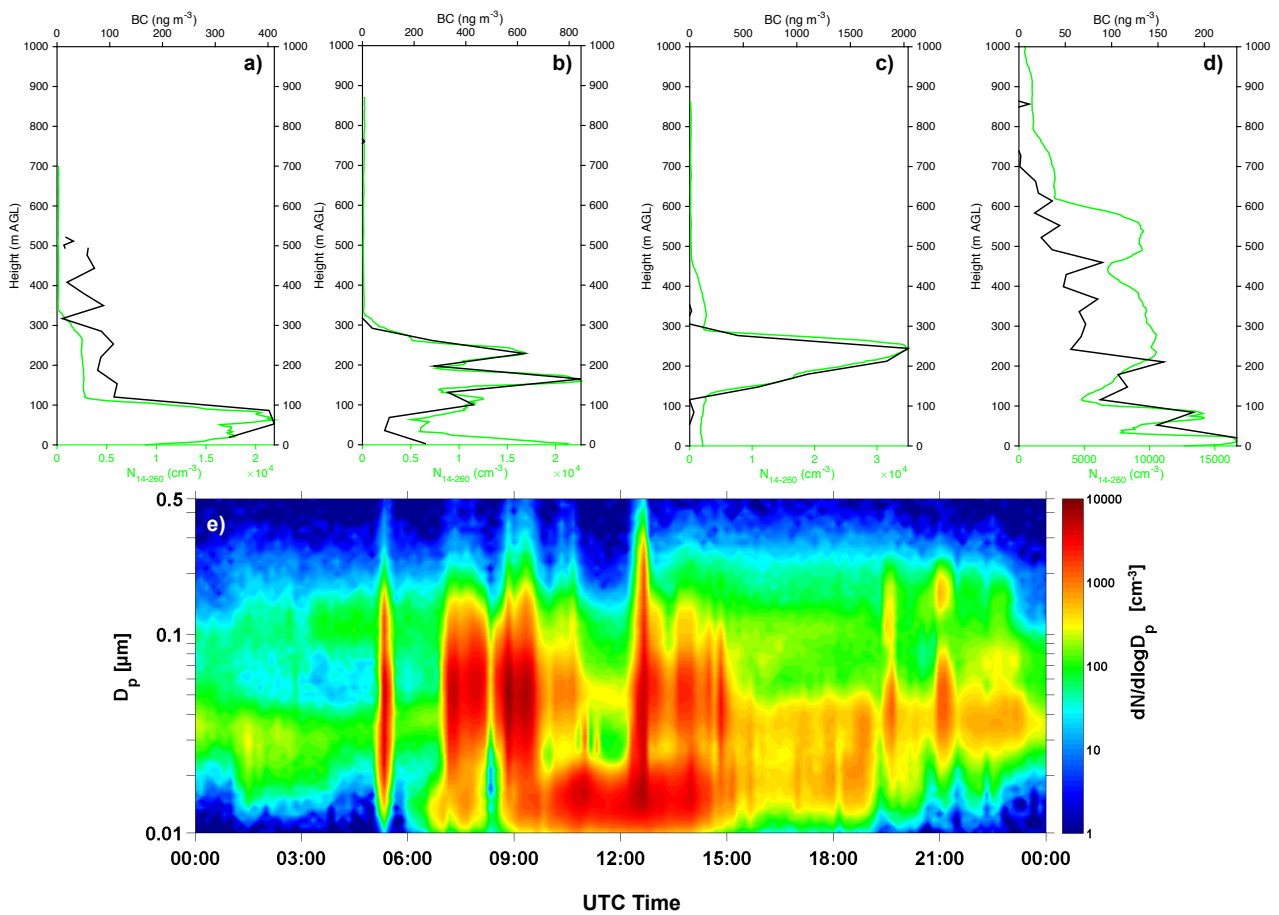


Figure 12. Case study of 6th July 2011 when four ships anchored (not simultaneously) in the harbor of Ny-Ålesund. Vertical profiles of N_{14-260} (green line) and BC (black line) (0740 UTC, 0901 UTC, 0932 UTC and 1340 UTC) are reported in panels from a) to d) together with ground SMPS data collected at Gruvebadet (e). Note the change in BC scale to progressively increasing BC values during the peak of the ship activity at mid-day.